# JOURNAL OF APPLIED PHYSICS

# JOURNAL OF APPLIED PHYSICS

Vol. 16, No. 7 JULY, 1945


## *In This Issue*


*Page*

**Bibliography of Electron Microscopy. III**
CLAIRE MARTON AND SAMUEL SASS 373

**Hipersil—A Greatly Improved Transformer Iron**
T. D. YENSEN 379

*Contributed Original Research*

**Comparison of Some Elastic Properties of Tire Cords**
HELMUT WAKEHAM, EDITH HONOLD, AND EVALD L. SKAU 388

**On the Distribution of Current along Asymmetrical Antennas**
LIEUTENANT COMMANDER CHARLES W. HARRISON, JR. 402

**Correction of X-Ray Diffraction Intensities for Lorentz and Polarization Factors**
M. J. BUERGER AND GILBERT E. KLEIN 408

**Determination of Molecular-Weight Distribution in High Polymers by Means of Solubility Limits**
D. R. MOREY AND J. W. TAMBLYN 419

**Techniques for Evaporation of Metals** LEONARD O. OLSEN, CHARLES S. SMITH, AND E. C. CRITTENDEN, JR. 425

**Letter to the Editor:**

**Adaptation of Special Specimen Holders to Commercial Electron Microscopes** L. MARTON 387

*In Every Issue*

**Here and There** 386

**Recent Applications of Physics** 434

**Index to Advertisers** xxvi



**BOARD OF EDITORS**

ELMER HUTCHISSON, *Editor*

*Associate Editors*

R. B. BARNES
OTTO BEECK
W. F. BUSSE
S. H. CALDWELL
CLARK GOODMAN
SELIG HECHT
W. J. LYONS
MORRIS MUSKAT
THOMAS H. OSGOOD
PAUL E. SABINE
FREDERICK SEITZ
J. R. TOWNSEND

Publication of the
**American Institute of Physics**

**ADMINISTRATIVE STAFF**

HENRY A. BARTON, *Director*

MARGARET S. GRIFFIN, *Publications Manager*

THEODORE VORBURGER, *Business Manager*

JOHN T. TATE, *Adviser on Publications*

**GOVERNING BOARD**

PAUL E. KLOPSTEG, *Chairman*

WALLACE WATERFALL, *Secretary*

GEORGE B. PEGRAM, *Treasurer*

T. D. COPE
R. B. DOW
L. A. DUBRIDGE
FLOYD A. FIRESTONE
HARVEY FLETCHER
R. C. GIBBS
K. S. GIBSON
HERMANN MARK
A. G. WORTHING
JOHN T. TATE
L. W. TAYLOR
N. W. TAYLOR
WALLACE WATERFALL



The JOURNAL OF APPLIED PHYSICS, published monthly at Prince and Lemon Sts., Lancaster, Pa., is devoted to physics in its role as the science basic to other natural sciences and to the arts and industries. Previous to 1937 this publication was known as PHYSICS. The JOURNAL OF APPLIED PHYSICS publishes editorials, news of physicists, and reviews, as well as technical papers of applied physics.

**Manuscripts** should be submitted to Elmer Hutchisson, Editor Case School of Applied Science, Cleveland 6, Ohio.

**Subscriptions** and orders for back numbers should be addressed to Prince and Lemon Streets, Lancaster, Pa. or to the American Institute of Physics, 57 East 55 Street, New York 22, N. Y.

| Subscription Price | U. S. AND CANADA | ELSEWHERE |
|---|---|---|
| To members of scientific societies | $5.00 | $5.70 |
| To all others | 7.00 | 7.70 |

**Back Number Prices**

Complete set: Vol. 1, July, 1931–Vol. 15, 1944—$94.50
Yearly back number rate: $7.70
Single copies: $0.70 each.

**Changes of address** and proofs should be addressed to the Publications Manager.

**Advertising rates** supplied on request. Orders, advertising copy, and cuts should be sent to the American Institute of Physics.

Entered as second class matter January 22, 1937, at the Post Office at Lancaster, Pennsylvania, under the Act of March 3, 1879
Accepted for mailing at the special rate of postage provided for in the Act of February 28, 1925, authorized May 2, 1932.



Copyright 1945, by the American Institute of Physics.

Journal
of
Applied Physics

Volume 16, Number 7 July, 1945

# A Bibliography of Electron Microscopy. III

COMPILED BY

CLAIRE MARTON
*Division of Electron Optics, Stanford University, Stanford University, California*

AND

SAMUEL SASS*
*In Charge of Physics and Observatory Libraries, University of Michigan, Ann Arbor, Michigan*

THE interest evidenced in the first two parts of our bibliography published in this journal[1] seemed to warrant the present effort to bring it up to date so far as is possible under existing conditions. As in the earlier parts, the material is arranged in eight groups; within each group the arrangement is chronological and within each year alphabetical by author and title. No papers came to our attention which would fall into Group VI (Electron Speeds Above 100 kv).

In the April, 1944, issue of *Kolloid Zeitschrift* (**107**, 2–16), E. Ruska published a paper summarizing the development and applications of the electron microscope in Germany up to the end of 1943. This paper includes a summary in table form of the types of electron microscopes, the application of each type, and the number of papers about each type published in Germany up to the end of 1943. The compilers thought it would be of interest to publish a translation of this table and, for purposes of comparison, to construct a similar table showing the number of papers published in countries exclusive of Germany during the same period. Table I is the translation of Ruska's table and Table II gives the same information concerning papers published outside of Germany.

We wish to thank Professor F. O. Koenig, Stanford University, for his help with the translation of German titles, and the assistance of Professor L. Marton, Stanford University, is gratefully acknowledged.

January 31, 1945.

### I. BOOKS

1941

**Eitel, W.** *The electron microscope as an instrument for quantitative measurements in silicate research.* Das Übermikroskop als Forschungsmittel, 48. Berlin, 1941.

**Meldau, R.** *Task of the electron microscope in dust research.* Das Übermikroskop als Forschungsmittel, 78. Berlin, 1941.

**Schmieder, F.** *Examples of the application of the electron microscope to chemical-technical problems.* Das Übermikroskop als Forschungsmittel, 67. Berlin, 1941.

1943

**Beischer, D.** *Results of electron microscopy.* Kolloidchemisches Taschenbuch, second edition, 425, 1943.

1944

**Hatschek, P.** *Electron-optics*, trans. by Artur Palme. Amer. Photogr. Pub. Co., Boston, 1944.

**Prebus, A. F.** The electron microscope. In Alexander, J., *Colloid Chemistry*, Vol. 5, 152–235. Reinhold, New York, 1944.

1945

**Hawley, G. G.** *Seeing the Invisible.* Alfred A. Knopf, New York, 1945.

* Now at General Electric Laboratory, Pittsfield, Massachusetts.

[1] J. App. Phys. **14**, 522–531 (1943); **15**, 575–579 (1944).

### II. EMISSION MICROSCOPY

1942

**Kinder, E.** Emission electron microscopy with magnetic lenses. *Naturwiss.* **30**, 591–592 (1942).

### III. TRANSMISSION TYPE MICROSCOPE

1944

**Levy, G. B.** Dark field illumination in electron microscopy. *J. App. Phys.* **15**, 623–625 (1944).

**Marton, L.** Stereoscopy with the electron microscope. *J. App. Phys.* **15**, 726–727 (1944).

**Marton, L.** A 100 kv electron microscope. *Science* **100**, 318–320 (1944).

### IV. OPTICS OF THE TRANSMISSION TYPE ELECTRON MICROSCOPE

1940

**Brüche, E.** On the application of electric and magnetic fields in electron optics. TFT **29**, 1 (1940).

1942

**Henneberg, W. and Brüche, E.** Concepts and notation in geometrical electron optics. *Arch. Tech. Messen* **138**, 133–134 (1942).

1943

**Brüche, E.** Glass lenses and electron lenses. *Wissen-u. Fortschritt/Technik. f. Alle* **1**, 8 (1943).

**Mollwo, E.** Interference phenomena from scattering particles in an interference field. *Zeits. f. Physik* **120**, 618–626 (1943).

1944

**Boersch, H.** On edges in electron microscope imaging. *Kolloid Zeits.* **106**, 169–174 (1944).

**Calbick, C. J.** Historical background of electron optics. *J. App. Phys.* **15**, 685–690 (1944).

**Marton, L. and Hutter, R. G. E.** Optical constants of a magnetic type electron microscope. *Proc. I.R.E.* **32**, 546–552 (1944).

**Siegbahn, K.** Formation of image in a strong magnetic lens. *Ark. Mat. Astr. fys.* **30A**, 1–12 (1944).

### V. IMAGE DEFECTS

1940

**Hillier, J.** Fresnel diffraction of electrons as a contour phenomenon in electron supermicroscope images. *Phys. Rev.* **58**, 842 (1940).

**Wendt, G.** Chromatic aberration of electron-optical image systems. *Zeits. f. Physik* **116**, 436–443 (1940).

1944

**Schlesinger, K.** A mechanical theory of electron-image formation. *Proc. I.R.E.* **32**, 483–493 (1944).

### VII. DIFFERENT RELATED INSTRUMENTS

1940

**Boersch, H.** Diffraction experiments with very narrow electron beams. *Zeits. f. Physik* **116**, 469–479 (1940).

1942

**Boersch, H.** A highly resolved image by means of ion rays (ion supermicroscopy). *Naturwiss.* **30**, 711–712 (1942).

1943

**Riedel, G.** An electrostatic precipitator for obtaining electron microscopic preparations. *Kolloid Zeits.* **103**, 228–232 (1943).

1944

Capacitator for electron microscope. *Ind. & Engin. Chem. (Anal. ed.)* **16**, 278 (1944).

**Hillier, J. and Baker, R. F.** Microanalysis by means of electrons. *J. Appl. Phys.* **15**, 663–675 (1944).

**Picard, R. G.** Studies with the electron microscope diffraction adapter. *J. Appl. Phys.* **15**, 678–684 (1944).

**Schulz, L. G.** Design of a vacuum photographic plate chamber. *Rev. Sci. Instrum.* **15**, 78–80 (1944).

**Zworykin, V. K.** Using electrons for microanalysis. *Science* **99**, 334–335 (1944).

### VIII. APPLICATIONS OF THE TRANSMISSION TYPE MICROSCOPE

1939

**Ruska, H.** Electron microscopical research technique. *Naturwiss.* **27**, 287–292 (1939).

1940

**Borries, B. von and Ruska, E.** The influence of electron interference on the image of crystals in the electron microscope. *Naturwiss.* **28**, 366 (1940).

**O'Daniel, H. and Radczewski, O. E.** Electron microscopy and diffraction of the same specimen of highly dispersed minerals. *Naturwiss.* **28**, 628 (1940).

**Jacob, A. and Loofman, H.** Electron microscopic investigations of soil minerals of uniform composition $<2\mu$. *Bodenkunde u. Pflanzenernährg.* **66/67**, 666 (1940).

**Meldau, R.** On the air plankton. *Staub, Veröffentlichungen der Staubbekämpfungsstelle* **14**, 317 (1940).

**Müller, R.** Colloidal sulphur in dermatology. *Jb. Heyden*, 143 (1940).

1941

**Ardenne, M. von.** On an electron microscopic investigation of the structure of reflection reducing layers and on the measurement of such layers. *Z. angew. Photogr.* **3**, 13 (1941).

**Ardenne, M. von, Friedrich-Freksa, H., and Schramm, G.** Electron microscopic investigation of the precipitin reaction of tobacco mosaic virus with rabbit antiserum. *Arch. ges. Virusforsch.* **2**, 80 (1941).

**Ardenne, M. von and Hofmann, U.** Electron microscope and x-ray investigations of the structure of carbon black. *Z. physik. Chem. Abt.* B. **50**, 1–12 (1941).

**Brüche, E.** From microscope to electron microscope. *Schweiz. Arch. angew. Wiss. Tech.* **7**, 46–54 (1941).

**Elöd, E.** The structure of wool fibers. *Kolloid Zeits.* **96**, 284–301 (1941).

**Franz, E., Wallner, L. and Schiebold, E.** Contribution to the interpretation of electron micrographs of fibrous specimens. *Kolloid Zeits.* **97**, 36–37 (1941).

**Heering, H., Gizycki, I. von and Kirseck, A.** Investigation of carbon black with the electron microscope. *Kautschuk* **17**, 55 (1941).

**Hess, K., Kiessig, H. and Gundermann, J.** X-ray and electron microscopic investigation of the process of grinding of cellulose. *Z. physik. Chem. Abt.* B. **49**, 64–82 (1941).

**Hofmann, U., Ragoss, A. and Sinkel, F.** The structure of fine crystalline carbon colloids. *Kolloid Zeits.* **96**, 231–237 (1941).

**Jentgen, H.** Can we see the cellulose molecule? *Kunstseide u. Zellwolle* **23**, 76–79 (1941).

**Kausche, G. A., Pfankuch, E. and Ruska, H.** Observations on the effect of sound and supersonics on the protein of tobacco mosaic virus. *Naturwiss.* **29**, 573 (1941).

**Koch, H. W.** Particle size and shape in gold sols. *Z. Elektrochem.* **47**, 717–721 (1941).

**Kühn, J.** Electron microscopic investigations of asbestos dust and asbestos lungs. *Arch. Gewerbepathol. Gewerbehyg.* **10**, 473–485 (1941).

**Kuhn, W.** Electron microscopic investigations of natural and synthetic cellulose fibers. *Melliands Textilber.* **22**, 249 (1941).

**Mahl, H.** Electron microscopic investigations of oxide surface films. *Korros. u. Metallschutz* **17**, 1 (1941).

**Mahl, H.** On the plastic printing process for the electron microscopic examination of surfaces. *Zeits. tech. Physik* **22**, 33–38 (1941).

**Mahl, H.** Electron microscope observations of etch structures of aluminum. *Zentrbl. Mineral Geol.* A, 182–191 (1941).

**Meldau, R. and Teichmüller, M.** On the morphology of extremely fine lead oxide sublimates. I. *Z. Elektrochem.* **47**, 95 (1941).

**Meldau, R. and Teichmüller, M.** On the morphology of extremely fine lead oxide sublimates. II. *Z. Elektrochem.* **47**, 191 (1941).

**Meldau, R. and Teichmüller, M.** Electron microscopic observations on air elutriated carbon dusts of different degrees of carbonization. *Öl und Kohle* **37**, 751–755 (1941).

**Radczewski, O. E. and Richter, H.** Electron microscopic investigation of silicic acid sols. *Kolloid Zeits.* **96**, 1–6 (1941).

**Riedel, G. and Ruska, H.** Electron microscopic determination of the number of particles of a sol over its aerodisperse state. *Kolloid Zeits.* **96**, 86–96 (1941).

**Ruska, H.** On a new kind of structure arising in cytolysis by bacteriophage. *Naturwiss.* **29**, 367 (1941).

**Schoon, Th. and Beger, E.** Influence of carrier structure and method of preparation on Pt catalysts. *Z. physik. Chem. Abt.* A. **189**, 171–182 (1941).

**Schoon, Th. and Klette, H.** The structure of typical adsorbents. *Naturwiss.* **29**, 652–653 (1941).

**Schoon, Th. and Koch, H. W.** Studies of rubber fillers. I. Particle size and shape of carbon black and their influence on the properties of rubber mixtures as observed on electron micrographs. *Kautschuk* **17**, 1–7 (1941).

**Schramm, G. and Friedrich-Freksa, H.** The precipitin reaction of tobacco mosaic virus with rabbit and hog antiserum. *Physiol. Chem.* **270**, 233 (1941).

**Zahn, H.** Electron micrographs of isolated spindle cells of sheep wool. *Melliands Textilber.* **22**, 305 (1941).

1942

**Ardenne, M. von and Endell, K.** Melting of clinker-minerals $C_3A$ and $C_4AF$ and of the fraction $>3\mu$ of some Portland cement clinkers in the heating electron microscope. *Zement*, 313 (1942).

**Arnold, A. and Gölz, E.** Zinc oxide studies, I. *Kautschuk* **18**, 39 (1942).

**Bennek, H., Rüdiger, O., Stablein, F. and Volk, K. E.** Structural examination of steel with the electron microscope. *Arch. Eisenhüttenwessen* **15**, 431–436 (1942).

**Calfas, P.** The electron microscope for 45,000X magnification. *Genie Civil* **119**, 313–315 (1942).

**Elöd, E., Novotny, H. and Zahn, H.** On the structure and chemistry of wool fibers. *Kolloid Zeits.* **100**, 283 (1942).

**Frey-Wyssling, A.** Remark on the discussion on electron microscopy of cellulose fibers. *Kolloid Zeits.* **100**, 304–305 (1942).

**Feitknecht, W., Signer, R. and Berger, A.** On sols with flake-shaped particles. On colloidal nickel hydroxide. *Kolloid Zeits.* **101**, 12, (1942).

**Hamann, A.** The behavior of cellulose fibers in the electron microscope. *Kolloid Zeits.* **100**, 248–254 (1942).

**Hass, G.** Electron microscopic and electron diffraction studies of the structure of evaporated metal films. *Kolloid Zeits.* **100**, 230–242 (1942).

**Hess, K., Steurer, E. and Fromm, H.** Influence of the grinding process on the properties of high polymers (cellulose and polystyrene) and on the nature of its action. Parts I and II. *Kolloid Zeits.* **98**, 148–159; 290–304 (1942).

**Kottmann, U.** Morphological observations on "taches vierges" on coli cultures. *Arch. ges. Virusforsch.* **2**, 388 (1942).

**Mahl, H.** On thermally produced oxide films on aluminum. *Kolloid Zeits.* **100**, 219 (1942).

**Mahl, H. and Stranski, I. N.** Etch figures on aluminum crystal surfaces. *Zeits. physik. Chem.* **51**, 319–346 (1942).

**Reumuth, H.** The microscopic fine structure of wool. Contributions to morphology, histology and anatomy. *Kleipzigs Textilzeitschrift* **45**, 149 (1942).

**Ruska, H.** Electron microscopic investigations of asbestos dust and asbestos lungs. (Appendix to the paper of Kühn, J.) *Arch. Gewerbepath. Gewerbehyg.* **11**, 575–578 (1942).

**Ruska, H.** Morphological findings in cytolysis by bacteriophage. *Arch. ges. Virusforsch.* **2**, 345 (1942).

**Thiessen, P. A.** Reciprocal adsorption of colloids. *Z. Elektrochem.* **48**, 675–681 (1942).

**Thiessen, P. A.** Relation between shape and properties of colloidal conglomerates. *Kolloid Zeits.* **101**, 241–248 (1942).

**Wallner, L.** The possibilities of electron microscopic structure determination of fibers. I, II, III. *Melliands Textilber.* **23**, 158: 211 (1942).

**Wergin, W.** What conclusions does electron microscopy permit concerning the structure of cellulose? *Kolloid Zeits.* **98**, 131 (1942).

**Zahn, H.** Electron micrographs of isolated spindle cells of sheep wool, II. *Melliands Textilber.* **23**, 157 (1942).

1943

**Ardenne, M. von.** The production of electron microscope films. *Forschungen u. Fortschr.* **19**, 77–78 (1943).

**Ardenne, M. von and Endell, K.** The sintering of clay minerals and of sludge in naturally occurring moulding sands in the heating electron microscope. *Giesserei vereinigt mit Giesserei-Ztg.* H. **1**, 6 (1943).

**Ardenne, M. von, Endell, K. and Lehmann, H.** The sintering of ceramic raw materials in the heating electron microscope. *Ber. Dtsch. keram. Ges.* **24**, 73–88 (1943).

**Baylor, M. R. B., Nalbandov, A. and Clark, G. L.** Electron microscope study of sperm. *Proc. of the Soc. Exp. Biology & Med.* **54**, 229–232 (1943).

**Beischer, D.** Electron microscopic investigations for the structure determination of colloidal particles. 10. Electron microscopic investigations for the structure determination of colloidal systems. *Z. Elektrochem. angew. physik. Chem.* **49**, 463 (1943).

**Big, E. J.** The electron microscope: an opening to new scientific frontiers. *Bios* **14**, 128–138 (1943).

**Clark, G. L., Quaife, M. L., and Baylor, M. R. B.** Electron microscope studies of proteins including some hemocyanins and nucleoproteins. *Biodynamica* **4**, 153–162 (1943).

**Eisenhut, O. and Kuhn, E.** Light microscopic and electron microscopic investigations of natural and synthetic cellulose fibers. *Melliands Textilber.* **24**, 210 (1943).

**Eitel, W.** Electron microscopy and electron diffraction of silicate metaphases. I. On metahallaysite (Eitel, W. and Radczewski, O. E.). II. The metaphase of brucite (Eitel, W. and Kedesdy, H.). III. The metaphase of the dehydration of talc (Eitel, W. and Kedesdy, H.). IV. Metakaolin (Eitel, W. and Kedesdy, H.) *Abh. Preuss. Akad. Wiss., Math.-naturwiss. Kl.* Nr. 5 (1943).

**Eitel, W.** The electron microscope and its application to ceramic problems. *Ber. Dtsch. keram. Ges.* **24**, 37–53 (1943).

**Endell, K. and Ardenne, M. von.** Representation of sintering and melting of ceramic raw materials of glass mixtures, of slags, and of coal ashes in the heating electron microscope. *Kolloid Zeits.* **104**, 223 (1943).

**Endell, K. and Ardenne, M. von.** Representation of sintering and melting of glass mixtures, soda and soda slags in the heating electron microscope. *Glasstechn. Ber.* **21**, 121 (1943).

**Endell, K., Zinsen, A. and Ardenne, M. von.** On the sintering and melting of coal ashes in the heating electron microscope and the importance of slag viscosity for the fueling of melting furnaces. *Feuerungstechn.* **31**, 73 (1943).

**Franz, E. and Schiebold, E.** On the structure of bacterial cellulose. *J. makromol. Chem.* 3. Reihe, **1**, 4 (1943).

**Franz, E., Schiebold, E. and Weygand, C.** On the morphological structure of bacterial cellulose. *Naturwiss.* **31**, 350 (1943).

**Franz, E., Schiebold, E. and Wallner, L.** Contributions of the electron microscope to the morphology of cellulose. *Forschungsberichte des Zellwolle- und Kunstseide-Rings* H. **3**, 114 (1943).

**Gard, S.** Comparative physico-chemical and electron microscopic studies of purified poliomyelitis virus preparations. *Ark. Kem. Mineral. Geol.* **17B**, 1 (1943).

**Gärtner, K.** The action of sulfonamide as revealed by fluorescent- and electron-microscopy. *Zent. f. Bakt.* **150**, 97–115 (1943).

**Günther, F.** A contribution to the study of the influence of method of preparation on the electron microscope image of some highly polymeric organic substances. *Forschungsberichte des Zellwolle- und Kunstseide-Rings* H. **3**, 9 (1943).

**Hagemann.** The electron microscope and motion picture camera. *Kinotech.* **25**, 14–15 (1943).

**Hanke, W.** Determination of the size and shape of ultramicroscopic particles. *Zeits. f. Physik* **121**, 438–458 (1943).

**Hess, K.** Changes in air elutriated organic high polymers. *Z. Ver. Dtsch. Ing., Beih. Verfahrenstechn. Folge* Nr. **3**, 61 (1943).

**Hofmann, U.** The structure and technical properties of carbons. *Wien. Chem. Ztg.* **46**, 97–106 (1943).

**Husemann, E.** Electron microscopic investigations of ground cellulose fibers. *J. makromol. Chem.* 3 Reihe, **1** (1943).

**Husemann, E. and Carnap, A.** Electron microscopic investigations of hydrolitically split fibers. *J. makromol. Chem.* 3 Reihe, **1**, 16 (1943).

**Kedesdy, H.** Electron microscopic investigations of the roasting of talc and of steatite. *Ber. Dtsch. keram. Ges.* **24**, 201–232 (1943).

**Kossel, W.** Lines of uniform thickness of crystals in the electron microscope. *Naturwiss.* **31**, 323–324 (1943).

**Krause, F. and Mahl, H.** Electron microscopic surface representation of medico-biological objects with replica technique. *Kolloid Zeits.* **105**, 53–55 (1943).

**Lepsius, R.** Methods of structural analysis of macromolecules. *Kunststoffe* **33**, 133–138 (1943).

**Mahl, H.** Progress in surface electron microscopy with the replica method. *Metallwirtschaft* **22**, 9–12 (1943).

**Mahl, H. and Stranski, I. N.** The block structure of cadmium single crystals. *Z. f. Metallkunde* **35**, 147–151 (1943).

**Marx, Th. and Wehner, G.** Electron microscopic representation of the lamellar structure of magnesium hydroxide. *Kolloid Zeits.* **105**, 226–227 (1943).

**Pfankuch, E. and Piekenbrock, F.** On the splitting of the virus proteins of the tobacco mosaic group. *Naturwiss.* **31**, 94 (1943).

**Ragoss, A., Hofmann, U. and Holst, R.** The graphitizing of Thermax-carbon. *Kolloid Zeits.* **105**, 118 (1943).

**Ruska, E.** The origin of the fringes around particles in electron micrographs and their variation with the optical focus. *Kolloid Zeits.* **105**, 43–52 (1943).

**Ruska, H.** Attempt at a classification of the virus species. *Arch. ges. Virusforsch.* **2**, 480 (1943).

**Ruska, H.** Results of bacteriophage research and their interpretation by morphological findings. *Erg. Hyg. Bakt., Immunitatsforschng. u. exper. Ther.* **25**, 437 (1943).

**Ruska, H.** On the virus of chickenpox and herpes. *Klin. Wochenschr.* **22**, 703 (1943).

**Ruska, H. and Kausche, G. A.** On the form, size-distribution and structure of some elementary virus bodies. *Zbl. Bakteriol., Parasitenkunde Infektionskrankh.* **150**, 311 (1943).

**Schaefer, V. J.** Dry stripped replicas for the electron microscope. *Science* **97**, 188 (1943).

**Schramm, G.** On the splitting of tobacco mosaic virus into low molecular proteins and the reformation of high molecular proteins from the products of the splitting. *Naturwiss.* **31**, 94–96 (1943).

**Semmler-Alter, E.** Electron microscopic surface representation of some metallographic materials with replica technique. *Metallwirtschaft* **22**, 303–307 (1943).

**Semmler-Alter, E.** Methods and results of electron microscopy applied to metallurgy. *Rev. de Métallurgie* **40**, 301–309 (1943).

**Semmler, E.** Electron microscope studies with aluminum surfaces. *Aluminum*, **24**, 302–307 (1942); *Light Metals* **6**, 20–24 (1943).

**Staudinger, M.** Macromolecular compounds. Microscopic and electron microscopic investigations of macromolecular materials. *Chem. Ztg.* **67**, 316–320 (1943).

**Strunz, H.** Contributions to the pyrolusite problem. *Naturwiss.* **31**, 89–91 (1943).

**Thiessen, P. A.** The cause of dichroism of colloidal metals. *Zeits. anorg. u. Allg. Chem.* **250**, 352–356 (1943).

**Thomson, G. P.** The electron microscope. *Endeavor* **2**, 125–135 (1943).

**Watson, J. H. L.** Applied electron microscopy. *Can. J. Res.* **21**, 89–98 (1943).

**Wolpers, C.** Transverse striation in collagens and basic material. *Klin. Wochenschr.* **22**, 624 (1943).

**Zahn, H.** Electron micrographs of isolated epithelial cells of sheep wool. *Melliands Textilber.* **24**, 154 (1943).

1944

**Abrams, I. M. and McBain, J. W.** A closed cell for electron microscopy. *J. App. Phys.* **15**, 607–609 (1944).

**Abrams, I. M. and McBain, J. W.** A closed cell for electron microscopy. *Science* **100**, 273–274 (1944).

**Baker, R. F. and Nicoll, F. H.** On the silica replica method of surface examination with the electron microscope. *J. App. Phys.* **15**, 803–805 (1944).

**Banca, M. C.** The electron microscope. *Can. Chem. Process Ind.* **28**, 10–12 (1944).

**Barrett, C. S.** Electron microscope in metallurgical research. *J. App. Phys.* **15**, 691–696 (1944).

**Baylor, M. R. B., Severens, J. M. and Clark, G. J.** Electron microscope studies of the bacteriophage of Salmonella pullorum. *J. Bact.* **47**, 277–282 (1944).

**Borries, B. von and Glaser, W.** On the rise in temperature of objects in the electron microscope. *Kolloid Z.* **106**, 123–128 (1944).

**Crane, H. R.** Direct centrifugation onto electron microscope specimen film. *Rev. Sci. Instrum.* **15**, 253 (1944).

**Donovan, G. E.** Biological applications of the electron microscope. *Nature* **154**, 356–358 (1944).

**Dubin, J. N. and Sharp, D. G.** Comparison of the morphology of bacillus megatherium with light and electron microscopy. *J. Bact.* **48**, 313–329 (1944).

**Hall, C. E., Hauser, E. A., Le Beau, D. S., Schmitt, F. O. and Talalay, P.** Natural and synthetic rubber fibers; electron microscope studies. *Ind. Eng. Chem.* (*Ind. ed.*) **36**, 634–640 (1944).

**Heidenreich, R. D. and Matheson, L. A.** Electron microscopic determination of surface elevations and orientations. *J. App. Phys.* **15**, 423–435 (1944).

**Hofer, A. W.** Flagellation of Azotobacter. *J. Bact.* **48** (6) 697–701 (1944).

**Ingelman, B. and Siegbahn, K.** Dextran and levan molecules studied with the electron microscope. *Nature* **154**, 237–238 (1944).

**Johnson, F. H.** Observations on the electron microscopy of B. cereus, and Tyrothricin action. *J. Bact.* **47**, 551–557 (1944).

**Keller, F. and Geisler, A. H.** Application of electron microscope to study of aluminum alloys. *Metals Technology* **11**, Tech. Pub. 1700, 1–17 (1944).

**Keller, F. and Geisler, A. H.** Extending microscopic examination of metals. *J. App. Phys.* **15**, 696–704 (1944).

**Kratky, O., Sekora, A. and Weber, H. H.** New small-angle interferences in myosin. *Naturwiss.* **31**, 91 (1944).

**Ladd, W. A.** Electron microscope studies of colloidal carbon in vulcanized rubber. *Ind. & Eng. Chem.* (*Anal. ed.*) **16**, 642–644 (1944).

**Mrgudich, J. N. and Clock, R. C.** X-ray and electron microscope evaluation of carbon black. *Electrochemical Soc.* Preprint **86/29**, 329–341 (1944).

**Mudd, S. and Anderson, T. F.** Pathogenic bacteria, Rickettsias and viruses as shown by the electron microscope. *J. Am. Med. Ass.* **126**, 561–571; 632–639 (1944).

**Picard, R. G. and Smith, P. C.** The electron microscope for metals. *Metals and Alloys* **20**, 636–641 (1944).

Progress in electron microscopy and new results with the Siemens electron microscope. *Schweizer. Arch. f. angew. Wiss. u. Tech.* **10**, 86–88 (1944).

**Rawlins, T. E.** Stream double refraction studies on the orientation of tobacco mosaic virus particles. *Science* **99**, 447–449 (1944).

**Rees, A. L. G.** The electron microscope and its applications. *Paper-Maker* **107**, 11–14 (1944).

**Richards, A. G. and Thomassen, L.** Microstructures of tooth surfaces as revealed by the electron microscope. *Amer. Dental Assoc. J.* **31**, 772–776 (1944).

**Ruska, E.** The development of electron microscopy and its relation to colloid research. *Kolloid Zeits.* **107**, 2–16 (1944).

**Sharp, D. G., Taylor, A. R., McLean, I. W., Jr., Beard, D. and Beard, J. W.** Density and size of influenza virus A (PR8 strain) in solution. *Science* **100**, 151–153 (1944).

**Sollner, K. and Anderman, J.** Structure of the collodion membrane and its electrical behavior. *J. Gen. Physiol.* **27**, 433–460 (1944).

**Stanley, W. M.** The size of influenza virus. *J. Exper. Med.* **79**, 267–283 (1944).

**Taylor, A. R., Sharp, D. G., McLean, I. W., Jr., Beard, D., Beard, J. W., Dingle, J. H. and Feller, A. E.** Purification and character of the swine-influenza virus. *J. Immunology* **48**, 361–379 (1944).

**Weiss, L. J.** Electron micrographs of pleuropneumonia-like organisms. *J. Bact.* **47**, 523–527 (1944).

**Williams, R. C. and Wyckoff, W. G.** Thickness of electron microscopic objects. *J. App. Phys.* **15**, 712–716 (1944)

TABLE I.

| Means of image formation | Transmission | Vertical illumination | Emission |
|---|---|---|---|
| Enlarging lenses (focusing microscopes) | Most important instrument for many applications<br>m.l. EM 1931 SM 1933 2 mμ<br>e.l. EM 1933 SM 1939 8 mμ<br>341 papers | Instrument for metallographic investigations<br>m.l. EM 1933 SM 1940 25 mμ<br>e.l. ——<br>6 papers | Instrument for metallographic and cathode investigations<br>m.l. EM 1932 SM 1942 140 mμ<br>e.l. EM 1931 SM 1942 40 mμ<br>5 papers |
| Point projection (shadow microscope, field emission microscope) | Resolution limited by distortion<br>m.l. EM —— SM ——<br>e.l. EM —— SM 1939 25 mμ<br>5 papers | | Special instrument for the investigation of finest points<br>m.l. EM —— SM ——<br>e.l. EM —— SM 1937 4 mμ<br>7 papers |
| Scanning (scanning microscope) | Resolution limited by scanning lines<br>m.l. EM —— SM 1938<br>e.l. EM —— SM ——<br>40 mμ<br>2 papers | Imaging system possible, no microscopical devices known up to now | |

Abbreviations: m.l. = magnetic lens, e.l. = electrostatic lens, EM = electron microscope, SM = super microscope.

TABLE II.

| Means of image formation | Transmission | Vertical illumination | Emission |
|---|---|---|---|
| Enlarging lenses (focusing microscopes) | Most important instruments for many applications<br>m.l. 2 mμ<br>e.l. 10 mμ<br>180 papers | Instrument for metallographic investigations<br>m.l. ——<br>e.l. ——<br>—— | Instrument for metallographic and cathode investigations<br>m.l. 1 μ?<br>e.l. ——<br>13 papers |
| Point projection (shadow microscope, field emission microscope) | Resolution limited by distortion<br>m.l. ——<br>e.l. 50 mμ?<br>1 paper | —— | Special instrument for the investigation of finest points and of fine wires<br>m.l. 1 μ for wires<br>e.l. 4 mμ for points<br>3 papers |
| Scanning (scanning microscopes) | Resolution limited by scanning lines<br>m.l. ——<br>e.l. ——<br>—— | m.l. ——<br>e.l. 50 mμ<br>1 paper | —— |

Abbreviations: m.l. = magnetic lens, e.l. = electrostatic lens, EM = electron microscope, SM = super microscope.

# Hipersil†—A Greatly Improved Transformer Iron*

BY T. D. YENSEN

*Westinghouse Electric Corporation, East Pittsburgh, Pennsylvania*

WHEN silicon-iron was first introduced 40 years ago through the efforts of Hadfield in England and Gumlich in Germany, it revolutionized the transformer industry. Because of its high electrical resistivity and better magnetic properties, it cut losses in two, made it possible to operate transformers at 50-percent higher inductions, thereby decreasing volume and weight, and incidentally eliminated aging through better heat treatment practices.

For 35 years silicon-iron was without a competitor as core material for distribution and power transformers. Many attempts were made to find substitutes but without success. Because of their high initial permeability iron-nickel alloys like Hipernik (40–60 percent nickel) have found a place in the radio and instrument transformer field, and higher nickel alloys like Permalloy in the telephone field, but their high cost and low saturation values have precluded their use in the ordinary transformers.

While no successful substitute was found for silicon-iron, an enormous amount of research and development work was done to improve upon Hadfield's original alloy. As a measure of the success of this work might be mentioned that the commercial hot rolled silicon-iron in common use today has a core loss of less than one-half of that of the alloy used 40 years ago, and a maximum permeability of more than double. The high density permeability, however, has not been materially improved.

That there was plenty of room for still further improvements has been known for a long time. In the first place, the work done at the Westinghouse Research Laboratories[1] since 1916 had shown that it was quite possible to reduce the hysteresis loss to still lower values by removal of impurities, particularly carbon (Fig. 1) and increase in grain size (Fig. 2).

In the second place, it has been known for the last 15 years that iron and iron-silicon alloys are magnetically anisotropic, i.e., that the magnetic properties, particularly the high density permeability, are different in different crystallographic

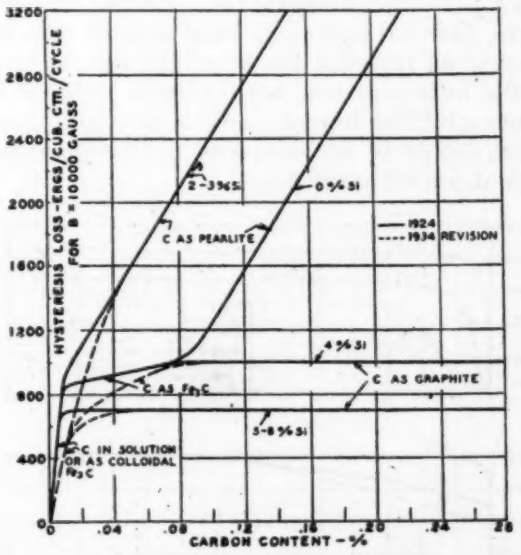


FIG. 1. Effect of carbon on the magnetic properties of iron-silicon alloys.

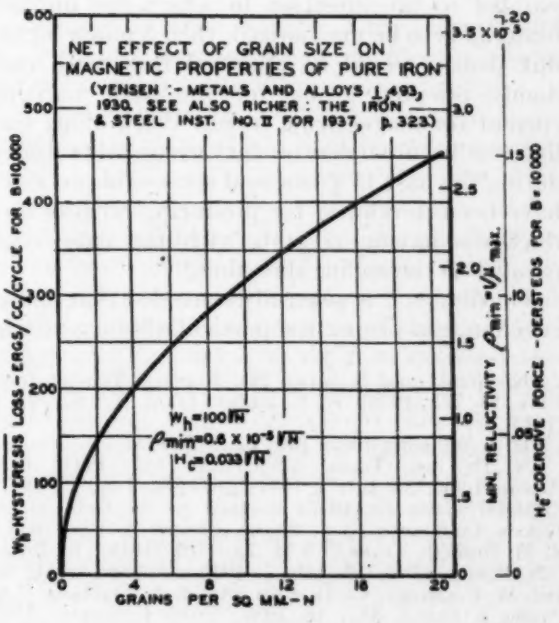
NET EFFECT OF GRAIN SIZE ON MAGNETIC PROPERTIES OF PURE IRON
(YENSEN :- METALS AND ALLOYS 1, 493, 1930. SEE ALSO RICHER : THE IRON & STEEL INST. NO. II FOR 1937, p. 323)
Wh=100√N
ρmin=0.8 X 10⁻⁵ √N
Hc=0.033√N
Wh-HYSTERESIS LOSS - ERGS/CC/CYCLE FOR B=10,000
MIN. RELUCTIVITY ρmin=1/μmax.
Hc-COERCIVE FORCE - OERSTEDS FOR B=10000
GRAINS PER SQ. MM.-N
0
4
8
12
16
20
3.5 X 10⁻⁵

FIG. 2.

† Westinghouse trademark.

* This paper was presented at the April, 1944 meeting of the American Physical Society in Pittsburgh.

[1] T. D. Yensen, Trans. A.I.E.E. **43**, 145 (1924); U. S. Patent 2,050,408, August 11, 1936.

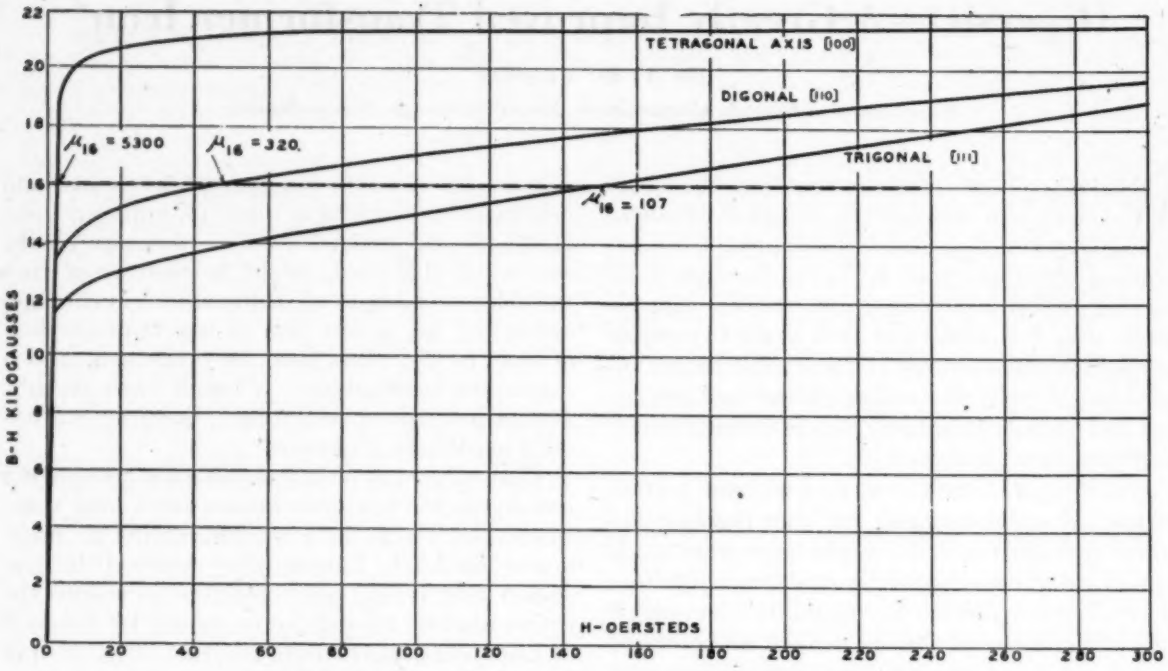


FIG. 3. Effect of grain orientation on the magnetic properties of iron.

directions, as shown in Fig. 3 for iron,[2] and Fig. 4 for silicon iron.[3] If the alloy could be treated in such a way that all or most of the crystal grains could be oriented with their cube edges, [100], parallel to the direction in which the finished material is to be magnetized, then a much higher flux density could be obtained than with randomly oriented grains for the same exciting current (or magnetizing force). Work along this line has been carried on in various laboratories during the past 15 years, and successful processes have been developed for producing strip of any thickness having crystals with the cube edge parallel to the rolling direction.[4]

Thirdly, as it is generally conceded that aging, i.e. change in properties, particularly increases in hysteresis loss at operating temperatures, is caused by precipitation of impurities from a super-saturated solid solution, it follows that aging can be eliminated by reducing the impurities to the solubility limit at room temperatures. This naturally goes hand in hand with the process for reducing the hysteresis loss, so that, if the hysteresis loss is sufficiently reduced by eliminating the impurities to a very low value, there should be no aging effect. This point has been definitely established.

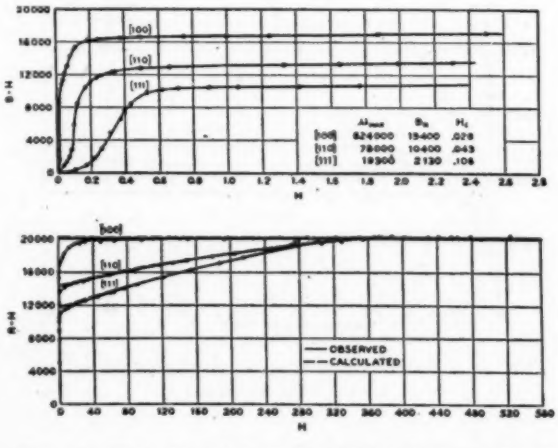


FIG. 4. The observed and calculated magnetization curves for the (100), (110) and (111) directions of single crystals of 3.85 percent silicon-iron.

[2] K. Honda and S. Kaya, Sci. Reports, Tohoku Imp. Univ. **15**, 721 (1926). W. E. Ruder, Trans. A.S.S.T. **23**, 8 (1925).

[3] H. J. Williams, Phys. Rev. **52**, 747 (1937).

[4] N. P. Goss, Trans. A.S.M. **23**, 1107 (1935). U.S. Patents 1,965,559, July 3, 1934; 2,084,336, June 22, 1937; 2,084,337, June 22, 1937; assigned to the Cold Metal Process Company; K. J. Sixtus, Physics **6**, 105 (1935); R. M. Bozorth, Trans. A.S.M. **23**, 1107 (1935); F. Bitter U.S. Patent 2,046,717, July 7, 1936. Assigned to W. E. and M. Company; G. H. Cole and R. L. Davison, U.S. Patent 2,158,065, May 16, 1939; V. W. Carpenter, U.S. Patent, 2,236,519, April 1, 1941; V. W. Carpenter, U.S. Patent, 2,287,466, June 23, 1942; V. W. Carpenter and John M. Jackson, U.S. Patent 2,287,467, June 23, 1942. The last four patents are assigned to the American Rolling Mill Company.

Lastly, magnetostriction, i.e., change in dimensions on magnetization, produces vibration in the core, and as 60-cycle current results in 120 vibrations per second for the fundamental flux and double frequencies for each of the upper harmonics, all transformers emit more or less noise, depending on the amount of magnetostriction in the core material. As magnetostriction is a function of domain orientation, it so happens that the treatment that has been developed for the production of low hysteresis loss and preferred orientation also results in lowered magnetostriction.

Hipersil is the name that we have applied to a silicon-iron alloy in which all the above desirable properties, i.e. low impurities, large grain size, and crystal orientation, have been combined, and is therefore an ideal transformer material. The alloy, containing from 3 to 4 percent Si, after hot rolling to a thickness of 2 to 3 mm (about 0.1″) is put through a combination rolling and heat treating process that produces a maximum of preferred lattice orientation resulting in a flux density in the rolling direction for operating magnetizing forces that is from 20 to 30 percent higher than that of the best standard silicon-iron sheet. The annealing process removes the impurities, of which the most important are oxygen,

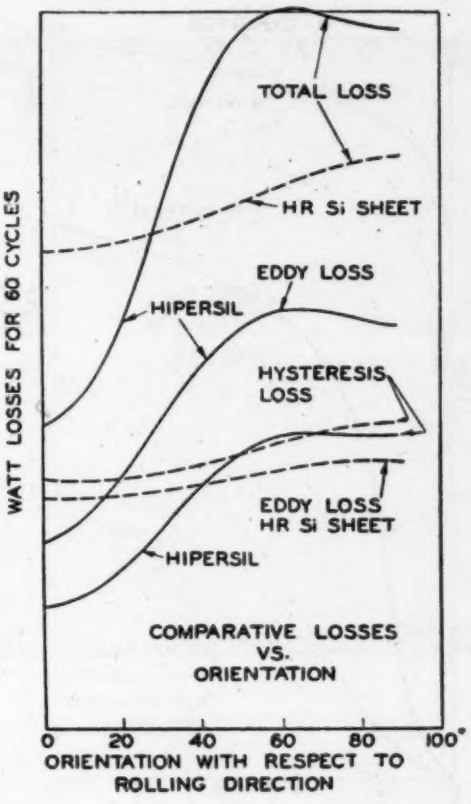


FIG. 6.

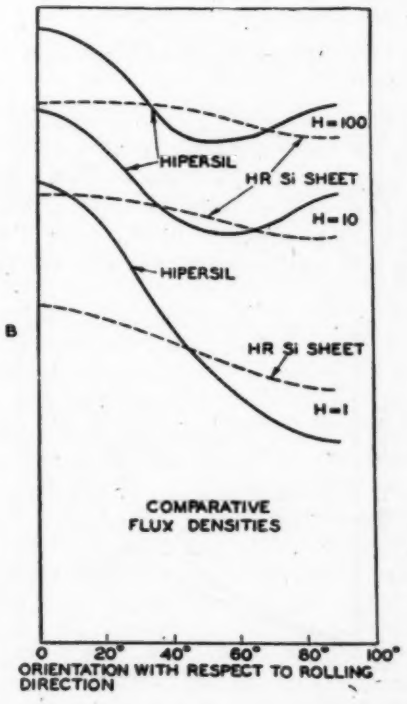


FIG. 5.

carbon, and sulphur, down to a few thousandths of a percent and at the same time produces grain growth and the preferred grain orientation.

Transformers with this material were built some nine years ago, and have been in constant service; but it is only during the past four years that manufacturing processes, both for the manufacture of Hipersil and for the construction of the transformers, have been perfected to the point where large scale applications have been possible. This development is the result of close cooperation first between the Research and Development Departments of the American Rolling Mill Company and Westinghouse Electric Corporation and then between the operating departments of these two companies.

One feature in this development that merits particular mention is the construction of the core. It is obvious that, because of the preferred crystal orientation of Hipersil, it must be used in such a way that the flux will be generated in the direction of rolling in order that any benefit can be derived from its use. This means that the core must be built in one of two possible ways:

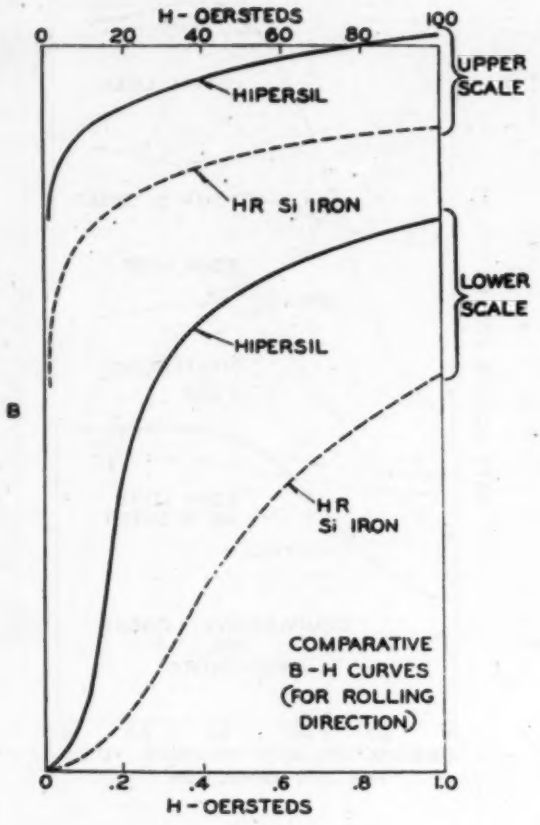


FIG. 7.

(1) either it must be built with plates sheared so that the direction of the flux throughout the core will be parallel to the rolling direction, or (2) the core must be wound up like a clockspring.

Large transformers are still built in accordance with a modification of the first scheme, which has been orthodox for many years, overlapping the joints at the corners. For smaller (distribution) transformers L-shaped punchings were previously used, and these were punched from sheets or strips at an angle of 30 to 45° depending on the ratio of the length of the two legs. This practice saved material and labor, eliminated half of the joints and enabled the engineers to take advantage of the fact that the rolling technique, current at the time, produced a sheet in which the high density permeability was somewhat higher at 45° than parallel to the rolling direction. The joints, of course, were staggered.

With Hipersil such a scheme obviously cannot be used; it would result in the worst possible magnetic properties. Consequently wound cores have been resorted to. To make these, one company has developed an ingenious process for threading the strip through the completed primary and secondary windings, resulting in a circular core. Another company has developed a scheme for winding the copper coils on to the finished cores. The Westinghouse Transformer Department, on the other hand, has developed and perfected another process that appears to have several obvious advantages. The cores and coils are completed separately in accordance with optimum designs as to size and shape (usually rectangular). After

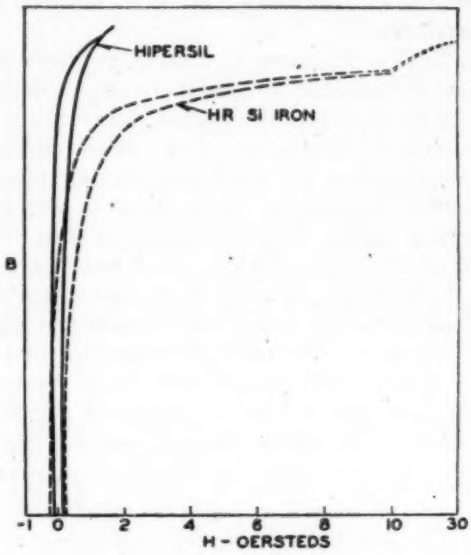


FIG. 8. Comparative hysteresis loops.

being "strain annealed" so as to remove winding strains, the cores are impregnated with an insulating compound so as to make them solid, then cut in two, the sections ground, polished and etched so as to make as nearly perfect joints as possible and finally assembled with the coils into

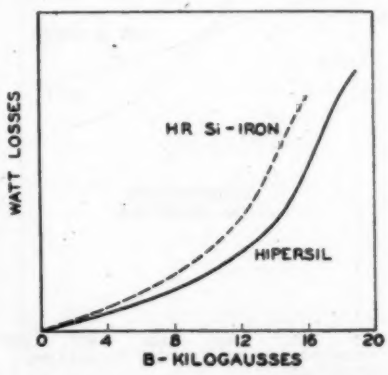


FIG. 9. Comparative core losses for 60 cycles (in rolling direction).

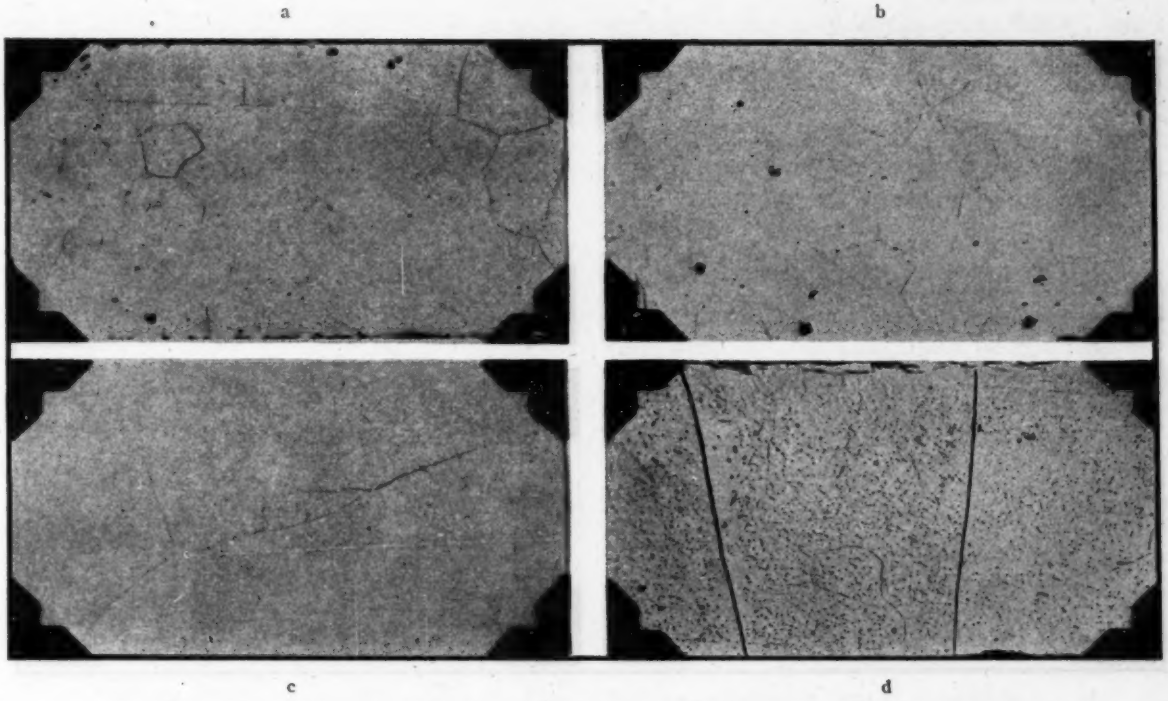


FIG. 10a. (100×) Commercial 3.5 percent H.R. Si-iron. mill annealed, slowly cooled. Not aged. Hysteresis loss—1400 ergs.
FIG. 10b. (100×) Same. Aged 600 hrs. at 100°C. Hysteresis loss—1420 ergs. ∴ No aging.
FIG. 10c. (100×) Same. Reannealed at 1200°C to redissolve impurities. Cooled 100°C per hour. Not aged. Hysteresis loss—480 ergs.
FIG. 10d. (100×) Same. Aged 600 hrs. at 100°C. Hysteresis loss—730 ergs. ∴ 50 percent aging.

a completed transformer. The joints thus made are equivalent to airgaps of the order of a fraction of a mil (i.e., less than 0.001″) in length. This results in simplicity of construction, minimum of volume, maximum of efficiency, and ease of repairs in case of accidents.

The magnetic properties of Hipersil are shown in Figs. 5 and 6 as functions of orientation with respect to the rolling direction. The fact that the lowest permeabilities and highest losses for high flux densities do not occur at 90° can be explained on the basis, supported by experimental evidence, that the grains are largely oriented with a cube edge, [100] axis, parallel to the rolling direction, but with a face diagonal, [110], at right angles to the rolling direction in the plane of the strip. This makes the 55° direction parallel to a body diagonal, [111] axis, which is the direction of most difficult magnetization (see Fig. 4).[5]

The eddy loss also varies with orientation and the total loss curves are of the same general shape as the hysteresis loss curves, as shown in Fig. 6.

In Figs. 7 and 8 are shown *B-H* curves and hysteresis loops, respectively, for a typical Hipersil sample in comparison with ordinary hot rolled silicon iron, both cut parallel to rolling direction. As transformers are usually operated with exciting currents corresponding to a magnetizing force of 10 to 20 oersteds, Fig. 7 shows that Hipersil can be operated at a flux density of 20 to 30 percent higher than is practical with hot rolled sheet. This means a decrease in core cross section of 20 to 30 percent, and Fig. 9 shows that this can be done with about the same total core loss at the higher induction as is possible with hot rolled sheet at the lower induction. The importance of this improvement is obvious to electrical engineers.

One of the advantages of silicon-iron is that it supposedly does not age. However, this depends largely on the kind of heat treatment it has been subjected to. With a carbon content of 0.01 to 0.02 percent all silicon-iron alloys may age, if cooled at the rate of 50° to 100°C per hour from the annealing temperature. An increase in

[5] Another interpretation of the x-ray evidence is that at right angles to the rolling direction the grains are more or less randomly oriented; but the relative effect on the magnetic properties would be about the same in the two cases.

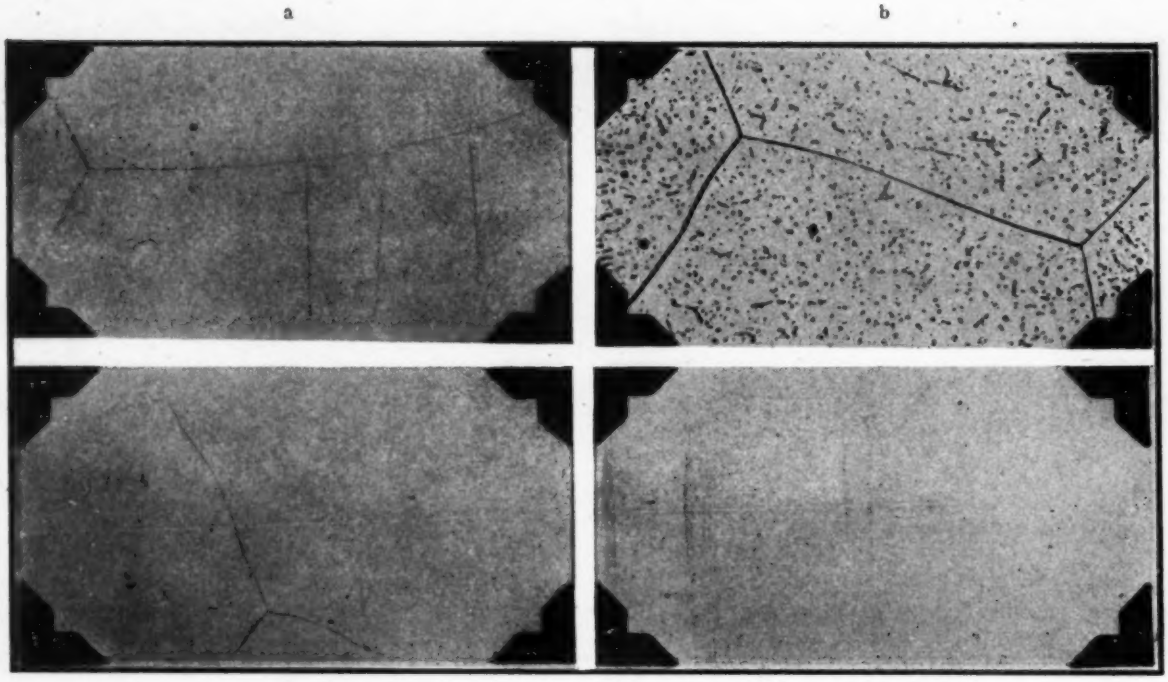


FIG. 11a. (×300) 3.25 percent Hipersil base. Annealed in cont. furnace at 1100°C. Not aged. Hysteresis loss—630 ergs. 0.007 percent C.
FIG. 11b. (×300) Same. Aged 600 hrs. at 100°C. Hysteresis loss—1350 ergs. ∴ 115 percent aging.
FIG. 11c. (×300) 3.25 percent Hipersil base annealed in cont. furnace at 1100°C. Reannealed at 1200°C to eliminate impurities. Not aged. Hysteresis loss—365 ergs 0.004 percent C.
FIG. 11d. (×300) Same. Aged 600 hrs. at 100°C. Hysteresis loss—375 ergs. ∴ No aging.

hysteresis loss of 100 percent or more is often obtained on subsequent heating for several hundred hours at 100°C. This is probably caused, as previously stated, by precipitation of carbon in the form of colloidal particles of iron carbide from the super-saturated solid solution, as the solubility limit of carbon in $\alpha$-iron at 100°C is of the order of only 0.001 percent. Our present hypothesis postulates that these colloidal particles of carbide produce a distortion of the crystal lattice surrounding them that causes this increase in hysteresis loss. In the ordinary process of annealing silicon-iron sheet, the cooling rate is so low that the carbon is given a chance to precipitate during the cooling period under conditions that prevent the strains that are produced when the precipitation takes place at 100°C.

Figure 10 shows photomicrographs before and after aging at 100°C of a 3.5-percent hot rolled silicon iron alloy: 10-a and b after annealing in the ordinary way, i.e., after very slow cooling; 10-c and d after reannealing to redissolve and partly remove impurities, followed by fairly rapid cooling (about 100°C per hour).[6] After the first aging treatment (Fig. 10-b), there is no visible precipitate and no appreciable increase in hysteresis loss, while after the latter (Fig. 10-d) the grains are full of minute spots and the hysteresis loss has increased by over 50 percent. We interpret these spots as being caused by strains surrounding the colloidal particles rather than representing the particles themselves. Similar phenomena are found for all silicon contents, although to a lesser degree for 4 percent Si than for lower silicon contents. The spots and the accompanying increase in hysteresis loss can be largely eliminated by reannealing at a low temperature (500° to 700°C) for several hours, the explanation being that such a treatment, while it may to some extent further remove impurities, eliminates the aging largely by eliminating the strains in the lattice surrounding the precipitates.

[6] These photomicrographs were obtained by Miss Mildred Fergusion, of the Westinghouse Research Laboratories using a special technique to bring out the spots caused by aging.

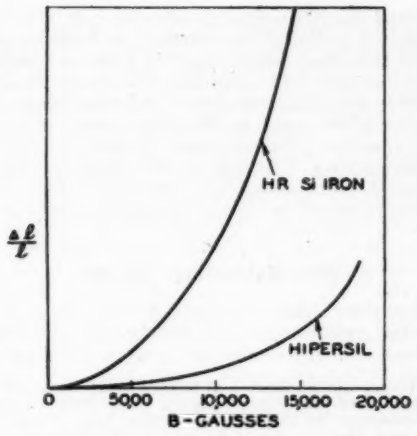


FIG. 12. Comparative magnetostriction.

Another and surer way of eliminating the effect of aging, as already stated, is to reduce the impurities to the solubility limit at 100°C, which can be done by the special annealing process already referred to. This is accompanied by a greatly decreased hysteresis loss, so that this treatment serves a double purpose.

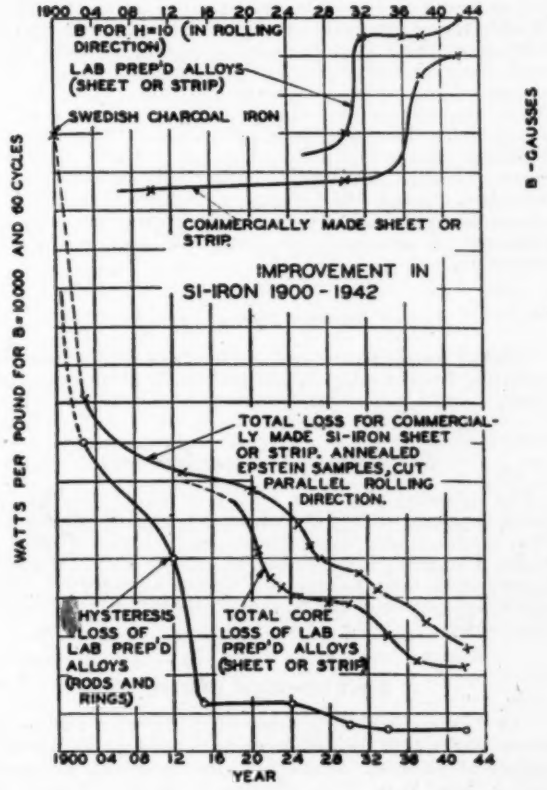
1900 04 08 12 16 20 24 28 32 36 40 44
B FOR H=10 (IN ROLLING DIRECTION)
LAB PREP'D ALLOYS (SHEET OR STRIP)
SWEDISH CHARCOAL IRON
COMMERCIALLY MADE SHEET OR STRIP
IMPROVEMENT IN SI-IRON 1900 - 1942
TOTAL LOSS FOR COMMERCIALLY MADE SI-IRON SHEET OR STRIP, ANNEALED EPSTEIN SAMPLES, CUT PARALLEL ROLLING DIRECTION.
HYSTERESIS LOSS OF LAB PREP'D ALLOYS (RODS AND RINGS)
TOTAL CORE LOSS OF LAB PREP'D ALLOYS (SHEET OR STRIP)
WATTS PER POUND FOR B=10,000 AND 60 CYCLES
B-GAUSSES
YEAR

FIG. 13.

In the case of Hipersil the aging situation is the same as for ordinary silicon-iron. As ordinarily made the finished strip may contain 0.01 to 0.02 percent carbon. When annealed at a high temperature in a continuous furnace in which the cooling rate is very high, the carbon content may drop to less than 0.01 percent and the hysteresis loss to 6–700 ergs for $B=10{,}000$ (Fig. 11-a), but aging may increase this by over 100 percent and is accompanied by a precipitate as shown in Fig. 11-b. When reannealed at 500 to 700°C the hysteresis loss may return to the original value and the spots disappear. But a far more beneficial effect is obtained by the special purifying annealing process whereby a very low hysteresis loss is obtainable and all aging effects are eliminated, as shown in Fig. 11-c and d. The ultimate magnetic properties are then, as shown in Figs. 7, 8, and 9.

It is a very fortunate circumstance, as has already been stated, that the same heat treatment that produces low losses and eliminates aging, also decreases magnetostriction to such an extent that noise ceases to be a serious problem. Figure 12 shows magnetostriction curves for Hipersil, as compared with standard hot rolled sheet.

## SUMMARY

Hipersil is a silicon-iron alloy that, by a combination of hot and cold rolling processes, followed by a refining annealing process has reached such superior magnetic properties, as to cause just as great improvements in present day transformer iron as were obtained at the time of the introduction of silicon-iron. The 1905 4 percent silicon-iron cut losses roughly in two; subsequent improvements again cut losses in two. Hipersil has now cut the losses to one-half once again, making them $\frac{1}{4}$ of those of Hadfield's alloy and with ten times the maximum permeability. Figure 13 shows graphically the development from 1900 to the present time.

# Here and There

### New Appointments

Donald E. Stearns has been appointed Professor of Civil Engineering and Chairman of the Department of Civil Engineering in the College of Applied Science, Syracuse University, Syracuse, New York. In recent years he has been associated with the firm of Fay, Spofford and Thorndike, consulting engineers, Boston, Massachusetts, as engineer in the Sanitary Division.

David Gordon, recently chief engineer for the Interchemical Corporation, has joined the staff of Foster D. Snell, Inc., as director of engineering. He will have complete responsibility for all engineering projects and serve as consulting engineer.

Arthur H. Compton, chairman of the department of physics, University of Chicago, has been named chancellor of Washington University, St. Louis, Missouri, to succeed George R. Throop, who retired in June 1944.

Frank Hovorka, professor of chemistry, Western Reserve University, has been appointed acting head of the university's department of physics, succeeding Dr. Harry W. Mountcastle, who has retired after 38 years of service with Western Reserve.

### Lincoln Foundation Awards

A 12-page brochure, covering the object and purpose of the Award Program for Textbooks in Modern Design and setting forth all rules and conditions governing the program, has been published by trustees of The James F. Lincoln Arc Welding Fountlation, Cleveland 1, Ohio. The brochure is the official document of the Award Program announced by the Foundation in April to encourage preparation of textbooks on design for use of engineering undergraduates in machine design and in structural design for fabrication by all processes including welding. It covers thoroughly the types of subject matter to be treated in these fields, listing the awards which are divided into the two classes and which total $20,000. It carries explanatory paragraphs on royalties for manuscripts of award-winning authors, method of payment of awards, eligibility requirements, bases of judgment in rating papers, how to present subject matter, and other pertinent facts designed to assist prospective participants. The brochure may be obtained gratis by anyone interested. Address requests to the Secretary of the Foundation.

### Electron Optics Fellowships

The Westinghouse Educational Foundation has provided three fellowships in electron optics at The Ohio State University—one post-doctoral fellowship with a stipend of $3000 per year and two pre-doctoral fellowships with stipends of $1000 per year. These fellowships are open to graduates in physics, mathematics, and electrical engineering. Application forms may be obtained from the Dean of the Graduate School of The Ohio State University, Columbus, Ohio.

### American Society for Testing Materials

The regular annual meeting of the American Society for Testing Materials, scheduled for Buffalo, New York, June 18–22, has been cancelled because of the transportation situation. Instead a business session or sessions will be held probably the last week in June in New York City. The Society will proceed with the printing of its technical papers that would normally have been presented, and these will be distributed to the members as is customary. The Society's technical committees are holding meetings at various times and places, and its work on specifications and tests for materials continues intensively. The Society is extending its standardization activities in the field of ultimate consumer goods and is appointing a new administrative committee to direct this. Another phase of work to be undertaken is "the study, development, and standardization of methods of tests of materials, parts, and assemblies, in actual or simulated service conditions."

### New Meteorology Journal

The American Meteorological Society has initiated a new quarterly publication entitled *Journal of Meteorology*. The table of contents of the first issue is as follows:

**On the Theory of Cyclones**—J. Bjerknes and J. Holmboe
**Determination of the Normal Regions of Heating and Cooling in the Atmosphere by Means of Aerological Data**—Harry Wexler
**Temperature Changes during Formation and Dissipation of West Coast Stratus**—Morris Neiburger
**The Recurvature of Tropical Storms**—H. Riehl and R. J. Shafer

### Research Index

Research data of immense importance, much of which is buried in the many departments of the technical schools and universities, is now being unearthed for the first time. Master theses are being made available to industry. Information which is not easily accessible is being made available in carefully indexed form. Through the cooperation of the leading technical schools and universities, Master theses that are of importance to industry and research will be indexed in the technical *Digest-Index* issued by The National Research Bureau, Inc., 415 North Dearborn Street, Chicago 10, Illinois. They will be supplied on microfilm through the Library of Industrial Research, a non-profit organization acting as a clearing house for the exchange of technical, scientific, and management information.

### Einstein Retirement

Albert Einstein has retired and has been named professor emeritus, Institute for Advanced Study, Princeton, New Jersey.

### New National Academy Members

The following physicists have been elected to the National Academy of Sciences: Enrico Fermi, E. P. Wigner, Otto Stern. Among the engineers elected were Mervin J. Kelly, Executive Vice President of the Bell Telephone Laboratories, and George W. Lewis, Director of Aeronautical Research of the National Advisory Committee on Aeronautics.

### Electrochemical Officers

The Electrochemical Society, Inc., elected the following officers at its 44th Annual Meeting: President, William R. Veazey of Midland, Michigan; Vice President, James A. Lee of New York City; Treasurer, W. W. Winship of New York City; Secretary, Colin G. Fink of New York City.

### Honorary Degree

Dr. John T. Tate received the honorary degree of Doctor of Science at Case School of Applied Science on April 22. He delivered the commencement address entitled "The Role of Science in Society."

### New Buildings at Bell Telephone Laboratories

As soon as war restrictions permit, the facilities of Bell Telephone Laboratories at Murray Hill, New Jersey, will be greatly augmented, according to an announcement by Dr. Oliver E. Buckley, president of the Laboratories. The proposed addition is approximately the same size as the initial buildings, which were opened in 1941 and cost more than $2,000,000. The new building will extend the lines of the present one about five hundred feet in a northeasterly direction. Old and new buildings will be joined by a bridge with a sheltered bus terminal beneath. The accompanying picture shows the architects' sketch of the complete building group with roadways and tree-shaded parking areas.

Since the present building was opened in the fall of 1941, about one hundred groups from varied industries, Government departments, and some from abroad have come to study its new features. The unique requirement of a laboratory is that it must be designed for change. Prominent among new features which visitors come to see are the quickly movable partitions and the ease with which wires, cables, and pipes may be installed or removed and yet concealed from view.

There are no permanent partitions in the buildings except those around the stair wells and elevator shafts. All others are built of easily movable metal panels. The outside surfaces of these units are sheet steel and they are separated by a three-inch space which is packed with rock wool to prevent the transmission of sound and heat. Doors and transoms are made in one unit which can be interchanged with a partition in any part of the buildings. Along the outside wall of the buildings there is sheet steel wainscoting under the windows and up the piers between them. This is the same in appearance as the partition panels. The wainscoting is removable without special tools to give access to service pipes and wiring which are installed behind it. Similar wainscoting is applied around interior columns.

At intervals, small wings jut out from the main building providing well-lighted offices for physicists, chemists, and engineers conveniently close to their laboratories. Shops, library, medical department, and restaurant all fit into the pleasing functional pattern. The fields and woods, courtyards, and shaded lawns all tend to make it a pleasant place in which to work.

People are all important to an institution whose products are discovery, invention, and design—creations of the intellect. In choosing this two-hundred acre site the Bell Telephone Laboratories management sought a pleasant and healthful countryside in the midst of desirable home communities which spread over a wide area in towns along the Orange Mountain Range and the adjoining valleys. There is no intention of creating a company community in the immediate vicinity of the buildings. Murray Hill is about twenty-five miles from the New York headquarters.

The executive offices of Bell Telephone Laboratories will continue to be at 463 West Street, New York City and a majority of the employees will continue to work there. With the addition at Murray Hill, however, about two thousand employees will work at the new location compared with more than one thousand employed there during the war. This will include all of the research work, and most of the work of apparatus development.

Though designed for peace-time use, the present new laboratory opened just as war was breaking and its new and adaptable space proved to be a great aid to Bell Laboratories' war service. Within its walls scores of war projects have been started, some small and completed quickly, others large and expanding from a room to whole sections of the building. The completion of the Murray Hill building project will find Bell Telephone Laboratories well equipped to design better and more economical telephone and radio equipment for the Bell Telephone System. It will also be ready and equipped to continue its record of achievement in developments for the Army and Navy as they may have need for its services in the future.

# Letter to the Editor

## Adaptation of Special Specimen Holders to Commercial Electron Microscopes

L. MARTON
*Division of Electron Optics, Stanford University, California*
May 4, 1945

SEVERAL inquiries came to this laboratory concerning the use in commercial electron microscopes of the specimen holder described in an earlier issue of this journal.[1] The specimen holder can be very easily adapted to such instruments by transforming the "cartridge" or other support into a kind of tongs. This adaptation can be described by using the cartridges of the RCA Type B instruments as examples. Figure 1 represents the general

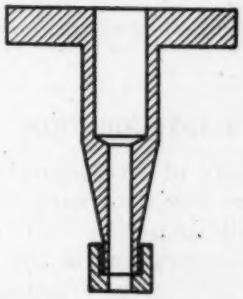

FIG. 1. "Cartridge" of RCA Type B microscopes.

appearance of the cartridge as supplied with these instruments. For the special specimen holders of the Stanford instrument, a similar cartridge can be made (Fig. 2) by

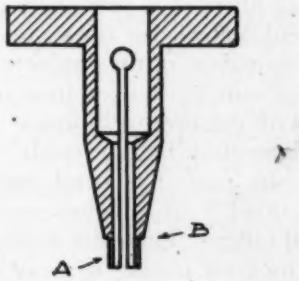


FIG. 2. Modified "cartridge" to serve as tongs for specimen holder.

omitting the cap normally holding the wire screen, and splitting the body of the cartridge. First the lower end of the cartridge, marked *A*, is turned to the inside diameter of the eyelet in which the screen is mounted. The surface of this turned part should not be too finely polished so that a certain degree of surface roughness helps to hold the eyelet from the inside. After turning to the right diameter, the cartridge is split as indicated on Fig. 2, and slightly spread. The shoulder, *B*, provides the fixed depth to which the tongs can be inserted into the eyelet. By varying the length of the cartridge, the same type of operation at different magnifications can be achieved as indicated, for instance, by Burton, Barnes, and Rochow.[2]

[1] L. Marton, J. App. Phys. 16, 134 (1945).
[2] C. J. Burton, R. B. Barnes, and T. G. Rochow, Ind. Eng. Chem. 34, 1429 (1942).

# Contributed Original Research

## A Comparison of Some Elastic Properties of Tire Cords

HELMUT WAKEHAM, EDITH HONOLD, AND EVALD L. SKAU
*Southern Regional Research Laboratory, New Orleans, Louisiana*[1]

(Received January 25, 1945)

Additional information concerning the elastic properties of tire cords is needed since the present criteria involving breaking strength and elongation are considered insufficient to enable prediction of tire cord performance. The elastic behavior of Nylon, of rayon, and of unstretched and stretched cotton tire cords are compared with respect to their rates of elongation during measurement of the stress-strain curves and their elongation under static loads at various temperatures between 25° and 200°C. Elongations under the influence of cyclic loads are shown for cotton and rayon cords, and an apparatus for determining mechanical hysteresis of tire cords during cyclic loading is described. The temperature and moisture content of the cord are shown to have considerable effect upon its elastic properties.

### I. INTRODUCTION

THE necessity of satisfactory correlation of laboratory test data with the service behavior of textile materials such as tire cords confronts the investigator in this field all too frequently, in view of the enormous amount of fundamental and theoretical work which has been done on the mechanical properties of fibers and yarns. The fund of information available does not yet permit successful prediction of the physical properties of such a combination of filaments or fibers as is present in a tire cord. In fact, present knowledge does not even allow a complete statement of the characteristics desired in an "ideal" tire cord, even if such a cord could be made with existing techniques.

This failure may be due to the overemphasis which, in the past, has been placed upon the "breaking load"[2] in judging serviceability of mechanical fabrics. There are evidences that the trend in tire cord testing is away from the sole dependence upon tensile tests to the view that no one laboratory test, or even three, will satisfactorily predict tire cord behavior in the tire. Careful investigations of additional tire cord properties should aid, therefore, in obtaining a more useful set of requirements for a good cord.

In the present work, some elastic properties of four commercial and five experimental cotton tire cords were compared over a wide range of loads, temperatures, etc., to show how these properties might be expected to change under varying conditions. The results reported here are preliminary in the sense that considerably more study will be required to investigate completely each factor involved. For this reason, no attempt is made to interpret all the phenomena described in terms of the known fundamental elastic characteristics of these textile materials. Some of the experiments mentioned are, furthermore, being extended and are here reported only to indicate the nature of the characteristic being investigated. They will be discussed in greater detail in a later paper.

### II. PREVIOUS WORK

The elastic properties of tire fabrics or cords were investigated in the pioneering researches of King and Truesdale,[3] of Gurney and Davis,[4] and of Stavely and Shepard.[5] These workers all agreed that breaking strength and ultimate elongation are not sufficient information for proper evaluation of a tire cord, and that elasticity under repeated stressing is an important characteristic of cords used in tire service. The method by which this property was

[1] This is one of the laboratories of the Bureau of Agricultural and Industrial Chemistry, Agricultural Research Administration, U. S. Department of Agriculture.

[2] The term "breaking load" (frequently referred to incorrectly as "tensile strength") as used in this paper refers to the maximum load developed in a tension test carried to rupture. The values herein reported were obtained with a Scott pendulum-type cord tester and do not take into account the gage of the cord.

[3] F. C. W. King and R. Truesdale, Text. Recor. **41**, 41, 88 (April); 86, 99 (June) and 103 (July 1923).

[4] H. P. Gurney and E. H. Davis, Text. World **68**, 219 (1925).

[5] F. W. Stavely and N. A. Shepard, Ind. Eng. Chem. **19**, 296 (1927).

TABLE I. Physical properties of tire cord samples.

| Identification of cords | | Group A—Commercial tire cords 1 Nylon | 2 Rayon | 3 Ordinary cotton | 4 Mercerized cotton[a] | Group B—Experimental cotton tire cords 1 Unstretched | 2 Stretched | 3 Unstretched | 4 Stretched | 5 "Dual-stretched" |
|---|---|---|---|---|---|---|---|---|---|---|
| Gage | | 0.016 | 0.023 | 0.033 | 0.028 | 0.028 | 0.027 | 0.035 | 0.031 | 0.033 |
| Construction[b] | | 210/4/2 | 1100/2 | 18.3/4/3 | 11/3/2 | 22.75/4/3 | 22.75/4/3 | 17/4/3 | 17/4/3 | 17/4/3 |
| Cord number (Hanks/lb.) | | 2.86 | 2.18 | 1.26 | 1.52 | 1.56 | 1.65 | 1.16 | 1.23 | 1.19 |
| Twists per inch | Cord | 10 "s" | 11.5 "s" | 10.0 "s" | 10.4 "z"[c] | 10.5 "s" | 10.0 "s" | 10.4 "s" | 10.2 "s" | 10.1 "s" |
| | Ply | 0 | 10.7 "z" | 18.7 "z" | 22.0 "s" | 26.7 "z" | 25.7 "z" | 20.6 "z" | 20.1 "z" | 19.3 "z" |
| | Single | 0 | —— | 12.1 "z" | 7.8 "z" | 10.8 "z" | 11.6 "z" | 10.0 "z" | 9.7 "z" | 10.5 "z" |
| Test under standard conditions | Breaking load in lbs. | 25.2 | 14.2 | 19.2 | 19.0 | 17.9 | 19.1 | 23.4 | 24.7 | 26.2 |
| | Percent elongation at break | 12.4 | 9.8 | 10.8 | 8.0 | 9.0 | 6.0 | 14.7 | 6.2 | 9.6 |
| | Moisture content, % of dry weight | 22.0 | 16.6 | 20.0 | 10.8 | 13.4 | 9.3 | 21.8 | 11.8 | 14.3 |
| | | 4.0 | 14.5 | 7.8 | 9.4 | 8.2 | 8.0 | 7.9 | 8.3 | 8.4 |
| Bone dry test | Breaking load in lbs. | 25.4 | 18.0 | 17.7 | 19.1 | 15.9 | 17.9 | 18.5 | 22.0 | 24.2 |
| | Percent elongation at break | 11.8 | 4.5 | 6.0 | 4.8 | 7.3 | 5.9 | 10.4 | 6.0 | 11.1 |
| | | 22.0 | 10.8 | 8.7 | 7.1 | 10.3 | 8.2 | 15.4 | 9.4 | 15.7 |
| Hot break, 130°C. | Breaking load in lbs. | — | 13.5 | 12.6 | 11.8 | 10.9 | 13.0 | 13.7 | 15.7 | 16.1 |
| | Percent elongation at break | — | 8.0 | 6.5 | 5.7 | 7.8 | 5.6 | 9.9 | 4.8 | 10.0 |
| | | — | 11.0 | 7.5 | 6.1 | 8.0 | 6.6 | 12.1 | 7.0 | 12.9 |

[a] This mercerized cord was manufactured and treated by commercial methods and equipment but has not been used in other than experimental or test tires to the knowledge of the authors.
[b] The first figure represents size of single yarns (denier for Nylon and rayon and yarn number for cotton); the second figure represents number of single yarns per ply; and the third figure represents number of plies in the cord.
[c] Note that the twist of the mercerized cord differed from that of the other cotton cords.

tested, however, varied; some investigators used flexing machines, whereas others simply measured elongations as loads were applied or removed at regular intervals.

Gurney and Davis[6] followed this preliminary work with a more fundamental study of the elastic properties of tire cords. They called attention to the work of Barratt,[7] who showed that cotton fibers after being stretched do not recover completely, and pointed out that the elastic properties of a tire cord are necessarily conditioned by the elastic properties of the fiber. They demonstrated, however, that cotton cords with high and low twists have different elongations and different degrees of recovery, proving that the elastic properties of cords depend, at least to some extent, upon the cord construction.

Midgley and Peirce,[8] in studying the influence of the time factor on the breaking load of yarns and fibers, found that although the apparent "tensile strength" varied with the rate of loading, the ultimate elongation observed was about the same in each case. This indicated the possibility of a flow phenomenon, which was more thoroughly investigated by Smith and Eisenschitz[9] for the case of rayon filaments. They found that the rate of elongation with respect to time for a static load increases rapidly with increasing temperature. Recently, this subject has received further attention by Press[10] and by Leaderman.[11]

Practically no data are available in the literature on the effect of temperature on the elastic properties of tire cords. Busse and coworkers[12] reported the "growth" of tire cords at various temperatures and loads. Loaded cotton and Nylon cords under conditions of negligible creep were found to contract when the temperature was raised, analogous to the effect observed with rubber and other high polymers. The breaking loads of cotton and rayon tire cords were shown to decrease at 350°F by about 35 percent and 20 percent, respectively, of their normal values. But this work was limited in scope, and a direct comparison between cords of different types was not made.[12a]

Although an enormous amount of research has been done on the fundamental characteristics of high polymeric fibers and yarns, mostly at

[6] H. P. Gurney and E. H. Davis, J. Text. Inst. **21**, T463 (1930).
[7] T. Barratt, J. Text. Inst. **13**, T17 (1922).
[8] E. Midgley and F. T. Peirce, J. Text. Inst. **17**, T330 (1926).
[9] H. D. W. Smith and R. Eisenschitz, J. Text Inst. **22**, T170 (1931).
[10] J. J. Press, J. App. Phys. **14**, 224 (1943).
[11] H. Leaderman, *Elastic and Creep Properties of Filamentous Materials and Other High Polymers*, The Textile Foundation, Washington, D. C. (1943).
[12] W. F. Busse, E. T. Lessig, D. L. Loughborough and L. Larrick, J. App. Phys. **13**, 715 (1942).
[12a] In a paper which appeared after the manuscript for this article was submitted, J. H. Dillon and I. B. Prettyman, J. App. Phys. **16**, 159 (1945), report an interesting comparison of the breaking loads, elongations, and creep characteristics of tire cords at various temperatures and humidities.

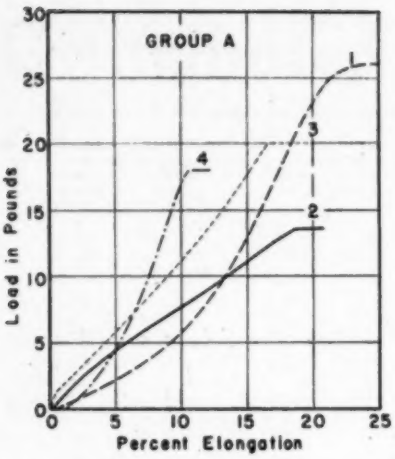


FIG. 1a. Tensilgrams for tire cords. Group A. Commercial tire cords: 1. Nylon; 2. rayon; 3. ordinary cotton; 4. mercerized cotton. For further data on these cords see Table I.

room temperature,[13] much work remains to be done on the effect of temperature on the elastic properties of tire cords, especially in view of the higher temperatures generated in service by synthetic rubber tires.

### III. EXPERIMENTAL

The cords tested were chosen for their differences in the properties ordinarily measured. A compilation of these characteristics is shown in Table I. These data, with the exception of results of "bone-dry" tests and "hot breaks," were obtained on the cords under the ASTM standard testing conditions of 70°F and 65 percent relative humidity.[14] Breaking loads under bone-dry conditions were determined in the manner commonly employed by commercial testing laboratories.[15] The hot breaks are breaking load values obtained in a special chamber mounted on the tester[12] and maintained at such a temperature that the cord is at approximately 130°C. These high temperature values give some indication of the loss in strength to be expected when the cord is hot. Such values could not be obtained with this equipment on the Nylon cord because of its high elongation.

The experimental tire cords in group B were made in this laboratory as part of the research program on cotton cords. The cotton used was of the Wilds-13 variety (1942 crop) with a staple length of $1\frac{5}{16}$ inches. The treatments indicated in Table I were given to the cords for the purpose of increasing breaking strength and controlling elongations at 10-pound loads rather than to vary the properties discussed below. The "dual-stretched" cord (B5) was treated by a process described by Philipp and Conrad[16] for producing a stretched cotton cord with high strength and a relatively high elongation.

In the experiments described below, the cords and the apparatus used were kept in a room at constant conditions so that the cord samples were exposed to the same atmosphere. A temperature of 25°C and a relative humidity of 65 percent were chosen rather than some others because of the ease with which these conditions can be reproduced. The recent histories of the cords were thus more comparable than they might have been had each sample been subjected to some individual conditioning treatment immediately before testing. Since it is quite possible that the moisture content of the tire cord in actual use may vary over a considerable range, no attempt was made in these experiments to control the moisture in the cord other than to

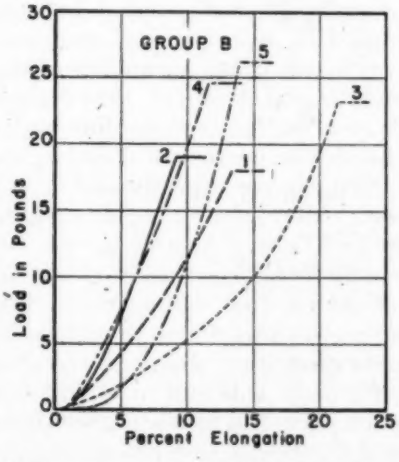


FIG. 1b. Tensilgrams for Tire Cords. Group B. Experimental cotton cords: 1. 22.75/4/3 construction, unstretched; 2. 22.75/4/3 construction, stretched; 3. 17/4/3 construction, unstretched; 4. 17/4/3 construction, stretched; 5. 17/4/3 construction, dual-stretched. For further data on these cords see Table I.

[13] For summaries of this work, the reader is referred to the reviews to be found in Section 10 of E. Ott's *Cellulose and Cellulose Derivatives*, Vol. V of High Polymers (Interscience Publishers, Inc., New York, 1943) and in R. Houwink's *Elasticity, Plasticity and Structure of Matter* (Cambridge University Press, London, 1940). Excellent bibliographies may also be found in the publications of Press (reference 10) and Leaderman (reference 11).

[14] A.S.T.M. Standards, Part III, D179–42, p. 625 (1942).

[15] For a fairly complete discussion of the bone-dry technique used, see G. B. Haven's *Mechanical Fabrics* (John Wiley and Sons, Inc., New York, 1932).

[16] H. J. Philipp and C. M. Conrad, J. App. Phys. **16**, 32 (1945).

maintain the room at constant conditions. Some of the phenomena described, therefore, were due to temperature and drying effects combined.

All cords tested were compared under identical sets of load, temperature, and humidity conditions so far as it was possible to reproduce them. The method of measuring elongations of the cords under equal fractions of their breaking loads and the one for determining count-strength products were considered no more satisfactory than the scheme here employed. Any basis for comparison of tire cord properties may be subject to numerous criticisms because the conditions imposed on the cord in actual service are still largely matters of conjecture.[17]

### 1. Change of Rate of Elongation with Load

While such variables as rate of loading, moisture content, and temperature have long been known to affect the stress-strain curves for cellulose yarns and cords[18] little effort has been made to analyze these curves for various cords. Two cords may have the same elongation at some given load, but the rate of elongation with load may vary markedly. Figure 1 is a graphical representation of load *vs.* elongation relationships (tensilgrams) for the cords in groups A and B. The differences indicated are probably better demonstrated by plotting the change of rate of elongation at various loads, i.e., the reciprocal of the slope of the stress-strain curves against the corresponding load. The resulting curves calculated from the tensilgrams are shown in Fig. 2. Some cords exhibit the major portion of their elongation at low loads, whereas the reverse appears to be true for the others. For example, the rayon cord does not reach its maximum rate of elongation until about half of the breaking load has been applied. This was found to be characteristic of all of a large number of rayon tire cord samples tested in this laboratory.[19]

It is interesting to note in this connection that although the curves for the cotton cords are similar in shape, it is possible, by proper construction and treatment, to alter somewhat the rate of elongation at various load ranges. Thus, the stretched cords B2 and B4 have elongation rates which are approximately uniform over the whole load range. Whether or not this characteristic would make them more serviceable as tire cords is still unknown.

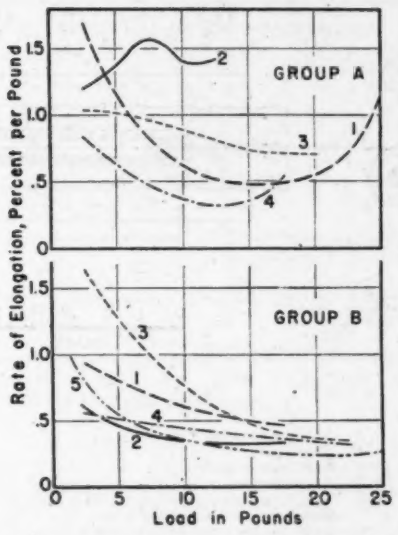


FIG. 2. Change of rate of elongation with load. Calculated from the slopes of the tensilgrams in Fig. 1 at various loads.

The "dual-stretching" treatment given cord B5 can be controlled to produce ten-pound bone-dry elongations anywhere between the original elongation of the unstretched cord and the lowest value obtainable by single stretching.[16] Elongation exceeding the low value of four percent, however, appears at stresses below one or two pounds. (Compare the tensilgrams for cords B4 and B5 in Fig. 1b.) This elongation at low loads may be useful in tire manufacturing, but its value in tire performance is still problematical, since this extra elongation is probably removed in manufacture and inflation of the tire.

### 2. Elongation under Static Loads

Elongation or flow curves with static loads have been reported by many authors for various types of cellulose fibers,[20] but no thorough study of the effect of temperature on this phenomenon has been published. Experiments to determine the temperature effect may be conducted in two ways: (1) the cord may be heated to the higher temperature before the load is applied, or (2) the load may be applied at room temperature, and the elongation observed while the temperature increases. Both of these methods were used in this investigation.

For these experiments, a special oven was constructed, a ½-inch copper tube, 54 inches

[17] For an analysis of the stresses on tire fabrics, see H. F. Schippel, Ind. Eng. Chem. **15**, 1121 (1923).

[18] See reference 13, E. Ott, pp. 1031–35; and R. Houwink, pp. 258–60.

[19] For an interesting explanation of this behavior of cellulosic materials, see reference 13, E. Ott, pp. 1034–35.

[20] Reference 13, E. Ott, p. 1020; Reference 11.

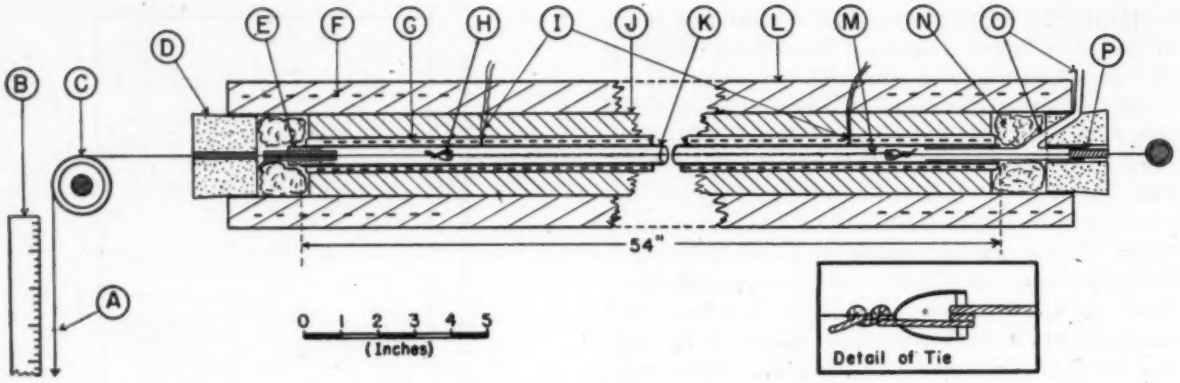


FIG. 3. The constant temperature oven.

*A*—Marker on wire.
*B*—Steel scale.
*C*—Frictionless pulley.
*D*—Cork stopper.
*E*—Small cork stopper with capillary tube.
*F*—End heater of Nichrome wire.
*G*—Tube heater of nichrome ribbon.
*H*—Stirrup.
*I*—Thermocouples soldered to copper tube.
*J*—1" pipe lagging.
*K*—1" inner copper tube.
*L*—2" pipe lagging.
*M*—Cord sample.
*N*—Cotton plug.
*O*—Glass tube inlet for dry air.
*P*—Brass connector.

long, being used as the inner chamber. (See Fig. 3.) The tube, covered with a thin layer of asbestos insulation, was heated and controlled electrically by a Nichrome ribbon heater wrapped around it. Pipe lagging and end heaters were added to help maintain a reproducible temperature uniform to .1°C along the useful length of the tube. The temperature along the chamber was measured by means of a traveling thermocouple which could be held taut in the tube at the same position as that to be occupied by the cord. The thermocouple junction was at first wrapped with single yarns of the various cords tested to eliminate the possibility of errors from radiation effects, but the difference between the temperatures with the thermocouple wrapped and unwrapped was found to be less than the one degree tolerance. Other thermocouples soldered to the outside of the copper tube at points along its length were used to detect any changes in temperature while the cord was in position.

The cord was tied at each end to a small metal stirrup as shown in the insert of Fig. 3. The entire length of the cord was kept in the uniform temperature zone. Steel wires fastened to the stirrups led to supports beyond each end of the tube. The elongation (both thermal and elastic) of the wires was taken into consideration, but it was less than one percent of the cord elongation in nearly all cases. Lengths were accurately measured from a marker on the left-hand wire by means of a Geneva cathetometer and an accurate steel scale. The wire at the left end passed over a special "frictionless" ball-bearing pulley to weights which were hung below the marker.

For the series of experiments in which the temperature of the cord was raised before application of the load, the procedure was as follows: A proper length of cord from the conditioned spool, after being carefully tied to the two stirrups, was quickly pulled into the tube and secured at the right-hand end. The ends of the tube were then closed, and a 0.31-pound weight was hung on the movable wire. After sufficient time had been allowed for the temperature to

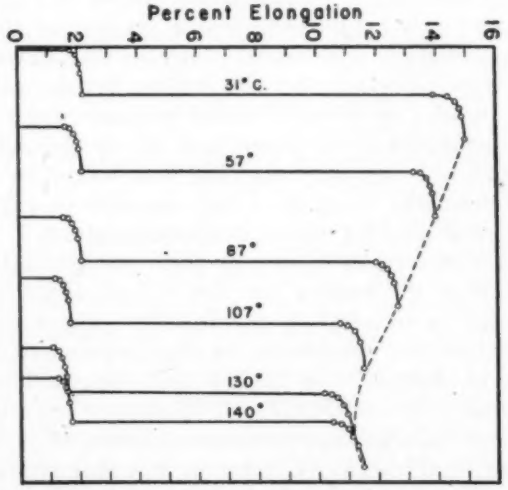


FIG. 4. Elongations at static loads of 1 and 7 pounds for cord B3 at various temperatures. (The 1-pound and the 7-pound elongations have been plotted against time for each temperature. Curves have been spaced according to the temperature of the measurement as explained in the text.)

reach equilibrium, as previously determined with the traveling thermocouple, the position of the marker was read, and, from the calibrated length of the wire, the "zero" length and position of the cord were determined. A 1-pound weight was then suspended from the wire, and the elongation was observed for a period of one hour. An additional six pounds were then added, and the elongation was again observed for one hour. This scheme of loading to 1 pound and then to 7 pounds was adopted to permit comparison between this experiment and the cyclic loading experiments described later, and also to make possible a calculation of the elongation obtainable between the 1- and 7-pound tensions. This latter elongation is probably of greater significance than the total elongation at 7 pounds, since the normal load on the cord in an inflated tire is usually at least one pound. Actually, the elongation obtained by loading to 7 pounds directly differs only slightly from that obtained by the above method.

A number of such runs were made at each temperature for several samples of each cord, in order to eliminate to some extent differences between individual samples. For the most part, these differences were of the order of 0.1- or 0.2-percent elongation, but in some cases the range from maximum to minimum for different samples of the same cord was as much as 2 percent. In these latter cases, more experiments were run to give a larger number of results from which to compute the average elongation.

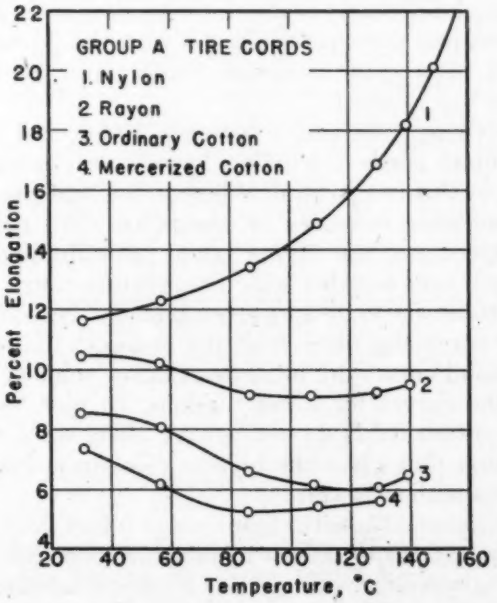


FIG. 5. Temperature-elongation curves for 7-pound static load. Group A.

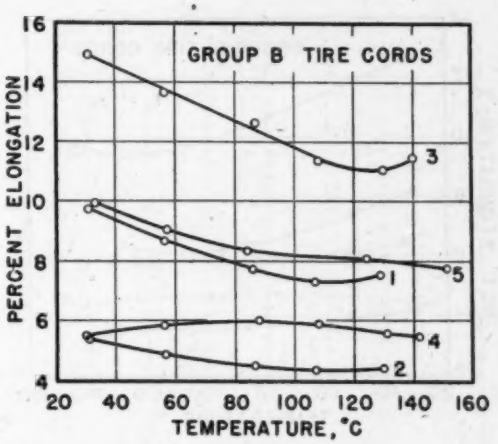


FIG. 6. Temperature-elongation curves for 7-pound static load. Group B. Experimental cotton cords: 1. 22.75/4/3 construction, unstretched; 2. 22.75/4/3 construction, stretched; 3. 17/4/3 construction, unstretched; 4. 17/4/3 construction, stretched; 5. 17/4/3 construction, dual-stretched.

Figure 4 shows the results of a number of such measurements for cord B3 at various temperatures. In this figure, the percent elongations for the 1-pound load and then the 7-pound load have been plotted against time for each temperature. The curves have been spaced according to the temperature of the measurement as labelled so that the dotted curve connecting the final percent elongations shows the change of this elongation with temperature. Such curves are shown in Figs. 5 and 6 for the cords in groups A and B, respectively.

These curves show interesting fundamental differences between the tire cords examined. Whereas the elongations of the commercial cotton samples, A3 and A4, and of the rayon, A2, decrease with increasing temperature, up to about 100°C, the elongation of the Nylon, A1, increases over the entire range to a value at 160°, which is more than double that at 30° with the same load. The curves for the experimental cords in group B also show differences which may be ascribed to differences in structure or treatment of the cords. The unstretched cords, B1 and B3, exhibit temperature elongation characteristics essentially similar to those of the commercial cotton cords in group A. Sample B1 has a lower elongation than B3, probably because there is a lower angle of twist in the B1 cord. (See Table I.) The stretching treatment, which reduces the elongation and gage of the cord, changes the shape of the elongation-temperature curves.

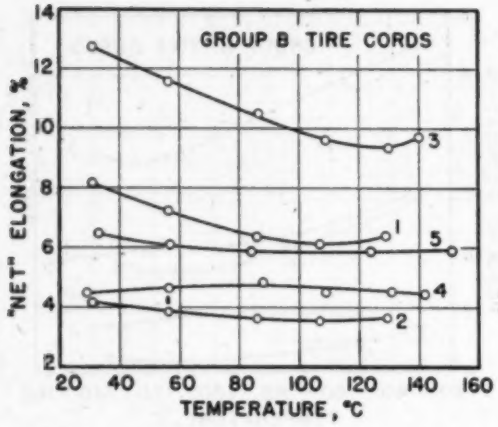


FIG. 7. Temperature-"net" elongation curves for tire cords of Group B. Net elongations were obtained by subtracting the 1-pound elongations from the 7-pound values.

Thus, B2 and B4 show flat curves in which the temperature effect is considerably reduced. In fact, B4 actually increases in elongation with rising temperature over the lower part of the range. This unusual effect was checked by repeating the experiments at each temperature several more times than was customary with the other cords to make certain that this result was not due to differences between individual samples of cord. The elongation and slope of the single-stretched cord are restored somewhat by the dual-stretching treatment as shown by the curve for B5.

The 1-pound elongations shown in Fig. 4 are practically unaffected by temperature; this was also found to be the case, within rather narrow limits, of all the cords tested, with the exception of the Nylon, A1, and the dual-stretched experimental cord, B5. Both the 1-pound and the 7-pound elongations of Nylon increased with temperature in a continuous manner; so the resultant obtained by subtracting the 1-pound value from the 7-pound extension also showed an increase with temperature. In the case of the dual-stretched cord, the 1-pound elongations decreased with increasing temperature almost as rapidly as the 7-pound elongations. The resultant stretch, due to the additional six pounds of load, was approximately the same over the entire temperature range. This is shown in Fig. 7 in which the resultant or "net" elongation obtained between the 1- and 7-pound loads is plotted against the temperature for the experimental cords. All of the stretched cords exhibit nearly constant net elongations over the entire temperature range studied. It appears, therefore, that one result of the stretching treatment for cotton cords is to reduce the effect of temperature on static elongations observed after the initial low-load stretch has been taken out.

The tubular oven described above was also used for determining the change of elongation with increasing temperature. A schedule for periodically adjusting the heater control was worked out empirically so the temperature of the cord was elevated at a uniform rate. This procedure was checked several times with the traveling thermocouple and found to give satisfactory reproducibility. A time-temperature curve (approximately a straight line) was plotted; this served as a calibration curve from which the temperature could be determined fairly accurately from the time of heating.

The cord to be tested was placed in the tube at room temperature and the load was applied immediately. When an equilibrium elongation had been reached (30 to 90 minutes were required, depending upon the load and the characteristics of the cord) heating was begun; the additional elongation was measured at intervals during the 90 minutes required for the temperature to reach 200°C. Temperature-elongation curves were thus obtained for tensions of 0.13, 1.0, 2.4, 4, and 7 pounds. These are shown for the commercial tire cords in Figs. 8–11. A sufficient number of duplicate experiments were run with various loads to show that the single curves traced in these figures illustrate typical differences between the cords tested. The rayon and cotton cords broke with the 7-pound load before the maximum temperature of the runs was reached.

Striking differences between Nylon and the cellulose cords (including rayon) are brought out in this comparison. Whereas the latter show appreciable increases in elongation with rising temperature, the Nylon seems to maintain its length over a rather wide temperature range for loads between one and seven pounds. The cellulose cords also differ from the Nylon in that the 7-pound curves are in all cases below some or all of the curves for lower tensions. In fact, even the cotton cords do not behave alike, since the tension that gives the highest elongation curve varies with each cord.

In connection with these results, it is of interest to note the differences in moisture contents of the conditioned commercial cords as tabulated in Table I. The rayon, which had the highest moisture content (14.5 percent), exhibited the

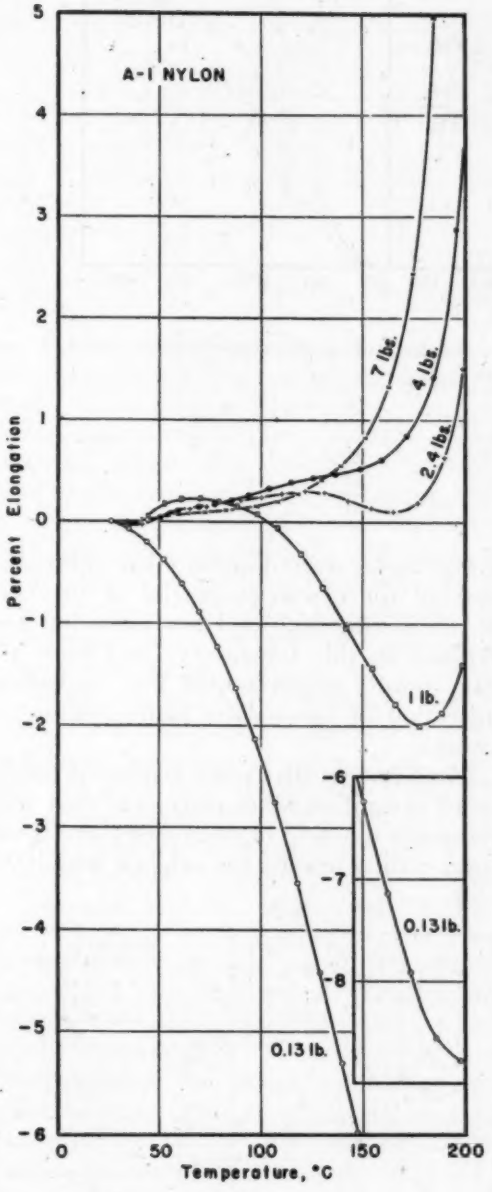


FIG. 8.

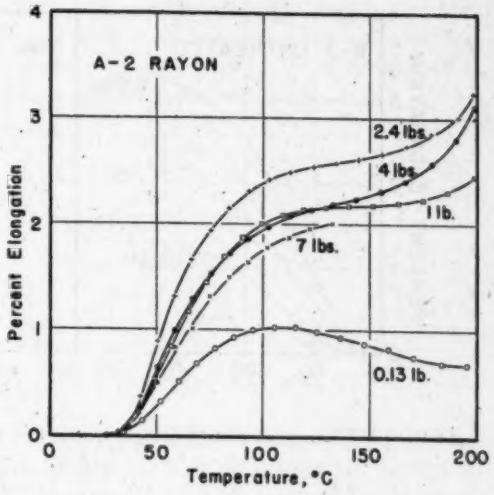


FIG. 9.

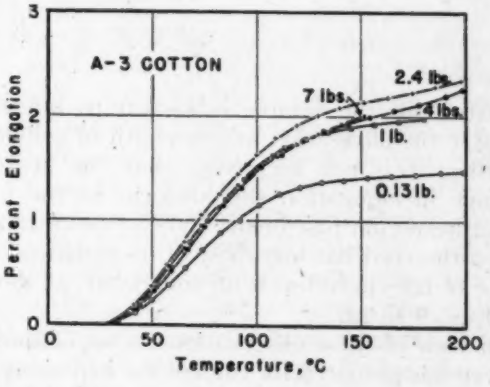


FIG. 10.

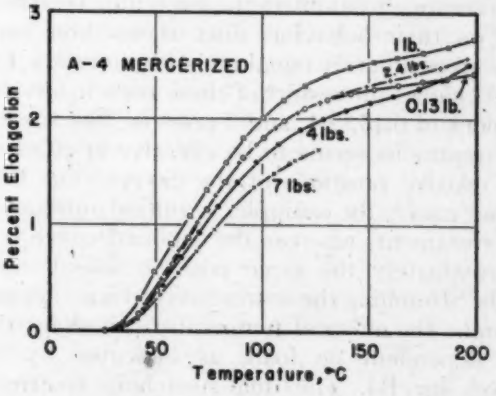


FIG. 11.

FIGS. 8, 9, 10, 11. Change in elongation of Group *A* tire cords at various loads as the temperature is raised.

greatest change in elongation with rising temperature for the range 50°–100°C except at the lowest load of 0.13 lb. Nylon, with the lowest moisture content (4.0 percent), showed the least change, and the cotton cords, with moisture contents of 7.8 percent to 9.4 percent, fitted in between these extremes. As will be shown in Section 5 of this paper, it is in the range of 50°–100°C that the cord probably undergoes its maximum change in moisture content. Since

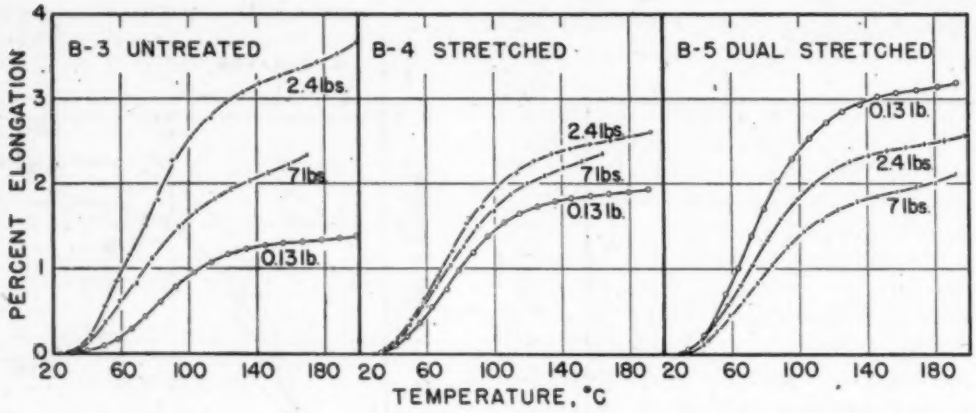


FIG. 12. Change in elongation for cords B3, B4, and B5 at various loads as the temperature is raised.

Equilibrium Elongations at 25° C.

| Load | B3 | B4 | B5 |
|---|---|---|---|
| 0.13 pound | 0.007% | 0.022% | 0.042% |
| 2.4 pounds | 5.23 | 2.93 | 6.12 |
| 7.0 pounds | 11.12 | 6.02 | 9.52 |

moisture of the sample is known to influence greatly the elongation and strength of cellulosic textiles, it is not surprising that the greatest change in elongation should occur in the temperature region just below 100°C. Above 100°C, when the cord has lost most of its moisture, the slope of the curve levels off somewhat, as shown by Figs. 9 to 12.

In view of these observations, a set of similar curves was prepared for each of the experimental cotton cords of 17/4/3 construction (B3, B4, B5) to determine what effect the stretching treatment had on their behavior, since these three cords had approximately equal moisture contents. Figure 12 shows the results of these tests made with tensions of 0.13, 2.4, and 7 pounds. The stretching treatment seems to be effective in changing the relative positions of the curves. The 0.13-pound curve, for example, is shifted upward by the treatment, whereas the 7-pound curve is in approximately the same position for all three cords. Stretching the untreated cord once appears to make the effect of temperature on elongation less dependent on load, as indicated by the curves for B4. The dual-stretching treatment seems to reverse the load effect; that is, the highest curve is for the lowest load, and conversely the lowest curve is for the highest (7-pound) load.

### 3. Elongation with Cyclic Loads

There are indications that the behavior of the cord under cyclic loadings is entirely different from that under static loading.[21] For this reason, a study of the elastic properties of tire cords under alternating high and low loads has been undertaken in this laboratory, and some preliminary results are presented here to indicate the direction of the results being obtained in this work.

It is well known that when tension is applied to a cord elongation takes place, and that when the tension is removed or decreased there is only a partial return toward the original length.[22] If

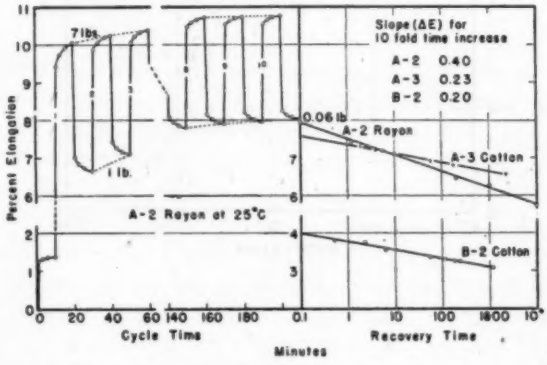


FIG. 13. Growth and recovery of tire cords with cyclic loading treatment.

[21] S. G. Barker and N. Tunstall, Trans. Faraday Soc. 25, 103 (1929).

[22] Numerous workers have studied this process, and various explanations and mechanical analogies have been used to account for the phenomena observed in this connection. See reference 13, for examples.

TABLE II. Percent elongations for cyclic loading (0.06 lb. load equivalent to "0" elongation).

| No. of 10-min. cycle | A-2 Rayon | | | A-3 Cotton | | | B-2 Stretched Cotton | | |
|---|---|---|---|---|---|---|---|---|---|
| | 1 lb. | 7 lb. | $\Delta E$ | 1 lb. | 7 lb. | $\Delta E$ | 1lb. | 7 lb. | $\Delta E$ |
| 1 | 1.37 | 10.06 | 8.69 | 3.27 | 10.08 | 6.81 | 2.32 | 6.32 | 4.00 |
| 2 | 6.66 | 10.25 | 3.59 | 7.34 | 10.21 | 2.87 | 4.01 | 6.37 | 2.36 |
| 3 | 7.10 | 10.39 | 3.29 | 7.72 | 10.29 | 2.57 | 4.36 | 6.41 | 2.05 |
| 4 | 7.33 | 10.48 | 3.15 | 7.90 | 10.36 | 2.46 | 4.45 | 6.43 | 1.98 |
| 5 | 7.50 | 10.55 | 3.05 | 8.06 | 10.42 | 2.36 | 4.51 | 6.45 | 1.94 |
| 6 | 7.63 | 10.60 | 2.97 | 8.19 | 10.44 | 2.25 | 4.57 | 6.48 | 1.91 |
| 7 | 7.73 | 10.66 | 2.93 | 8.26 | 10.46 | 2.20 | 4.61 | 6.49 | 1.88 |
| 8 | 7.81 | 10.72 | 2.91 | 8.32 | 10.50 | 2.18 | 4.64 | 6.50 | 1.86 |
| 9 | 7.90 | 10.74 | 2.84 | 8.37 | 10.51 | 2.14 | 4.67 | 6.50 | 1.83 |
| 10 | 7.96 | 10.76 | 2.80 | 8.42 | 10.53 | 2.11 | 4.70 | 6.52 | 1.82 |
| 11 | 8.03 | | | 8.46 | | | 4.72 | | |

the load is reapplied, elongation again takes place but not to the same extent as before. The recovery, likewise, is modified by the previous application of tension so that the elongation curve for the second cycle is not like the first. This trend continues in additional cycles; that is, the cord "grows." The rate of growth of a cord subjected to such tension cycles should bear some relation to the long-time behavior of the cord in a tire. Furthermore, temperature should have some considerable effect on this rate.

In a preliminary investigation in which the cycle time was twenty minutes, two cotton cords (A3 and B2) and the rayon cord (A2) were each subjected to ten tension cycles with alternate loads of one pound and seven pounds. During the experiment, the cord was kept in the tubular oven already described. A typical series of curves for rayon at room temperature is shown in Fig. 13. At the end of the tenth cycle, the load was decreased to one pound for ten minutes as before. After this mechanical conditioning, the load was decreased again, this time to 0.06 pound, and with this load the recovery was observed over a period of about 24 hours. Plotting the elongation during recovery, based on the original length of the cord, against the logarithm of the time gave a straight line with a characteristic slope as shown in the right-hand part of Fig. 13.

Percent elongations for the end of each ten-minute half-cycle for the high and low loads, and the differences between these two values ($\Delta E$) for each cycle are tabulated in Table II. The second column under each type of cord shows the elongation with the 7-pound load at the end of each cycle. A steady increase in these values illustrates how the cord grows in length during the repeated cycles. Although the rate of growth became smaller with each additional cycle, the rayon still exhibited measurable growth after twenty cycles at room temperature. The tabulated data show that the rate of growth for the cotton cords studied was less than that for rayon.

The third column under each type of cord in Table II shows the extra elongation, $\Delta E$, obtained by the addition of six pounds of tension during the cycle. The magnitude of $\Delta E$ is seen to decrease with each cycle so that, at the end of the tenth cycle, the $\Delta E$ for a 6-pound increase is only about one-third that obtained in the first cycle. Such a decrease in elasticity may also occur in the tire and thus reduce the available elongation in the cord. If this is the case, the usefulness of the simple measurement of elongation from a tensilgram in predicting elongation behavior in a tire is questionable.

Recovery curves after ten-cycle mechanical conditioning treatments are also shown in Fig. 13 (right-hand part) for the two cotton cords studied, A3 and B2. The slopes of the recovery curves, or the logarithmic rate of recovery for these cotton cords, are approximately equal and

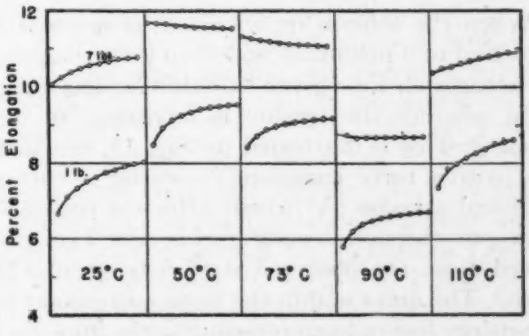


FIG. 14. Consecutive minimum and maximum elongations for 1- and 7-pound loading cycles with rayon for ten cycles at various temperatures.

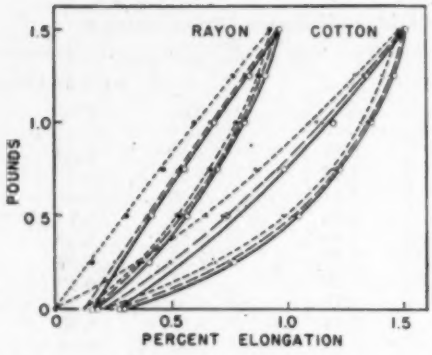


FIG. 15. Hysteresis loops for tire cords A2 and A3 with twenty-minute cycles. Order of loops: ------ first, – – – – – second, ——— third.

only about one-half of the corresponding slope for rayon.

Similar series of ten cycles were run with rayon at elevated temperatures. The envelopes of the curves for these series, similar to that indicated by the dotted lines in Fig. 13, were prepared from data obtained at temperatures of 25°, 50°, 73°, 90°, and 110°C and are represented in Fig. 14. These envelopes illustrate the profound effect that temperature and accompanying changes in the textile substance have on the behavior of rayon cord under cyclic stresses. The rapid drop in the elongation between 50° and 90°C is undoubtedly associated with the decrease in equilibrium moisture content of the rayon as the temperature is raised. Above 90°C the elongation, $\Delta E$, and cord growth, as illustrated by the upward slope of the envelope, appear to increase again, as one might expect from the greater tendency of the rayon filament to exhibit flow properties at higher temperatures.

### 4. Hysteresis

When the tension on a cord is progressively increased to a maximum and then lowered again, the elongation for a given load differs, depending upon whether the tension is increasing or decreasing. This is illustrated by Fig. 15, in which are plotted three complete cycles for a cotton (A3) and a rayon (A2) cord. After the cord had been put through several cycles, the loop obtained from the observed data was essentially closed. The areas within the loops correspond to the energy loss or hysteresis due to the imperfect elasticity of the cord. This phenomenon of elastic hysteresis, which has been reported upon for textile fibers by a number of experimenters,[21,22] was investigated by us for some of the tire cord samples herein described.

The apparatus used for measuring hysteresis is schematically depicted in Fig. 16. A calibrated spring $D$ served to give the necessary tension to the cord at various points in the cycle as the motor-driven eccentric $E$ gradually increased the pull on the cord $C$ and released it again. A two-meter length of the cord was used and was fastened to the wire leaders by means of the stirrups $T$ described earlier. Two pointers $M$ on the wires passed in front of two 23-cm scales $S$ in such a way that the position of the upper one gave the elongation of the spring, which could be converted to load; the difference between the positions of the two pointers permitted calculation of the elongation of the cord. Simultaneous positions of the pointers were recorded by means of a 16-mm moving-picture camera which had a maximum speed of 64 frames per second. Thus, sufficient points could be obtained with a one-second cycle to permit plotting a fairly good hysteresis loop.

Hysteresis curves for four tire cords were obtained under three sets of cycle conditions (load and time) at room temperature of 25°C and a relative humidity of approximately 50 percent. The results are depicted in Fig. 17. To ensure an essentially closed loop, each cord was put through the cycle approximately 50 to 100 times before a record was made. The plotted hysteresis loops were integrated graphically with a planimeter, and elastic moduli were calculated from the over-all slopes of the curves. The hysteresis values expressed as calories of heat generated per centimeter length of cord are tabulated with the elastic moduli in Table III.

The hysteresis values for these cords have been compared over similar load ranges. They

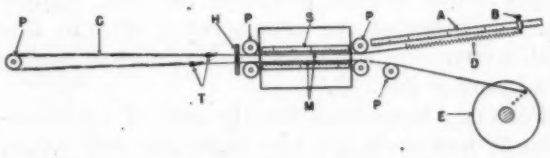


FIG. 16. Schematic diagram of apparatus for measuring hysteresis of tire cords.

*P*—Frictionless pulleys
*C*—Cord sample
*T*—Stirrups
*H*—Stirrup stops
*S*—Millimeter scales
*M*—Pair of markers on wire
*A*—Meter scale
*B*—Clamp
*D*—Spring
*E*—Motor-driven geared eccentric

[22] W. S. Denham and T. Lonsdale, Trans. Faraday Soc. **29**, 305 (1933).

TABLE III. Cyclic loading behavior for tire cords at room temperature.

| Cycle conditions | A–2 Rayon Elastic modulus dynes/cm² | A–2 Rayon Hysteresis cal./cm | A–3 Cotton Elastic modulus dynes/cm² | A–3 Cotton Hysteresis cal./cm | B–1 Unstretched cotton Elastic modulus dynes/cm² | B–1 Unstretched cotton Hysteresis cal/cm | B–2 Stretched cotton Elastic modulus dynes/cm² | B–2 Stretched cotton Hysteresis cal./cm |
|---|---|---|---|---|---|---|---|---|
| 7 sec./cycle, 2.0 to 4.4 lbs. | $5.4\times10^{10}$ | $12\times10^{-7}$ | $2.7\times10^{10}$ | $17\times10^{-7}$ | $3.6\times10^{10}$ | $13\times10^{-7}$ | $5.5\times10^{10}$ | $9\times10^{-7}$ |
| 7 sec./cycle, 5.0 to 11.1 lbs. | $7.9\times10^{10}$ | $39\times10^{-7}$ | $5.4\times10^{10}$ | $36\times10^{-7}$ | $7.5\times10^{10}$ | $13\times10^{-7}$ | $8.6\times10^{10}$ | $22\times10^{-7}$ |
| 1 sec./cycle, 5.0 to 10.9 lbs. | $8.3\times10^{10}$ | $23\times10^{-7}$ | $5.8\times10^{10}$ | $43\times10^{-7}$ | $8.0\times10^{10}$ | $18\times10^{-7}$ | $9.3\times10^{10}$ | $21\times10^{-7}$ |

might also have been compared for ranges of equal elongation. Actually, in the tire the cycle conditions probably vary so that neither the load nor the elongation ranges are constant. The comparison of hysteresis losses of cotton and rayon, for example, over the same load increment may not be valid because under equal service conditions the individual rayon cord may not be subjected to an equally high load, hence the hysteresis loop might be smaller.

Experience demonstrated that many improvements could be made in the apparatus used for hysteresis measurements. The mass of the moving system was too great to permit unhindered recovery of the cord during the second half of the cycle. The motor speed was not constant throughout the cycle; so a slightly longer time was required during the loading portion than during the unloading portion. These and other difficulties are being corrected in a new apparatus now being assembled for the purpose of obtaining better data on cyclic loading of tire cords at various temperatures, moisture contents, and load ranges.

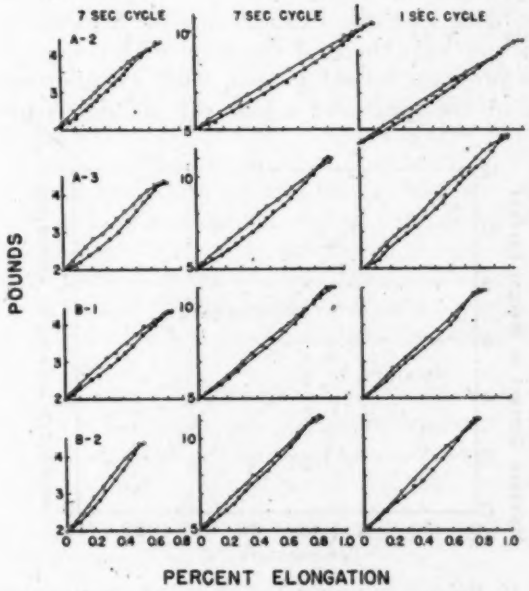


FIG. 17. Hysteresis loops for tire cords.

### 5. Effect of Moisture Content

It was pointed out earlier that some of the elasticity phenomena herein described are probably related, at least in part, to the moisture content of the tire cord. In order to determine the influence of this factor, some of the experiments were repeated on cords which had been dried and were maintained in a dry condition during the test period.

The drying was accomplished by the use of a second tubular oven similar to that described in connection with Fig. 3. The length of cord was placed inside a long glass tube which was then slipped into the oven heated to approximately 105°C. A slow stream of air from a drying train was passed through the glass tube for an hour. The glass tube containing the dry cord was then quickly transferred to the test oven and slipped out again, leaving the cord in the test chamber. The air passing into the test oven through the tube *O*, Fig. 3, was preheated to the temperature of the experiment so that the temperature equilibrium of the constant-temperature zone would not be disturbed by the introduction of the dry air. In this way, the predried cord was transferred to the test chamber without exposure to room air and was kept dry during the period of the experiment.

Measurements were made on an untreated cotton cord (B3), because the effects observed for this cord in undried condition were fairly large. Final elongations with a load of 1 pound for 1 hour followed by a load of 7 pounds for 1 hour were measured over the temperature range as described in Section 2 above. The results of these experiments are shown in the lower, solid curve of Fig. 18. A similar curve taken from Fig. 6

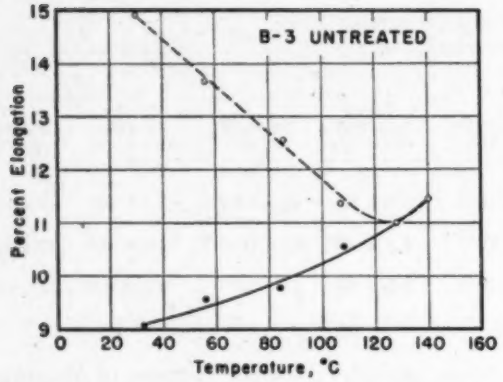


FIG. 18. Temperature-elongation curves for B3 with 7-pound static load. Dotted curve—cord initially conditioned; Solid curve—cord dried and kept dry.

for the undried cord is included in this figure for comparison.

On the basis of these results, one would be led to the conclusion that the decrease in elongation observed with increasing temperature (Figs. 5 and 6) is due to the concomitant decrease in moisture content of the cord. This conclusion is supported by the fact that both the dried and undried B3 cords have the same elongation at high temperatures when the moisture content in the undried cord approaches that of the dried cord. To confirm this view, an estimation of the moisture content of the cord at various temperatures in the experimental oven was made by a method of approximations, using psychrometric tables and the equilibrium moisture data for raw cotton published by Wiegerink.[24] The moisture contents and the differences between the static elongations of the dried and undried cords as determined from Fig. 18 are plotted against temperature in Fig. 19. Although these curves do not have identical shapes, probably due to inaccuracies in the elongation measurements and in the moisture estimations, they do have the same general negative slope. The ratio of moisture content to the difference in elongation at the various temperatures was found to be approximately constant, indicating good correlation between the two variables. Therefore, there is evidence that static elongation as measured in these experiments is a function of moisture content and of temperature.

The change of elongation with increasing temperature was investigated for the dried cord (B3) in another experiment to determine the effect of drying. The drying procedure described above and the elongation measurement outlined in the latter portion of Section 2 were followed. Figure 20 shows the elongations obtained as the temperature was elevated with loads between 0.13 and 7 pounds. A curve from Fig. 12 for the undried cord with a 2.4-pound load is included for comparison and orientation.

It is interesting to note that the elongation-temperature curve for the dried cord at temperatures above 50° is a straight line with any load between 1 and 7 pounds, and that the slope of this curve increases with load in a regular manner. This behavior suggests a thermal expansion coefficient which is a function of the load applied, but definite proof of this would require additional investigation.

## IV. DISCUSSION

The experiments on the elastic properties of tire cords which have been described are only "*in vitro*" tests of cords outside of the tire in which they are expected to perform certain vital functions. In the ultimate analysis, the only satisfactory test of a tire cord is an "*in vivo*" test in actual service in the tire. Except for a limited number of properties, such as breaking load, elongation, and possibly fatigue life, the correlation of laboratory tests with tire service must be made by a logical or deliberative attempt to visualize the part that the tire cord plays in its contribution to the serviceability of the tire.

A consideration of the rate of change of elongation with load, for example, would lead one to conclude that the best tire cord with respect to this property would be one with a rather low rate at low loads and a high rate at high loads.

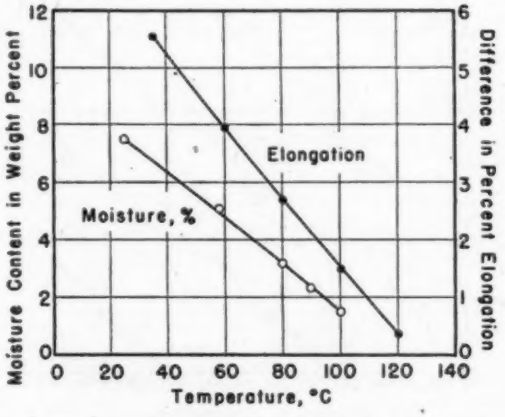


FIG. 19. Relation of temperature to moisture content and to difference between the curves shown in Fig. 18.

[24] J. G. Wiegerink, J. Research Nat. Bur. Stand. **24**, 645 (1940).

The tire made of such a cord should retain its shape under ordinary conditions and yet be able to withstand great impacts without cord rupture and subsequent blowouts.

In the tire, the cord is encased in rubber; so that its moisture equilibrium with the surroundings, may be altogether different from that experienced in free air. If the temperature is elevated, some of the moisture sorbed by the cord may be lost to the rubber, but a large part of it will probably be retained by the cord. Using a special technique for minimizing or eliminating moisture exchange between the cord and the atmosphere, the authors have made determinations of the moisture of cotton tire cords in a tire which had been run over 17,000 miles under the destructive conditions of the Army Ordnance test at Camp Normoyle, Texas,[25] and have found a moisture content of 4.5 percent. Since the elastic properties of a cord depend somewhat on its moisture content and since this content may be very low at 150°C in the tire, the behavior of the cord in service at high temperatures may be very unlike that observed in a laboratory test under atmospheric conditions.

The tire cord in the experimental oven described in Section 2 was subjected to temperature and humidity conditions somewhat analogous to the cord in the tire. Here the cord was kept in an enclosed tube in which the moisture lost by the cord because of increasing temperature tended to raise the humidity of the air in the tube, which in turn tended to maintain the moisture in the cord. For this reason, we believe the results described in Sections 2 and 3 have special significance with regard to the behavior of cord in the tire. The change of elongation with temperature as measured in the latter part of Section 2, for example, is a phenomenon which undoubtedly occurs when the inflated tire, containing cords under tension, is run under such conditions that the temperature of the cord is considerably increased. The tension on the cord also changes; so the conditions imposed upon the cord include varying loads and varying temperatures.

The elastic behavior of a tire cord is the net result of a multiplicity of factors, many of which are difficult to investigate. Elongation of a given cord is not merely a function of load, temperature, and moisture content, but depends also upon the element of time and upon the complete history of the cord. Further investigation of these factors should give scientific information that will be of value in the manufacture of better fabrics and in the preparation of more complete specifications for tire cords than have been set up in the past.

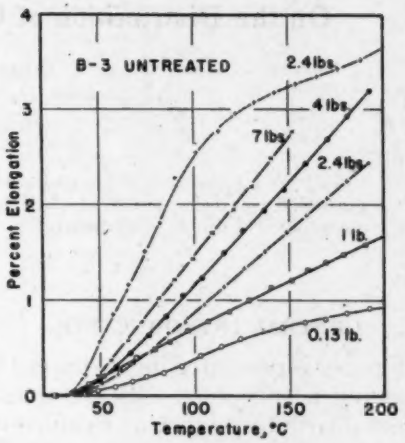


FIG. 20. Change in elongation of dry cord B3 as the temperature is raised. The dotted curve is for the same cord initially conditioned and was taken from Fig. 12.

## V. SUMMARY

The elastic properties of four commercial and five experimental tire cords have been compared over wide ranges of loads, temperatures, and moisture contents. The effect of temperature on elongations with various static loads has been investigated, and the influence of moisture content on the results has been pointed out. The partial recovery and growth of rayon and cotton cords subjected to cyclic loadings have been compared. A hysteresis test has been described in which the energy loss per cycle of loading and unloading may be calculated. The results of these tests have given considerable information concerning the possible behavior of the tire cord in the tire and should aid in setting up more complete criteria of the essential elastic requirements of a better tire cord.

## ACKNOWLEDGMENT

The authors are grateful to J. J. Brown, D. S. Dearie, R. M. Gerard, and W. S. Lewis of this Laboratory for their interest and cooperation in this work.

[25] B. J. Lemon and J. J. Robson, India Rubber World, 109, 463 and 582 (1944).

# On the Distribution of Current along Asymmetrical Antennas

LIEUT. COMDR. CHARLES W. HARRISON, JR.*
*Cruft Laboratory, Harvard University, Cambridge, Massachusetts*

(Received January 24, 1945)

In Part I a theoretical discussion is presented concerning the distribution of current along a grounded vertical antenna which is driven at an arbitrary point. In Part II the problem of the asymmetrical dipole is formulated.

## GENERAL INTRODUCTION

THIS paper is presented in two parts. Of these the first is concerned with the question of the current distribution along a grounded vertical radiator which is located over a perfectly conducting plane earth of infinite extent. In the second part, a brief analysis is given relative to the distribution of current along an isolated asymmetrical dipole.

## PART I

### Problem of the Grounded Vertical Radiator†

Numerous articles have appeared in the literature dealing with the current distribution along base-driven vertical radiators.[1-7] Now in practice it is difficult to locate the driving generator precisely at the base of the structure as this theory presupposes, but instead it may be situated some distance from ground. Figure 1 is intended to illustrate the point in mind. Here the antenna (and its image) lies along the $z$-axis of a system of cylindrical coordinates $r$, $\theta$, and $z$. The earth plane is at $z=0$; the generator is oriented at $z=s$; and the free end of the antenna is defined by $z=s+h$. Although a wire of constant radius is pictured, the radius of the wire in the interval $0\leqq z\leqq s$ is taken as $a_s$, and in the interval $s\leqq z\leqq s+h$ as $a_h$.

Electromagnetically, an antenna operated over a perfectly conducting earth is equivalent to the actual antenna and a second antenna so placed with respect to the first and the earth plane between them, that one is the geometrical image of the other when reflected in the plane. Both antennas are in empty space, and the plane between them has only mathematical reality. The same current amplitude distribution obtains in the two, but their time phases differ by one-half period. Applied to the present problem, one must analyze an *isolated antenna* driven at two points by identical generators, maintaining equal voltages in the same time phase across the input terminals. Additionally, a certain symmetry condition is imposed on the total current flowing in the antenna. It is

$$I(z)=I(-z). \tag{1}$$

(Hereafter the term "antenna" refers to the actual radiator and its image, *viz.*, a system extending over the range $-(s+h)\leqq z\leqq(s+h)$.)

Let it be assumed that the antenna is of infinite conductivity. This supposition is a good approximation in practice, as very little power transferred into a well constructed antenna is consumed in heat. Then the continuity of the tangential component of electric field at the surface of the antenna leads directly to the differential equation

$$d^2A(z)/dz^2+\beta^2A(z)=0. \tag{2}$$

---

* Now assigned to the Combined Research Group, U. S. Naval Research Laboratory, Washington, D. C.

† Readers may be interested in the following papers: "On the calculation of the impedance properties of parasitic antenna arrays involving elements of finite radius," J. Am. Soc. Naval Eng., May, 1945. "Mutual and Self-Impedance for Colinear Antennas" accepted for publication in the Proc. I.R.E. "A theory for three-element broadside arrays," submitted for publication in Proc. I.R.E. "Symmetrical antenna arrays," not yet presented for publication.

[1] E. Hallén, "Theoretical Investigations into the Transmitting and Receiving Qualities of Antennas," Nova Acta Upsalienses [4], **11**, 3–44 (1938).

[2] L. V. King, "On the Radiation Field of a Perfectly Conducting Base-Insulated Cylindrical Antenna Over a Perfectly Conducting Plane Earth, and the Calculation of Radiation Resistance and Reactance," Phil. Trans. Roy. Soc. (London) **236**, 381–422 (November 2, 1937).

[3] Léon Brillouin, "The Antenna Problem," Quart App. Math. **1**, 201–214 (1943).
Léon Brillouin, "Antennae for Ultra-High Frequencies," Elec. Communication **21**, 257–281 (1944).
Léon Brillouin, "Antennae for Ultra-High Frequencies," Elec. Communication **22**, 11–39 (1944).

[4] Ronold King and F. G. Blake, Jr., "The Self-Impedance of a Symmetrical Antenna," Proc. I.R.E. **30**, 335–348 (1942).

[5] Charles W. Harrison, Jr., "The Radiation Field of Long Wires, with Application to Vee Antennas," J. App. Phys. **14**, 537–544 (1943).

[6] Ronold King and Charles W. Harrison, Jr., "The Distribution of Current Along a Symmetrical Center-Driven Antenna," Proc. I.R.E. **31**, 548–567 (1943).

[7] Ronold King and Charles W. Harrison, Jr., "The Impedance of Short, Long, and Capacitively Loaded Antennas with a Critical Discussion of the Antenna Problem," J. App. Phys. **15**, 170–185 (1944).

Here $A(z)$ is the total vector potential on the surface of the antenna ($r=a_h$ when $s \leqq z \leqq (s+h)$ or $-s \geqq z \geqq -(s+h)$ and $r=a_s$ when $-s \leqq z \leqq s$).

$$\beta = 2\pi/\lambda, \tag{3}$$

where $\lambda$ is the wave-length.

Let intervals be defined for the antenna as follows:

Interval (1) $\quad s \leqq z \leqq (s+h), \tag{4a}$

Interval (2) $\quad 0 \leqq z \leqq s, \tag{4b}$

Interval (3) $\quad 0 \geqq z \geqq -s, \tag{4c}$

Interval (4) $\quad -s \geqq z \geqq -(s+h). \tag{4d}$

Subject to (4), the complete solution of (2) may be written

Interval (1)

$$A(z) = \frac{-j}{c}\{C_1 \cos \beta z + C_2 \sin \beta z\}, \tag{5a}$$

Interval (2)

$$A(z) = \frac{-j}{c}\{C_3 \cos \beta z + C_4 \sin \beta z\}, \tag{5b}$$

Interval (3)

$$A(z) = \frac{-j}{c}\{C_5 \cos \beta z + C_6 \sin \beta z\}, \tag{5c}$$

Interval (4)

$$A(z) = \frac{-j}{c}\{C_7 \cos \beta z + C_8 \sin \beta z\}. \tag{5d}$$

The following notation is used:

$c = 1/(\Pi\Delta)^{\frac{1}{2}} = 3\times 10^8$ meters per second, (6)

$\Pi = 4\pi \times 10^{-7}$ henry per meter, (7)

$\Delta = 8.85 \times 10^{-12}$ farad per meter, (8)

$C_1 \cdots C_8$ are arbitrary constants.

The constants involved in (5) may be evaluated by employing the following boundary conditions:

(a) The discontinuity in scalar potential at the driving point ($z=s$) equals the externally applied voltage $V_s^e$. That is

$$V_s^e = \operatorname*{Limit}_{z \to s} \{ \Phi_{\text{Int. (1)}} - \Phi_{\text{Int. (2)}} \}, \tag{9}$$

where

$$\Phi_{\text{Int. (1)}} = \frac{jc^2}{\omega}\left\{\frac{\partial A(z)}{\partial z}\right\}_{\text{Int. (1)}}, \tag{10a}$$

$$\Phi_{\text{Int. (2)}} = \frac{jc^2}{\omega}\left\{\frac{\partial A(z)}{\partial z}\right\}_{\text{Int. (2)}}, \tag{10b}$$

$$\omega = 2\pi f = c\beta. \tag{10c}$$

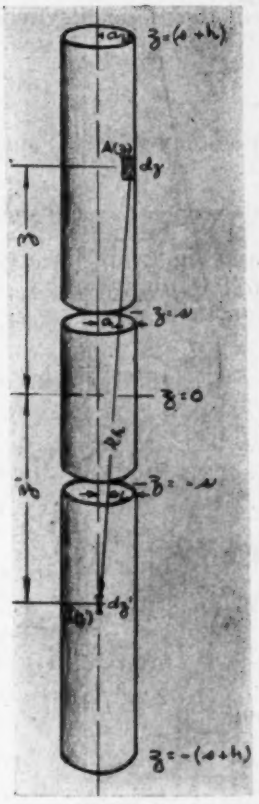

FIG. 1. Isolated antenna with two-generator drive.

(b) There is no discontinuity in scalar potential at the earth plane ($z=0$). Thus

$$0 = \operatorname*{Limit}_{z \to 0} \{ \Phi_{\text{Int. (2)}} - \Phi_{\text{Int. (3)}} \}, \tag{11a}$$

$$\Phi_{\text{Int. (3)}} = \frac{jc^2}{\omega}\left\{\frac{\partial A(z)}{\partial z}\right\}_{\text{Int. (3)}}. \tag{11b}$$

(c) The total vector potential $A(z)$, like the total current $I(z)$, satisfies the symmetry condition

$$A(z) = A(-z). \tag{12}$$

(d) The total current $I(z)$ is continuous across the driving point, thus insuring continuity of the vector potential $A(z)$ across the same point. (It is worth noting that the converse of this statement is not necessarily true.)

(e) The total current $I(z)$ vanishes at $z=s+h$. Applying (a) at the drive point $z=s$,

$$V_s^e = -(C_1 - C_3)\sin \beta s + (C_2 - C_4)\cos \beta s. \tag{13}$$

Applying (b) at the plane of symmetry ($z=0$),

$$C_4=C_6. \tag{14}$$

Applying (c),

$$(C_1-C_7)\cos\beta z+(C_2+C_8)\sin\beta z=0, \tag{15a}$$

and

$$(C_3-C_5)\cos\beta z+(C_4+C_6)\sin\beta z=0. \tag{15b}$$

Since $\cos\beta z$ and $\sin\beta z$ are linearly independent functions, it follows that

$$C_1=C_7, \tag{16a}$$

$$C_2=-C_8, \tag{16b}$$

$$C_3=C_5, \tag{16c}$$

$$C_4=-C_6. \tag{16d}$$

One now observes that (14) and (16d) require

$$C_4=C_6=0. \tag{17}$$

Equation (5) may now be rewritten in the form

$$\text{Interval (1)}\quad A(z)=\frac{-j}{c}\{C_1\cos\beta z+C_2\sin\beta z\}, \tag{18a}$$

$$\text{Interval (2)}\quad A(z)=\frac{-j}{c}\left\{\frac{V_s^e+C_1\sin\beta s-C_2\cos\beta s}{\sin\beta s}\right\}\cos\beta z, \tag{18b}$$

$$\text{Interval (3)}\quad A(z)=\frac{-j}{c}\left\{\frac{V_s^e+C_1\sin\beta s-C_2\cos\beta s}{\sin\beta s}\right\}\cos\beta z, \tag{18c}$$

$$\text{Interval (4)}\quad A(z)=\frac{-j}{c}\{C_1\cos\beta z-C_2\sin\beta z\}; \tag{18d}$$

or in short hand,

$$A(z)=\frac{-j}{c}\{C_1\cos\beta z+C_2\sin\beta|z|\}, \tag{19a}$$

for intervals (1) and (4);

$$A(z)=\frac{-j}{c}\left\{\frac{V_s^e+C_1\sin\beta s-C_2\cos\beta s}{\sin\beta s}\right\}\cos\beta z, \tag{19b}$$

for intervals (2) and (3). (The constants $C_1$ and $C_2$ remain to be evaluated from boundary conditions (d) and (e).)

The vector potential at any point on the surface of the antenna is given by

$$A(z)=\frac{\Pi}{4\pi}\int I(z')\frac{\exp(-j\beta R_{h,s})}{R_{h,s}}dz', \tag{20}$$

where the integration is to be carried out over the entire antenna length.

In (20), $I(z')$ is the complex current flowing in the element $dz'$. $R_{h,s}$ is the distance from the point $(a_{h,s}, \theta, z)$ where the vector potential is computed to the element $dz'$. That is

$$R_h=((z-z')^2+a_h^2)^{\frac{1}{2}} \quad \text{for intervals (1) and (4)}, \tag{21a}$$

$$R_s=((z-z')^2+a_s^2)^{\frac{1}{2}} \quad \text{for intervals (2) and (3)}. \tag{21b}$$

If $s\leqq z\leqq s+h$ or $-s\geqq z\geqq-(s+h)$, one may equate (20) to (19a). Thus

$$\int_{-(s+h)}^{-s} I(z')\frac{\exp(-j\beta R_h)}{R_h}dz'+\int_{-s}^{+s} I(z')\frac{\exp(-j\beta R_h)}{R_h}dz'+\int_{+s}^{s+h} I(z')\frac{\exp(-j\beta R_h)}{R_h}dz'$$

$$=-j\frac{4\pi}{R_c}\{C_1\cos\beta z+C_2\sin\beta|z|\}. \tag{22a}$$

Similarly, when $-s\leqq z\leqq s$,

$$\int_{-(s+h)}^{-s} I(z')\frac{\exp(-j\beta R_s)}{R_s}dz'+\int_{-s}^{+s} I(z')\frac{\exp(-j\beta R_s)}{R_s}dz'+\int_{+s}^{s+h} I(z')\frac{\exp(-j\beta R_s)}{R_s}dz'$$

$$=-j\frac{4\pi}{R_c}\left\{\frac{V_s^e+C_1\sin\beta s-C_2\cos\beta s}{\sin\beta s}\right\}\cos\beta z. \quad (22b)$$

In (22)

$$R_c=(\Pi/\Delta)^{\frac{1}{2}}=376.7 \text{ ohms}\approx 120\pi \text{ ohms}. \quad (23)$$

As far as the writer knows, no methods exist for obtaining exact solutions to simultaneous integral equations of the type occurring here. It is assumed, however, that approximate results are available by first expanding as in previous papers,[6,8] and second, by introducing a suitable subterfuge to take cognizance of the rather obvious fact that the second and third integrals in (22) play a comparable role when it comes to finding the current in the vicinity of $z=s$. Proceeding then, as in other papers, (22a) and the following equation are identities:

$$I(z)=-\frac{j4\pi}{\Omega_h R_c}\{C_1\cos\beta z+C_2\sin\beta|z|\}-\frac{1}{\Omega_h}I(z)f_h(z)-\frac{1}{\Omega_h}\int_s^{s+h}\frac{I(z')e^{-j\beta R}-I(z)}{R}dz'$$

$$-\frac{1}{\Omega_h}\int_{-(s+h)}^{-s} I(z')\frac{e^{-j\beta R}}{R}dz'-\frac{1}{\Omega_h}\int_{-s}^{+s} I(z')\frac{e^{-j\beta R}}{R}dz'. \quad (24a)$$

Similarly, (22b) may be rewritten in the form

$$I(z)-\frac{-j4\pi}{\Omega_s R_c}\left\{\frac{V_s^e+C_1\sin\beta s-C_2\cos\beta s}{\sin\beta s}\right\}\cos\beta z-\frac{1}{\Omega_s}I(z)f_s(z)-\frac{1}{\Omega_s}\int_{-s}^{+s}\frac{I(z')e^{-j\beta R}-I(z)}{R}dz'$$

$$-\frac{1}{\Omega_s}\int_{-(s+h)}^{-s} I(z')\frac{e^{-j\beta R}}{R}dz'-\frac{1}{\Omega_s}\int_s^{s+h} I(z')\frac{e^{-j\beta R}}{R}dz'. \quad (24b)$$

The following notation is used:

$$\Omega_h=\ln 2h/a_h, \quad (25)$$

$$\Omega_s=\ln 4s/a_s, \quad (26)$$

$$R_h\approx R_s\approx R=|z-z'|, \quad (27)$$

$$f_h(z)=\ln(a_h/2h)\left\{\frac{[(s+h-z)^2+a_h^2]^{\frac{1}{2}}+(s+h-z)}{[(s-z)^2+a_h^2]^{\frac{1}{2}}+(s-z)}\right\}, \quad (28)$$

$$f_s(z)=\ln(a_s/4s)\left\{\frac{[(s-z)^2+a_s^2]^{\frac{1}{2}}+(s-z)}{[(s+z)^2+a_s^2]^{\frac{1}{2}}-(s+z)}\right\}. \quad (29)$$

Upon introducing the fact that the current vanishes at $z=(s+h)$,

$$I(z)=-\frac{j4\pi}{\Omega_h R_c}\{C_1(\cos\beta z-\cos\beta(s+h))+C_2(\sin\beta|z|-\sin\beta(s+h))\}-\frac{1}{\Omega_h}I(z)f_h(z)$$

$$-\frac{1}{\Omega_h}\int_s^{s+h}\frac{I(z')e^{-j\beta R}-I(z)}{R}dz'+\frac{1}{\Omega_h}\int_s^{s+h} I(z)\frac{\exp(-j\beta R_1)}{R_1}dz'-\frac{1}{\Omega_h}\left\{\int_{-(s+h)}^{-s} I(z')\frac{e^{-j\beta R}}{R}dz'\right.$$

$$\left.-\int_{-(s+h)}^{-s} I(z')\frac{\exp(-j\beta R_1)}{R_1}dz'+\int_{-s}^{+s} I(z')\frac{e^{-j\beta R}}{R}dz'-\int_{-s}^{+s} I(z')\frac{\exp(-j\beta R_1)}{R_1}dz'\right\}, \quad (30)$$

[8] Ronold King and Charles W. Harrison, Jr., "Mutual and Self-Impedance for Coupled Antennas," J. App. Phys. 15, 481–495 (1944).

where

$$R_1 \approx |s+h-z'|. \tag{31}$$

One selects

$$(I(z))_0\} = (I(-z))_0\} = \frac{-j4\pi}{\Omega_h R_c}\{C_1(\cos\beta z - \cos\beta(s+h)) + C_2(\sin\beta|z| - \sin\beta(s+h))\}, \tag{32a}$$

to represent the zeroth-order approximation for the distribution of current within intervals (1) and (4), and

$$(I(z))_0\} = (I(-z))_0\} = \frac{-j4\pi}{\Omega_s R_c}\left\{\frac{V_s^e + C_1\sin\beta s - C_2\cos\beta_s}{\sin\beta s}\right\}\cos\beta z, \tag{32b}$$

to represent the zeroth-order approximation for the distribution of current within intervals (2) and (3). Subject to certain limitations, these expressions may be employed in (24b) and (30) for the purpose of computing a first-order correction to the current $I(z)$. Referring to (30), it is evident that (32a) should be used in the term involving $f_h(z)$, and in the following four integrals. Similarly in (24b), (32b) should be substituted in the term involving $f_s(z)$, and in the following integral. However, it cannot be maintained that it is a legitimate procedure to substitute (32a) in the last two integrals of (24b), nor can (32b) be substituted in the last two integrals of (30). If this substitution is made, no integral having the coefficient $1/\Omega_h\Omega_s$ is assigned its proper significance in the analysis. To circumvent this difficulty, it is convenient to make the reasonably good approximation that the force on charge within interval (2), caused by the presence of charge within interval (1) may be correctly represented by assuming a current of the form

$$[I(z')]\} = [I(-z')]\} = I_{\max}\sin\beta(s+h-|z'|), \tag{33}$$

to prevail within interval (1). Here $I_{\max}$ is the maximum complex current along the antenna. (If $h<\lambda/4$, one writes (33) in the form

$$[I(z')] = (I_s/\sin\beta h)\sin\beta(s+h-|z'|), \tag{34}$$

where $I_s$ is the complex current at the driving point $z=s$.) Conversely, one selects the expression

$$[I(z')]\} = [I(-z')]\} = I_s\frac{\cos\beta z'}{\cos\beta s}, \tag{35}$$

to represent the current distribution within interval (2), when computing the actual distribution of current along the portion of antenna lying within interval (1). The form of (35) is chosen to agree with the form of the vector potential distribution (19b). Equation (33) should be substituted in the last two integrals of (24b) and Eq. (35) is used in the last two integrals of (30).

Now a negligible error is committed by assuming that $I_{\max}$ occurs precisely at $z=s+h-(\lambda/4)$. (The current in the vicinity of $\lambda/4$ from the free end of the antenna is slowly variant with respect to distance along the radiator, and may be taken as $I_{\max}$ for all practical purposes.) $I_{\max}$ may be obtained from (30) by setting $z=s+h-(\lambda/4)$ throughout. This gives one relation between $I_{\max}$ and $I_s$. Next (24b) may be specialized to obtain the driving point current $I_s$, by writing $z=s$ throughout. Thus a second relation between $I_{\max}$ and $I_s$ is obtained. These simultaneous equations yield $I_{\max}$ and $I_s$ explicitly. One now applies boundary condition (d) by equating (24b) to (30) at $z=s$. A further restriction is imposed on $C_1$ and $C_2$ by requiring a vanishing current at

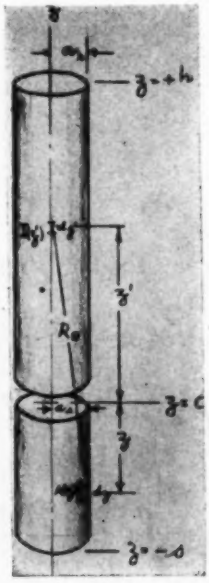

FIG. 2. Isolated asymmetrical dipole.

$z=s+h$ (boundary condition $e$). This is accomplished by writing $I(z)=0$ for $z=s+h$ in (24a). The currents appearing under the integral signs are given by (32a) and (35), respectively. Thus, one may determine the constants $C_1$ and $C_2$.

Having found $C_1$, $C_2$, $I_{max}$ as well as $I_s$, the input impedance $Z_s$ is available from

$$Z_s = V_s^e/I_s. \tag{36}$$

Persons desiring a numerical solution to the present problem will find that all integrals involved throughout the analysis may be readily evaluated in terms of the tabulated sine and cosine integral functions.

## PART II

### The Problem of the Isolated Asymmetrical Dipole

The antenna described is assumed to fall along the $z$ axis of a system of cylindrical coordinates, as shown in Fig. 2. The generator is located at $z=0$, and the ends of the antenna are defined by $z=+h$ and $z=-s$. The radius of the conductor over interval (1) $(0\leqq z\leqq h)$ is $a_h$. Over interval (2) $(0\geqq z\geqq -s)$ the radius is $a_s$.

Proceeding as in Part I, the vector potential along the surface of the antenna in the indicated intervals may be written

Interval (1)

$$A(z)=\frac{-j}{c}(k_1\cos\beta z+k_2\sin\beta z), \tag{37a}$$

Interval (2)

$$A(z)=\frac{-j}{c}(k_3\cos\beta z+k_4\sin\beta z). \tag{37b}$$

Applying boundary condition (a) Part I (at $z=0$),

$$V_0^e=k_2-k_4. \tag{38}$$

Here $V_0^e$ is the voltage applied across the input terminals to the antenna.

One now writes (37) in the form

Interval (1)

$$A(z)=\frac{-j}{c}(k_1\cos\beta z+k_2\sin\beta z), \tag{39a}$$

Interval (2)

$$A(z)=\frac{-j}{c}(k_3\cos\beta z+(k_2-V_0^e)\sin\beta z). \tag{39b}$$

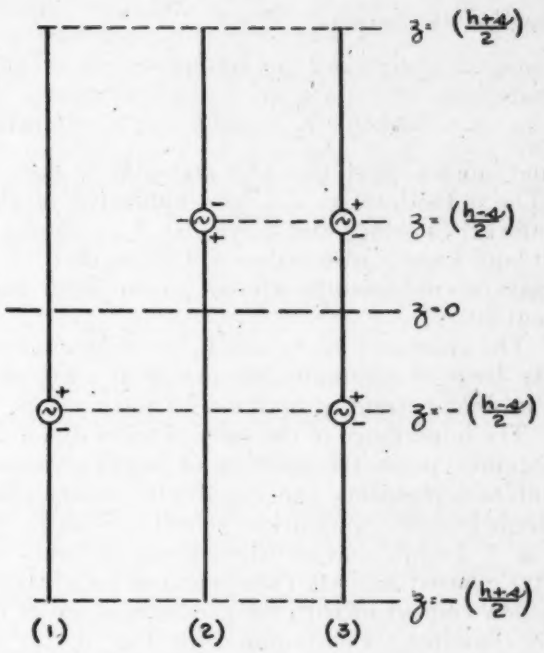


FIG. 3. Superposition of asymmetrical dipoles to obtain antenna with two generator drive.

The two simultaneous integral equations in the current are:

$$\int_{-s}^{0} I(z')\frac{\exp(-j\beta R_h)}{R_h}dz' + \int_{0}^{h} I(z')\frac{\exp(-j\beta R_h)}{R_h}dz' = \frac{-j4\pi}{R_c}(k_1\cos\beta z+k_2\sin\beta z) \tag{40a}$$

$$(0\leqq z\leqq +h).$$

$$\int_{-s}^{0} I(z')\frac{\exp(-j\beta R_s)}{R_s}dz' + \int_{0}^{h} I(z')\frac{\exp(-j\beta R_s)}{R_s}dz' = \frac{-j4\pi}{R_c}(k_3\cos\beta z+(k_2-V_0^e)\sin\beta z) \tag{40b}$$

$$(0\geqq z\geqq -s).$$

If the method of solution is to parallel the method already advanced, it is necessary to

assume the currents

$$[I(z')]=I_{1\max}\sin\beta(h-z'), \qquad (41a)$$

and

$$[I(z')]=I_{2\max}\sin\beta(s+z'). \qquad (41b)$$

and employ them like (33) and (35) in Part I. (The subscripts on $I_{\max}$ are indicative of the interval in which the particular $I_{\max}$ obtains.) If both $h$ and $s$ are less than $\lambda/4$ in length, $[I(z')]$ may be conveniently referred to the input current $I_0$.

The constants $k_1$, $k_2$ and $k_3$ are evaluated on the basis of continuity of current at $z=0$, and vanishing current at both $z=-s$ and $z=+h$.

The importance of the asymmetrical dipole as a prototype in the solution of more advanced antenna problems can hardly be overemphasized. For one application, reference is made to Fig. 3. Assume that an expression is available for $I(z)$ referred to $z=0$. (The origin of coordinates is now coincident with the geometrical center of the radiator.) Continuing with Fig. 3, (2) is derived from (1) by writing $-z$ for $z$ in $I(z)$. Next, one reverses the polarity of the driving generator in (2), and adds the currents in (1) to those in (2). The result is equivalent to the problem discussed in Part I, as shown in (3). The distance between generators is $h-s$. When $h-s\to 0$, a symmetrical center-driven antenna is obtained, having a voltage $2V_0$ applied across its input terminals. Assuming that the analysis of Part I will give poor results when $\Omega_a$ is small, the trouble will certainly be circumvented by super-imposing two asymmetrical dipoles in the way described.

Professor Ronold W. P. King of Harvard University made several useful suggestions which have been incorporated within the paper. The author hopes to use an expanded version of this report as part of a thesis on antennas to be submitted to fulfill one of the requirements for the D.Sc. Degree from Cruft Laboratory. The antenna sketches are by W. Thomson.

This article is presented in accordance with Navy Regulations governing the publication of professional articles by naval personnel. The opinions expressed are those of the writer, and are of course strictly unofficial.

---

## Correction of X-Ray Diffraction Intensities for Lorentz and Polarization Factors

M. J. Buerger and Gilbert E. Klein
*Massachusetts Institute of Technology, Cambridge, Massachusetts*

(Received February 3, 1945)

In crystal structure determination, it is necessary to apply corrections for Lorentz and polarization factors to the intensities of the x-ray diffraction spectra. Such corrections usually appear to take complicated form. It is shown that Lorentz factors can all be reduced to the comparatively simple form, $L=(1/S)\cdot(1/\sin\tau)$, where $S$ is a scale factor, constant for a particular recorded level of the reciprocal lattice, but differing in form depending on the method of recording. The factor can be eliminated from subsequent computation of corrections by proper timing of the photographs of the levels of the reciprocal lattice, and then all photographs have the same simple Lorentz correction, namely $\sin\tau$. The polarization factor, on the other hand, depends only on the reciprocal lattice coördinate, $\sigma$, and is independent of method of recording. Six tables are provided for simplifying the routine computation of Lorentz and polarization corrections, and the methods advocated for correction are illustrated by examples.

### INTRODUCTION

WHEN determining the positions of atoms in crystals, either by trial and error procedures or by employing any of the Fourier syntheses, it is necessary to make use of the relation,

$$I_0\sim L\cdot p\cdot F^2, \qquad (1)$$

for each reflection $hkl$. Here, $I_0$=the intensity of the reflection, $L$=the Lorentz factor for the reflection, $p$=the polarization factor for the reflection, and $F$=the structure factor for the reflection. In the Fourier syntheses, the $F$'s or their squares are the coefficients of a Fourier series. The diffraction experiment provides a series of $I$'s, and it is necessary to compute $F$'s from them with relation (1). When using trial and error procedures, it is customary to compute $I$ for each reflection of the trial structure and compare it with the experimentally observed $I$. In either case, it is necessary to apply a factor $L\cdot p$ for each reflection in order to obtain the desired list of computed $F$'s or $I$'s.

Lu[1] has recently presented a chart method of finding the correction for transforming the $I$'s of equi-inclination Weissenberg photographs to $F$'s for Fourier syntheses. One of us had already outlined[2] a much more general method of obtaining the correction. This method can be applied to any experimental procedure employing a rotating crystal, regardless of the inclination of the x-ray beam to the crystal rotation axis, and regardless of the angle of the diffraction cone. In this paper, a more detailed discussion of the application of this method is given, and appropriate tables of important functions used with it are provided.

## THE LORENTZ FACTOR

The general form of the Lorentz factor for diffraction methods employing a rotating crystal[2] is

$$L=1/\cos\mu\cos\nu\sin\Upsilon, \tag{2}$$

where $\mu$, $\nu$ and $\Upsilon$ have their usual significances.[3] This general form is necessary when general inclinations of the x-ray beam and diffraction cone are used. The only common instance of this occurs with the de Jong-Bouman method. The general expression reduces to the following special cases:

Normal beam, $\mu=0$:

$$L=1/\cos\mu\sin\Upsilon, \tag{3}$$

(rotating-crystal, oscillating crystal, normal-beam Weissenberg and Sauter methods).

Flat cone, $\nu=0$:

$$L=1/\cos\nu\sin\Upsilon, \tag{4}$$

(chiefly flat-cone Sauter method).

Equi-inclination, $\mu=-\nu$
Anti-equi-inclination, $\mu=\nu$
$$L=1/\cos^2\mu\sin\Upsilon \tag{5}$$

(chiefly Weissenberg method).

Each of these has the form

$$L=(1/S)\cdot(1/\sin\Upsilon), \tag{6}$$

where $S$ is a level-scale factor, constant for any level, but differing in form, as indicated in (2)–(5), with the various schemes of inclining the beam and diffraction cones.

When determining x-ray diffraction intensities by photographically recording the diffracted radiation (which is currently the common way of determining diffracted x-ray intensities), the intensity recorded on the photograph is proportional to the time of exposure, $t$, and the diffracted intensity, $I_0$:

$$I\sim tI_0. \tag{7}$$

Combining this with (1):

$$I\sim tLpF^2. \tag{8}$$

Substituting for $L$ in (8) from (6) gives,

$$I\sim[t(1/S)(1/\sin\Upsilon)]pF^2. \tag{9}$$

When working with a photographic diffraction method which records only one level at a time, such as the Weissenberg, de Jong-Bouman, Sauter, or precession methods, the simplest way of dealing with the Lorentz factor correction can be seen by combining it with the time factor indicated by (9), so that the time-Lorentz factor is

$$tL=t\cdot(1/S)(1/\sin\Upsilon). \tag{10}$$

It is evident that by appropriately selecting $t$ for recording a particular level, the product $t(1/S)$ can be made unity. To accomplish this, an exposure time must be selected so that

$$t=S. \tag{11}$$

The time of exposure, $t$, can be scaled up by any constant $T_0$, provided that the same constant is applied to the exposures of all levels. The length of time, $T_0$, is conveniently made the time of exposure for the zero level. If this is done, the intensity on the photographic film is

$$I\sim T_0t(1/S)(1/\sin\Upsilon)pF^2. \tag{12}$$

Since $t$ is made equal to $S$ by appropriately timing the exposures, and since $T_0$ is a constant for all exposures, (12) reduces to

$$I\sim(1/\sin\Upsilon)pF^2. \tag{13}$$

The required computation for each reflection is indicated by solving (13) for $F^2$, namely

$$F^2\sim\sin\Upsilon(1/p)I. \tag{14}$$

The computation requires one to have on hand only a table of sines, in degrees and decimals, and a table of the reciprocal of the polarization factor.

[1] Chia-Si Lu, Rev. Sci. Inst. **14**, 331–335 (1943).
[2] M. J. Buerger, Proc. Nat. Acad. Sci. **26**, 637–642 (1940).
[3] M. J. Buerger, *X-Ray Crystallography* (John Wiley & Sons, Inc., New York, 1942), p. 297.

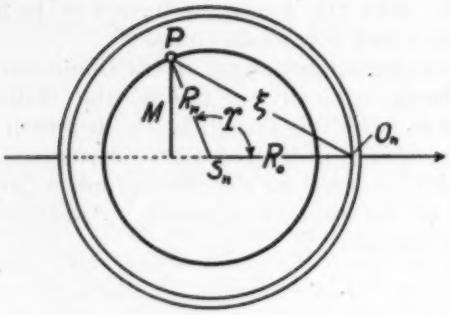


FIG. 1. The relation between quantities useful in the computation of the Lorentz factor for the de Jong-Bouman and precession methods.

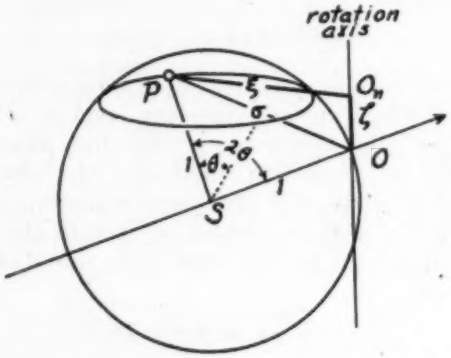


FIG. 2. The relation between quantities useful in the computation of the polarization factor.

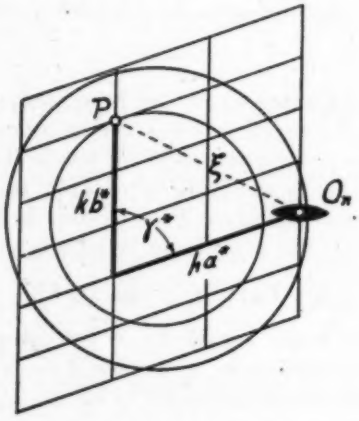


FIG. 3. Resolution of the coordinate $\xi$ into components along the reciprocal lattice axes, for the case of a level having twofold symmetry.

To apply the time-Lorentz factor, one proceeds as follows: Before starting the recording of levels, the appropriate level-scale factors are computed for each level as a function of the level coordinate, $\zeta$. For the several cases listed in (2)–(5), the factors are

General inclination:

$$S=\cos\mu\cos\nu\cos\sin^{-1}(\sin\nu-\zeta)\cos\nu. \quad (15)$$

($\nu$ is arbitrarily selected, and commonly held constant at 45° for de Jong-Bouman photographs.)

Normal-beam:

$$S=\cos\nu=(1-\zeta^2)^{\frac{1}{2}}. \quad (15')$$

Flat-cone:

$$S=\cos\mu=(1-\zeta^2)^{\frac{1}{2}}. \quad (16)$$

Equi-inclination:

$$S=\cos^2\mu=(1-[\zeta/2]^2)^{\frac{1}{2}}. \quad (17)$$

In making the exposures, each level is timed so that $t=T_0S$, where $T_0$ is the time of exposure of the zero level. This procedure leaves the correcting of the Lorentz factor merely a matter of applying a correction which is the same for any level, namely sin $\Upsilon$.

For rotating-crystal and oscillating-crystal photographs, the levels are not usually recorded separately and it is thus impossible to take advantage of eliminating the level-scale factor by time cancellation. For these photographs, the normal beam correction, $S=\cos\nu=(1-\zeta^2)^{\frac{1}{2}}$ must be applied according to level coordinate $\zeta$, and also the sin $\Upsilon$-factor must be applied according to the coordinate $\Upsilon$.

When the photographs are all made, the value of sin $\Upsilon$ can be found from the position of the reflection on the film. For cylindrical films placed coaxial with the rotation axis, such as employed in the rotating-crystal method, oscillating-crystal method, and the Weissenberg method, $\Upsilon$ is proportional to the distance of the reflection from the center line of the film. For cameras of the standard diameter,[4] 57.3 mm, $\Upsilon=2x^0$ where $x$ is the distance of the reflection from the center of the film, as measured in millimeters.

For de Jong-Bouman photographs, $\Upsilon$ is not so easily found. To make the correction for de Jong-Bouman photographs (and also for precession photographs), one must draw a circle[2] (Fig. 1) the size of the reflecting circle (to the same scale as the photograph) and place it so that, with the origin correctly located, the circle touches the reflection in question. The time-Lorentz factor is then

$$tL=1/\sin\Upsilon=R_n/M, \quad (18)$$

and the correction is $M/R_n=M/\cos\nu$.

[4] M. J. Buerger, see reference 3, p. 223.

For precession photographs,[5] the correction for the sin $\Upsilon$-part of the Lorentz factor is made as above. The level-scale correction, however, is

$$S=\sin\bar{\mu}\cos\bar{\mu}=\tfrac{1}{2}\sin 2\bar{\mu}, \qquad (19)$$

and level photographs should be timed accordingly.

### THE POLARIZATION FACTOR

The polarization factor, $p$, is invariant with the method of recording, and depends only on the deviation angle, $2\theta$:

$$p=(1+\cos^2 2\theta)/2. \qquad (20)$$

This factor can be computed and tabulated as a function of sin $\theta$ for the reflection. It is somewhat more straightforward and convenient to have it available as a function of some appropriate reciprocal lattice quantities. The transformation from sin $\theta$ to reciprocal lattice dimensions can be found with the aid of Fig. 2, which shows the direct x-ray beam enveloped by its sphere of reflection, and inclined at a general angle to the crystal rotation axis. The diffracted beam is $SP$ and makes an angle $2\theta$ with the direct beam $SO$. Since triangle $OSP$ has two sides which are the unit radii of the sphere, it is isosceles, and hence, $\sin\theta=\sigma/2$. It is therefore evident that if a tabulation of (20) for the argument sin $\theta$ is prepared, it can easily be converted to the argument $\sigma$ by doubling the value of the argument for each value of the function.

It should also be noted in Fig. 2 that $\sigma$ can be resolved into axial and radial components $\zeta$ and $\xi$, so that $\sigma$ can be computed for each reflection as a function of its reciprocal lattice coordinates from the relation

$$\sigma=(\zeta^2+\xi^2)^{\frac{1}{2}}. \qquad (21)$$

The term $\xi^2$ is a function of the reciprocal lattice translations of the level. If the level has no symmetry, the function is unduly complicated and should be found graphically. When the level has axial symmetry, the expression simplifies to the following forms:

| Level symmetry | $\xi^2$ | |
|---|---|---|
| 2-fold Fig. 3 | $h^2[a^{*2}]+k^2[b^{*2}]-hk[2a^*b^*\cos\gamma^*]$ | (22) |
| 2 $mm$ ($\gamma=90°$) | $h^2[a^{*2}]+k^2[b^{*2}]$ | (23) |
| 3-fold or 6-fold ($\gamma=120°$, $a^*=b^*$) | $(h^2+k^2+hk)[a^{*2}]$ | (24) |
| 4-fold ($\gamma=90°$, $a^*=b^*$) | $(h^2+k^2)[a^{*2}]$. | (25) |

The terms in brackets are constants for the crystal. Convenient tabulations of the functions $(h^2+k^2)$ for 4-fold levels and $(h^2+k^2+hk)$ for 6-fold and 3-fold levels are given in Tables I and II.

### APPLICATION

According to the discussion just given, the Lorentz factor is a function of $\Upsilon$ only (after the level-scale factor has been taken care of by the timing of the exposure), while the polarization factor is a function of $\sigma$ only. Success in computing Lorentz and polarization factors or their corrections depends upon the recognition that these two factor are conveniently referred to different coordinate systems.

To allow for Lorentz and polarization factors, one takes account of three things: (a) timing of the exposure of the level to eliminate the level-scale factor; (b) the sin $\Upsilon$ part of the Lorentz factor; (c) and the polarization factor, $(1+\cos^2 2\theta)/2$. The first is part of the experimental procedure and calls for different exposures for different levels. Since the several x-ray exposures must be accurately timed anyway, this does not give rise to additional trouble. The second part involves measuring the distance of the reflection, in millimeters, from the center line of the film, multiplying it by two to convert it to the angle $\Upsilon$, and looking up the factor in a table of sines. The third is the most troublesome of all, even though the value of the function varies only from 0.5 to 1.0. It involves computing, or graphically determining the reciprocal lattice distance, $\sigma$, for each point on the reciprocal lattice, and finding

[5] M. J. Buerger, "The photography of the reciprocal lattice," ASXRED Monograph Number 1 (1944).

TABLE I. $h^2+k^2$.

| h \ k | 0 | 1 | 2 | 3 | 4 | 5 | 6 | 7 | 8 | 9 | 10 | 11 | 12 | 13 | 14 | 15 | 16 | 17 | 18 | 19 | 20 | 21 | 22 | 23 | 24 | 25 | 26 | 27 | 28 | 29 | 30 | h \ k |
|---|---|---|---|---|---|---|---|---|---|---|---|---|---|---|---|---|---|---|---|---|---|---|---|---|---|---|---|---|---|---|---|---|
| 0 | 0 | 1 | 4 | 9 | 16 | 25 | 36 | 49 | 64 | 81 | 100 | 121 | 144 | 169 | 196 | 225 | 256 | 289 | 324 | 361 | 400 | 441 | 484 | 529 | 576 | 625 | 676 | 729 | 784 | 841 | 900 | 0 |
| 1 | 1 | 2 | 5 | 10 | 17 | 26 | 37 | 50 | 65 | 82 | 101 | 122 | 145 | 170 | 197 | 226 | 257 | 290 | 325 | 362 | 401 | 442 | 485 | 530 | 577 | 626 | 677 | 730 | 785 | 842 | 901 | 1 |
| 2 | 4 | 5 | 8 | 13 | 20 | 29 | 40 | 53 | 68 | 85 | 104 | 125 | 148 | 173 | 200 | 229 | 260 | 293 | 328 | 365 | 404 | 445 | 488 | 533 | 580 | 629 | 680 | 733 | 788 | 845 | 904 | 2 |
| 3 | 9 | 10 | 13 | 18 | 25 | 34 | 45 | 58 | 73 | 90 | 109 | 130 | 153 | 178 | 205 | 234 | 265 | 298 | 333 | 370 | 409 | 450 | 493 | 538 | 585 | 634 | 685 | 738 | 793 | 850 | 909 | 3 |
| 4 | 16 | 17 | 20 | 25 | 32 | 41 | 52 | 65 | 80 | 97 | 116 | 137 | 160 | 185 | 212 | 241 | 272 | 305 | 340 | 377 | 416 | 457 | 500 | 545 | 592 | 641 | 692 | 745 | 800 | 857 | 916 | 4 |
| 5 | 25 | 26 | 29 | 34 | 41 | 50 | 61 | 74 | 89 | 106 | 125 | 146 | 169 | 194 | 221 | 250 | 281 | 314 | 349 | 386 | 425 | 466 | 509 | 554 | 601 | 650 | 701 | 754 | 809 | 866 | 925 | 5 |
| 6 | 36 | 37 | 40 | 45 | 52 | 61 | 72 | 85 | 100 | 117 | 136 | 157 | 180 | 205 | 232 | 261 | 292 | 325 | 360 | 397 | 436 | 477 | 520 | 565 | 612 | 661 | 712 | 765 | 820 | 877 | 936 | 6 |
| 7 | 49 | 50 | 53 | 58 | 65 | 74 | 85 | 98 | 113 | 130 | 149 | 170 | 193 | 218 | 245 | 274 | 305 | 338 | 373 | 410 | 449 | 490 | 533 | 578 | 625 | 674 | 725 | 778 | 833 | 890 | 949 | 7 |
| 8 | 64 | 65 | 68 | 73 | 80 | 89 | 100 | 113 | 128 | 145 | 164 | 185 | 208 | 233 | 260 | 289 | 320 | 353 | 388 | 425 | 464 | 505 | 548 | 593 | 640 | 689 | 740 | 793 | 848 | 905 | 964 | 8 |
| 9 | 81 | 82 | 85 | 90 | 97 | 106 | 117 | 130 | 145 | 162 | 181 | 202 | 225 | 250 | 277 | 306 | 337 | 370 | 405 | 442 | 481 | 522 | 565 | 610 | 657 | 706 | 757 | 810 | 865 | 922 | 981 | 9 |
| 10 | 100 | 101 | 104 | 109 | 116 | 125 | 136 | 149 | 164 | 181 | 200 | 221 | 244 | 269 | 296 | 325 | 356 | 389 | 424 | 461 | 500 | 541 | 584 | 629 | 676 | 725 | 776 | 829 | 884 | 941 | 1000 | 10 |
| 11 | 121 | 122 | 125 | 130 | 137 | 146 | 157 | 170 | 185 | 202 | 221 | 242 | 265 | 290 | 317 | 346 | 377 | 410 | 445 | 482 | 521 | 562 | 605 | 650 | 697 | 746 | 797 | 850 | 905 | 962 | 1021 | 11 |
| 12 | 144 | 145 | 148 | 153 | 160 | 169 | 180 | 193 | 208 | 225 | 244 | 265 | 288 | 313 | 340 | 369 | 400 | 433 | 468 | 505 | 544 | 585 | 628 | 673 | 720 | 769 | 820 | 873 | 928 | 985 | 1044 | 12 |
| 13 | 169 | 170 | 173 | 178 | 185 | 194 | 205 | 218 | 233 | 250 | 269 | 290 | 313 | 338 | 365 | 394 | 425 | 458 | 493 | 530 | 569 | 610 | 653 | 698 | 745 | 794 | 845 | 898 | 953 | 1010 | 1069 | 13 |
| 14 | 196 | 197 | 200 | 205 | 212 | 221 | 232 | 245 | 260 | 277 | 296 | 317 | 340 | 365 | 392 | 421 | 452 | 485 | 520 | 557 | 596 | 637 | 680 | 725 | 772 | 821 | 872 | 925 | 980 | 1037 | 1096 | 14 |
| 15 | 225 | 226 | 229 | 234 | 241 | 250 | 261 | 274 | 289 | 306 | 325 | 346 | 369 | 394 | 421 | 450 | 481 | 514 | 549 | 586 | 625 | 666 | 709 | 754 | 801 | 850 | 901 | 954 | 1009 | 1066 | 1125 | 15 |
| 16 | 256 | 257 | 260 | 265 | 272 | 281 | 292 | 305 | 320 | 337 | 356 | 377 | 400 | 425 | 452 | 481 | 512 | 545 | 580 | 617 | 656 | 697 | 740 | 785 | 832 | 881 | 932 | 985 | 1040 | 1097 | 1156 | 16 |
| 17 | 289 | 290 | 293 | 298 | 305 | 314 | 325 | 338 | 353 | 370 | 389 | 410 | 433 | 458 | 485 | 514 | 545 | 578 | 613 | 650 | 689 | 730 | 773 | 818 | 865 | 914 | 965 | 1018 | 1073 | 1130 | 1189 | 17 |
| 18 | 324 | 325 | 328 | 333 | 340 | 349 | 360 | 373 | 388 | 405 | 424 | 445 | 468 | 493 | 520 | 549 | 580 | 613 | 648 | 685 | 724 | 765 | 808 | 853 | 900 | 949 | 1000 | 1053 | 1108 | 1165 | 1224 | 18 |
| 19 | 361 | 362 | 365 | 370 | 377 | 386 | 397 | 410 | 425 | 442 | 461 | 482 | 505 | 530 | 557 | 586 | 617 | 650 | 685 | 722 | 761 | 802 | 845 | 890 | 937 | 986 | 1037 | 1090 | 1145 | 1202 | 1261 | 19 |
| 20 | 400 | 401 | 404 | 409 | 416 | 425 | 436 | 449 | 464 | 481 | 500 | 521 | 544 | 569 | 596 | 625 | 656 | 689 | 724 | 761 | 800 | 841 | 884 | 929 | 976 | 1025 | 1076 | 1129 | 1184 | 1241 | 1300 | 20 |
| 21 | 441 | 442 | 445 | 450 | 457 | 466 | 477 | 490 | 505 | 522 | 541 | 562 | 585 | 610 | 637 | 666 | 697 | 730 | 765 | 802 | 841 | 882 | 925 | 970 | 1017 | 1066 | 1117 | 1170 | 1225 | 1282 | 1341 | 21 |
| 22 | 484 | 485 | 488 | 493 | 500 | 509 | 520 | 533 | 548 | 565 | 584 | 605 | 628 | 653 | 680 | 709 | 740 | 773 | 808 | 845 | 884 | 925 | 968 | 1013 | 1060 | 1109 | 1160 | 1213 | 1268 | 1325 | 1384 | 22 |
| 23 | 529 | 530 | 533 | 538 | 545 | 554 | 565 | 578 | 593 | 610 | 629 | 650 | 673 | 698 | 725 | 754 | 785 | 818 | 853 | 890 | 929 | 970 | 1013 | 1058 | 1105 | 1154 | 1205 | 1258 | 1313 | 1370 | 1429 | 23 |
| 24 | 576 | 577 | 580 | 585 | 592 | 601 | 612 | 625 | 640 | 657 | 676 | 697 | 720 | 745 | 772 | 801 | 832 | 865 | 900 | 937 | 976 | 1017 | 1060 | 1105 | 1152 | 1201 | 1252 | 1305 | 1360 | 1417 | 1476 | 24 |
| 25 | 625 | 626 | 629 | 634 | 641 | 650 | 661 | 674 | 689 | 706 | 725 | 746 | 769 | 794 | 821 | 850 | 881 | 914 | 949 | 986 | 1025 | 1066 | 1109 | 1154 | 1201 | 1250 | 1301 | 1354 | 1409 | 1466 | 1525 | 25 |
| 26 | 676 | 677 | 680 | 685 | 692 | 701 | 712 | 725 | 740 | 757 | 776 | 797 | 820 | 845 | 872 | 901 | 932 | 965 | 1000 | 1037 | 1076 | 1117 | 1160 | 1205 | 1252 | 1301 | 1352 | 1405 | 1460 | 1517 | 1576 | 26 |
| 27 | 729 | 730 | 733 | 738 | 745 | 754 | 765 | 778 | 793 | 810 | 829 | 850 | 873 | 898 | 925 | 954 | 985 | 1018 | 1053 | 1090 | 1129 | 1170 | 1213 | 1258 | 1305 | 1354 | 1405 | 1458 | 1513 | 1570 | 1629 | 27 |
| 28 | 784 | 785 | 788 | 793 | 800 | 809 | 820 | 833 | 848 | 865 | 884 | 905 | 928 | 953 | 980 | 1009 | 1040 | 1073 | 1108 | 1145 | 1184 | 1225 | 1268 | 1313 | 1360 | 1409 | 1460 | 1513 | 1568 | 1625 | 1684 | 28 |
| 29 | 841 | 842 | 845 | 850 | 857 | 866 | 877 | 890 | 905 | 922 | 941 | 962 | 985 | 1010 | 1037 | 1066 | 1097 | 1130 | 1165 | 1202 | 1241 | 1282 | 1325 | 1370 | 1417 | 1466 | 1517 | 1570 | 1625 | 1682 | 1741 | 29 |
| 30 | 900 | 901 | 904 | 909 | 916 | 925 | 936 | 949 | 964 | 981 | 1000 | 1021 | 1044 | 1069 | 1096 | 1125 | 1156 | 1189 | 1224 | 1261 | 1300 | 1341 | 1384 | 1429 | 1476 | 1525 | 1576 | 1629 | 1684 | 1741 | 1800 | 30 |

TABLE II. $h^2+k^2+hk$.

| h \ k | 0 | 1 | 2 | 3 | 4 | 5 | 6 | 7 | 8 | 9 | 10 | 11 | 12 | 13 | 14 | 15 | 16 | 17 | 18 | 19 | 20 | 21 | 22 | 23 | 24 | 25 | 26 | 27 | 28 | 29 | 30 | h \ k |
|---|---|---|---|---|---|---|---|---|---|---|---|---|---|---|---|---|---|---|---|---|---|---|---|---|---|---|---|---|---|---|---|---|
| 0 | 0 | 1 | 4 | 9 | 16 | 25 | 36 | 49 | 64 | 81 | 100 | 121 | 144 | 169 | 196 | 225 | 256 | 289 | 324 | 361 | 400 | 441 | 484 | 529 | 576 | 625 | 676 | 729 | 784 | 841 | 900 | 0 |
| 1 | 1 | 3 | 7 | 13 | 21 | 31 | 43 | 57 | 73 | 91 | 111 | 133 | 157 | 183 | 211 | 241 | 273 | 307 | 343 | 381 | 421 | 463 | 507 | 553 | 601 | 651 | 703 | 757 | 813 | 871 | 931 | 1 |
| 2 | 4 | 7 | 12 | 19 | 28 | 39 | 52 | 67 | 84 | 103 | 124 | 147 | 172 | 199 | 228 | 259 | 292 | 327 | 364 | 403 | 444 | 487 | 532 | 579 | 628 | 679 | 732 | 787 | 844 | 903 | 964 | 2 |
| 3 | 9 | 13 | 19 | 27 | 37 | 49 | 63 | 79 | 97 | 117 | 139 | 163 | 189 | 217 | 247 | 279 | 313 | 349 | 387 | 427 | 469 | 513 | 559 | 607 | 657 | 709 | 763 | 819 | 877 | 937 | 999 | 3 |
| 4 | 16 | 21 | 28 | 37 | 48 | 61 | 76 | 93 | 112 | 133 | 156 | 181 | 208 | 237 | 268 | 301 | 336 | 373 | 412 | 453 | 496 | 541 | 588 | 637 | 688 | 741 | 796 | 853 | 912 | 973 | 1036 | 4 |
| 5 | 25 | 31 | 39 | 49 | 61 | 75 | 91 | 109 | 129 | 151 | 175 | 201 | 229 | 259 | 291 | 325 | 361 | 399 | 439 | 481 | 525 | 571 | 619 | 669 | 721 | 775 | 831 | 889 | 949 | 1011 | 1075 | 5 |
| 6 | 36 | 43 | 52 | 63 | 76 | 91 | 108 | 127 | 148 | 171 | 196 | 223 | 252 | 283 | 316 | 351 | 388 | 427 | 468 | 511 | 556 | 603 | 652 | 703 | 756 | 811 | 868 | 927 | 988 | 1051 | 1116 | 6 |
| 7 | 49 | 57 | 67 | 79 | 93 | 109 | 127 | 147 | 169 | 193 | 219 | 247 | 277 | 309 | 343 | 379 | 417 | 457 | 499 | 543 | 589 | 637 | 687 | 739 | 793 | 849 | 907 | 967 | 1029 | 1093 | 1159 | 7 |
| 8 | 64 | 73 | 84 | 97 | 112 | 129 | 148 | 169 | 192 | 217 | 244 | 273 | 304 | 337 | 372 | 409 | 448 | 489 | 532 | 577 | 624 | 673 | 724 | 777 | 832 | 889 | 948 | 1009 | 1072 | 1137 | 1204 | 8 |
| 9 | 81 | 91 | 103 | 117 | 133 | 151 | 171 | 193 | 217 | 243 | 271 | 301 | 333 | 367 | 403 | 441 | 481 | 523 | 567 | 613 | 661 | 711 | 763 | 817 | 873 | 931 | 991 | 1053 | 1117 | 1183 | 1251 | 9 |
| 10 | 100 | 111 | 124 | 139 | 156 | 175 | 196 | 219 | 244 | 271 | 300 | 331 | 364 | 399 | 436 | 475 | 516 | 559 | 604 | 651 | 700 | 751 | 804 | 859 | 916 | 975 | 1036 | 1099 | 1164 | 1231 | 1300 | 10 |
| 11 | 121 | 133 | 147 | 163 | 181 | 201 | 223 | 247 | 273 | 301 | 331 | 363 | 397 | 433 | 471 | 511 | 553 | 597 | 643 | 691 | 741 | 793 | 847 | 903 | 961 | 1021 | 1083 | 1147 | 1213 | 1281 | 1351 | 11 |
| 12 | 144 | 157 | 172 | 189 | 208 | 229 | 252 | 277 | 304 | 333 | 364 | 397 | 432 | 469 | 508 | 549 | 592 | 637 | 684 | 733 | 784 | 837 | 892 | 949 | 1008 | 1069 | 1132 | 1197 | 1264 | 1333 | 1404 | 12 |
| 13 | 169 | 183 | 199 | 217 | 237 | 259 | 283 | 309 | 337 | 367 | 399 | 433 | 469 | 507 | 547 | 589 | 633 | 679 | 727 | 777 | 829 | 883 | 939 | 997 | 1057 | 1119 | 1183 | 1249 | 1317 | 1387 | 1459 | 13 |
| 14 | 196 | 211 | 228 | 247 | 268 | 291 | 316 | 343 | 372 | 403 | 436 | 471 | 508 | 547 | 588 | 631 | 676 | 723 | 772 | 823 | 876 | 931 | 988 | 1047 | 1108 | 1171 | 1236 | 1303 | 1372 | 1443 | 1516 | 14 |
| 15 | 225 | 241 | 259 | 279 | 301 | 325 | 351 | 379 | 409 | 441 | 475 | 511 | 549 | 589 | 631 | 675 | 721 | 769 | 819 | 871 | 925 | 981 | 1039 | 1099 | 1161 | 1225 | 1291 | 1359 | 1429 | 1501 | 1575 | 15 |
| 16 | 256 | 273 | 292 | 313 | 336 | 361 | 388 | 417 | 448 | 481 | 516 | 553 | 592 | 633 | 676 | 721 | 768 | 817 | 868 | 921 | 976 | 1033 | 1092 | 1153 | 1216 | 1281 | 1348 | 1417 | 1488 | 1561 | 1636 | 16 |
| 17 | 289 | 307 | 327 | 349 | 373 | 399 | 427 | 457 | 489 | 523 | 559 | 597 | 637 | 679 | 723 | 769 | 817 | 867 | 919 | 973 | 1029 | 1087 | 1147 | 1209 | 1273 | 1339 | 1407 | 1477 | 1549 | 1623 | 1699 | 17 |
| 18 | 324 | 343 | 364 | 387 | 412 | 439 | 468 | 499 | 532 | 567 | 604 | 643 | 684 | 727 | 772 | 819 | 868 | 919 | 972 | 1027 | 1084 | 1143 | 1204 | 1267 | 1332 | 1399 | 1468 | 1539 | 1612 | 1687 | 1764 | 18 |
| 19 | 361 | 381 | 403 | 427 | 453 | 481 | 511 | 543 | 577 | 613 | 651 | 691 | 733 | 777 | 823 | 871 | 921 | 973 | 1027 | 1083 | 1141 | 1201 | 1263 | 1327 | 1393 | 1461 | 1531 | 1603 | 1677 | 1753 | 1831 | 19 |
| 20 | 400 | 421 | 444 | 469 | 496 | 525 | 556 | 589 | 624 | 661 | 700 | 741 | 784 | 829 | 876 | 925 | 976 | 1029 | 1084 | 1141 | 1200 | 1261 | 1324 | 1389 | 1456 | 1525 | 1596 | 1669 | 1744 | 1821 | 1900 | 20 |
| 21 | 441 | 463 | 487 | 513 | 541 | 571 | 603 | 637 | 673 | 711 | 751 | 793 | 837 | 883 | 931 | 981 | 1033 | 1087 | 1143 | 1201 | 1261 | 1323 | 1387 | 1453 | 1521 | 1591 | 1663 | 1737 | 1813 | 1891 | 1971 | 21 |
| 22 | 484 | 507 | 532 | 559 | 588 | 619 | 652 | 687 | 724 | 763 | 804 | 847 | 892 | 939 | 988 | 1039 | 1092 | 1147 | 1204 | 1263 | 1324 | 1387 | 1452 | 1519 | 1588 | 1659 | 1732 | 1807 | 1884 | 1963 | 2044 | 22 |
| 23 | 529 | 553 | 579 | 607 | 637 | 669 | 703 | 739 | 777 | 817 | 859 | 903 | 949 | 997 | 1047 | 1099 | 1153 | 1209 | 1267 | 1327 | 1389 | 1453 | 1519 | 1587 | 1657 | 1729 | 1803 | 1879 | 1957 | 2037 | 2119 | 23 |
| 24 | 576 | 601 | 628 | 657 | 688 | 721 | 756 | 793 | 832 | 873 | 916 | 961 | 1008 | 1057 | 1108 | 1161 | 1216 | 1273 | 1332 | 1393 | 1456 | 1521 | 1588 | 1657 | 1728 | 1801 | 1876 | 1953 | 2032 | 2113 | 2196 | 24 |
| 25 | 625 | 651 | 679 | 709 | 741 | 775 | 811 | 849 | 889 | 931 | 975 | 1021 | 1069 | 1119 | 1171 | 1225 | 1281 | 1339 | 1399 | 1461 | 1525 | 1591 | 1659 | 1729 | 1801 | 1875 | 1951 | 2029 | 2109 | 2191 | 2275 | 25 |
| 26 | 676 | 703 | 732 | 763 | 796 | 831 | 868 | 907 | 948 | 991 | 1036 | 1083 | 1132 | 1183 | 1236 | 1291 | 1348 | 1407 | 1468 | 1531 | 1596 | 1663 | 1732 | 1803 | 1876 | 1951 | 2028 | 2107 | 2188 | 2271 | 2356 | 26 |
| 27 | 729 | 757 | 787 | 819 | 853 | 889 | 927 | 967 | 1009 | 1053 | 1099 | 1147 | 1197 | 1249 | 1303 | 1359 | 1417 | 1477 | 1539 | 1603 | 1669 | 1737 | 1807 | 1879 | 1953 | 2029 | 2107 | 2187 | 2269 | 2353 | 2439 | 27 |
| 28 | 784 | 813 | 844 | 877 | 912 | 949 | 988 | 1029 | 1072 | 1117 | 1164 | 1213 | 1264 | 1317 | 1372 | 1429 | 1488 | 1549 | 1612 | 1677 | 1744 | 1813 | 1884 | 1957 | 2032 | 2109 | 2188 | 2269 | 2352 | 2437 | 2524 | 28 |
| 29 | 841 | 871 | 903 | 937 | 973 | 1011 | 1051 | 1093 | 1137 | 1183 | 1231 | 1281 | 1333 | 1387 | 1443 | 1501 | 1561 | 1623 | 1687 | 1753 | 1821 | 1891 | 1963 | 2037 | 2113 | 2191 | 2271 | 2353 | 2437 | 2523 | 2611 | 29 |
| 30 | 900 | 931 | 964 | 999 | 1036 | 1075 | 1116 | 1159 | 1204 | 1251 | 1300 | 1351 | 1404 | 1459 | 1516 | 1575 | 1636 | 1699 | 1764 | 1831 | 1900 | 1971 | 2044 | 2119 | 2196 | 2275 | 2356 | 2439 | 2524 | 2611 | 2700 | 30 |

from this value the value of the function $2/(1+\cos^2 2\theta)$.

In order to facilitate this last step, we have prepared tables of the polarization factor correction, for the argument $\sigma$ and also sin $\theta$. We also present tables which combine Lorentz and polarization factor corrections for zero-level photographs taken under conditions $\mu=0$. *These particular tables should not be used for zero-level photographs where $\mu\neq 0$, nor for non-zero-level photographs.* The tables fall into the following categories:

| | | | Table |
|---|---|---|---|
| For transposing $I$ to $F$ (useful for deriving $F$'s for Fourier series) | as functions of $\sigma$ | $1/L\cdot p$ for zero levels, $\mu=0$ | III |
| | | $1/p$ for $n$-levels | IV |
| | as functions of sin $\theta$ | $1/L\cdot p$ for zero levels, $\mu=0$ | V |
| | | $1/p$ for $n$-levels | VI |

## EXAMPLES OF COMPUTATION OF CORRECTIONS

In this section we give some examples of the computation of Lorentz and polarization corrections for several cases which commonly arise in interpreting moving film photographs. The initial step is, in all cases, to time the exposures of the several levels so that $t=T_0S$. Here $T_0$ is the exposure time to be used for the zero-level photograph and $S$ is obtained for the several levels to be photographed from (15)–(17), according to the recording method. In the case of the precession method, the factor $S$ is sin $\bar{\nu}\,\frac{1}{2}\sin 2\bar{\mu}$, where $\bar{\mu}$ is selected and is ordinarily constant for the series of levels, and $\bar{\nu}$ is found from the relation $\cos\bar{\nu}=\cos\bar{\mu}+d^*$. If much work is to be done by the precession method, it is advisable to select a constant value of $\bar{\mu}$, and then find $S$ as a function of $d^*$ graphically.

In the example we assume that the equi-inclination Weissenberg method is to be used. We first lay out the form of Table VII, where the designations $\xi$, $\mu$, and $s$ have their usual Weissenberg significances. This table is not only prepared for the purpose of computing the timing of the photographs, but also for the purpose of providing the various Weissenberg settings. Column VII is computed from VI, but the character of the function in VI differs according to method as given in (15)–(17). In the equi-inclination Weissenberg case, here discussed, $S=\cos^2\mu$, so this column may be obtained by stages from column II. The exposures in column VII, according to (11), must be in proportion to $S$ of column VI. These values are scaled up so that the time, $T_0$, of the zero level is 20 hours. The final timings of the levels are then as given in the last column.

Table VIII indicates how to make the correction for Lorentz and polarization factors for the zero-level photograph where $\mu=0$ (for example, a zero-level, equi-inclination Weissenberg photograph). Such zero-level corrections are especially simple. Column II is derived from the $h$ and $k$ indices in Column I with the aid of Table II. Column III is the solution of (24) for the particular crystal used in the example, where $a^*=0.1779$. Column IV is the solution of (21). Column V is the required correction, as found from Table III. Column VII is obtained by multiplying the values in Columns V and VI.

Table IX shows the corresponding computation applied to data from an $n$-level (specifically the 2nd) equi-inclination Weissenberg photograph. Columns I, II, and III are computed in a manner identical with that of Table VIII. The computation of $\sigma$ for $n$-level photographs, however, requires taking account of the additional component shown in Column IV. The corrections for the $L$- and $p$-factors are also more complicated and must be made separately, and are found in Column VI and in Columns VII and VIII respectively. The $p$-correction of Column VI is taken directly from Table IV.

The computation for the correction of zero-level photographs taken for methods where $\mu\neq 0$ (as in the case of de Jong-Bouman and precession photographs) is different. In this case, $M/R_n=\sin\Upsilon$ must either be derived graphically, as in Fig. 1, or computed, whereas in the previous cases, $\Upsilon$ was directly measured on the photograph. With this exception the computations are the same. The form of Table X, which holds as it stands for the zero level, is also valid for $n$-levels provided allowance for the $c$-component of $\sigma$ is made as in Column IV of Table IX.

## TABLE III. Lorentz-polarization correction, $\frac{1}{L \cdot p}$

$$\left( = \sin 2\theta \frac{2}{1+\cos^2 2\theta} \right)$$

as a function of $\sigma$.

*Valid only for zero level when $\mu = 0$.*

| | .000 | .002 | .004 | .006 | .008 | | .000 | .002 | .004 | .006 | .008 | | .000 | .002 | .004 | .006 | .008 | | .000 | .002 | .004 | .006 | .008 |
|---|---|---|---|---|---|---|---|---|---|---|---|---|---|---|---|---|---|---|---|---|---|---|---|
| .00 | .0000 | .0020 | .0040 | .0060 | .0080 | .50 | .5485 | .5510 | .5537 | .5562 | .5587 | 1.00 | 1.3856 | 1.3899 | 1.3937 | 1.3980 | 1.4019 | 1.50 | 1.9539 | 1.9516 | 1.9493 | 1.9470 | 1.9448 |
| .01 | .0100 | .0120 | .0140 | .0160 | .0180 | .51 | .5615 | .5640 | .5666 | .5692 | .5718 | 1.01 | 1.4061 | 1.4102 | 1.4142 | 1.4182 | 1.4223 | 1.51 | 1.9425 | 1.9399 | 1.9372 | 1.9346 | 1.9320 |
| .02 | .0200 | .0220 | .0240 | .0260 | .0280 | .52 | .5744 | .5770 | .5797 | .5824 | .5851 | 1.02 | 1.4265 | 1.4304 | 1.4345 | 1.4386 | 1.4428 | 1.52 | 1.9294 | 1.9268 | 1.9238 | 1.9212 | 1.9183 |
| .03 | .0300 | .0320 | .0340 | .0360 | .0380 | .53 | .5879 | .5903 | .5931 | .5959 | .5984 | 1.03 | 1.4468 | 1.4510 | 1.4550 | 1.4592 | 1.4633 | 1.53 | 1.9153 | 1.9120 | 1.9091 | 1.9059 | 1.9030 |
| .04 | .0400 | .0420 | .0440 | .0460 | .0480 | .54 | .6013 | .6039 | .6064 | .6094 | .6120 | 1.04 | 1.4674 | 1.4715 | 1.4756 | 1.4797 | 1.4837 | 1.54 | 1.8997 | 1.8965 | 1.8932 | 1.8896 | 1.8864 |
| .05 | .0501 | .0521 | .0541 | .0561 | .0581 | .55 | .6146 | .6173 | .6203 | .6231 | .6258 | 1.05 | 1.4877 | 1.4919 | 1.4959 | 1.4999 | 1.5042 | 1.55 | 1.8829 | 1.8793 | 1.8758 | 1.8723 | 1.8685 |
| .06 | .0601 | .0621 | .0641 | .0661 | .0681 | .56 | .6285 | .6313 | .6341 | .6365 | .6394 | 1.06 | 1.5083 | 1.5124 | 1.5163 | 1.5205 | 1.5246 | 1.56 | 1.8650 | 1.8612 | 1.8574 | 1.8532 | 1.8495 |
| .07 | .0701 | .0722 | .0742 | .0762 | .0782 | .57 | .6423 | .6452 | .6477 | .6506 | .6532 | 1.07 | 1.5286 | 1.5328 | 1.5368 | 1.5408 | 1.5449 | 1.57 | 1.8457 | 1.8416 | 1.8376 | 1.8335 | 1.8292 |
| .08 | .0802 | .0822 | .0842 | .0862 | .0883 | .58 | .6562 | .6588 | .6618 | .6645 | .6676 | 1.08 | 1.5489 | 1.5530 | 1.5571 | 1.5610 | 1.5652 | 1.58 | 1.8252 | 1.8208 | 1.8165 | 1.8123 | 1.8077 |
| .09 | .0903 | .0923 | .0943 | .0963 | .0983 | .59 | .6702 | .6729 | .6761 | .6789 | .6817 | 1.09 | 1.5694 | 1.5733 | 1.5773 | 1.5813 | 1.5853 | 1.59 | 1.8034 | 1.7989 | 1.7944 | 1.7899 | 1.7851 |
| .10 | .1004 | .1024 | .1044 | .1065 | .1085 | .60 | .6845 | .6873 | .6901 | .6930 | .6959 | 1.10 | 1.5893 | 1.5934 | 1.5974 | 1.6003 | 1.6054 | 1.60 | 1.7806 | 1.7759 | 1.7709 | 1.7662 | 1.7615 |
| .11 | .1105 | .1125 | .1145 | .1166 | .1186 | .61 | .6988 | .7017 | .7047 | .7077 | .7102 | 1.11 | 1.6095 | 1.6134 | 1.6176 | 1.6215 | 1.6255 | 1.61 | 1.7565 | 1.7516 | 1.7464 | 1.7416 | 1.7364 |
| .12 | .1207 | .1227 | .1247 | .1268 | .1288 | .62 | .7133 | .7163 | .7194 | .7220 | .7252 | 1.12 | 1.6295 | 1.6335 | 1.6375 | 1.6415 | 1.6453 | 1.62 | 1.7313 | 1.7262 | 1.7209 | 1.7159 | 1.7106 |
| .13 | .1308 | .1329 | .1349 | .1369 | .1390 | .63 | .7283 | .7310 | .7342 | .7369 | .7396 | 1.13 | 1.6491 | 1.6532 | 1.6570 | 1.6609 | 1.6650 | 1.63 | 1.7053 | 1.6998 | 1.6943 | 1.6889 | 1.6835 |
| .14 | .1410 | .1431 | .1451 | .1472 | .1492 | .64 | .7429 | .7457 | .7491 | .7519 | .7547 | 1.14 | 1.6686 | 1.6728 | 1.6764 | 1.6804 | 1.6844 | 1.64 | 1.6779 | 1.6722 | 1.6667 | 1.6611 | 1.6554 |
| .15 | .1513 | .1533 | .1554 | .1575 | .1595 | .65 | .7582 | .7610 | .7639 | .7669 | .7698 | 1.15 | 1.6880 | 1.6920 | 1.6958 | 1.6995 | 1.7033 | 1.65 | 1.6499 | 1.6439 | 1.6383 | 1.6324 | 1.6265 |
| .16 | .1616 | .1636 | .1657 | .1677 | .1698 | .66 | .7728 | .7758 | .7794 | .7825 | .7855 | 1.16 | 1.7074 | 1.7112 | 1.7147 | 1.7185 | 1.7224 | 1.66 | 1.6205 | 1.6145 | 1.6085 | 1.6026 | 1.5964 |
| .17 | .1719 | .1739 | .1760 | .1781 | .1801 | .67 | .7886 | .7911 | .7943 | .7974 | .8006 | 1.17 | 1.7259 | 1.7298 | 1.7334 | 1.7373 | 1.7409 | 1.67 | 1.5903 | 1.5843 | 1.5780 | 1.5718 | 1.5657 |
| .18 | .1822 | .1843 | .1863 | .1884 | .1905 | .68 | .8039 | .8071 | .8104 | .8130 | .8163 | 1.18 | 1.7446 | 1.7483 | 1.7519 | 1.7556 | 1.7590 | 1.68 | 1.5596 | 1.5533 | 1.5468 | 1.5406 | 1.5342 |
| .19 | .1926 | .1947 | .1968 | .1988 | .2009 | .69 | .8197 | .8224 | .8258 | .8292 | .8319 | 1.19 | 1.7627 | 1.7665 | 1.7699 | 1.7734 | 1.7768 | 1.69 | 1.5377 | 1.5211 | 1.5147 | 1.5083 | 1.5017 |
| .20 | .2030 | .2051 | .2072 | .2093 | .2114 | .70 | .8354 | .8382 | .8418 | .8446 | .8482 | 1.20 | 1.7806 | 1.7841 | 1.7876 | 1.7912 | 1.7944 | 1.70 | 1.4952 | 1.4885 | 1.4817 | 1.4751 | 1.4684 |
| .21 | .2135 | .2156 | .2177 | .2198 | .2219 | .71 | .8511 | .8547 | .8576 | .8606 | .8643 | 1.21 | 1.7979 | 1.8012 | 1.8047 | 1.8080 | 1.8116 | 1.71 | 1.4618 | 1.4550 | 1.4482 | 1.4413 | 1.4345 |
| .22 | .2240 | .2261 | .2283 | .2304 | .2325 | .72 | .8673 | .8703 | .8741 | .8772 | .8803 | 1.22 | 1.8149 | 1.8182 | 1.8215 | 1.8248 | 1.8282 | 1.72 | 1.4276 | 1.4207 | 1.4138 | 1.4069 | 1.4000 |
| .23 | .2346 | .2367 | .2388 | .2410 | .2431 | .73 | .8842 | .8873 | .8905 | .8937 | .8969 | 1.23 | 1.8312 | 1.8345 | 1.8376 | 1.8409 | 1.8440 | 1.73 | 1.3930 | 1.3858 | 1.3787 | 1.3717 | 1.3646 |
| .24 | .2452 | .2473 | .2495 | .2516 | .2537 | .74 | .9001 | .9033 | .9066 | .9099 | .9132 | 1.24 | 1.8471 | 1.8502 | 1.8532 | 1.8563 | 1.8594 | 1.74 | 1.3574 | 1.3504 | 1.3432 | 1.3360 | 1.3287 |
| .25 | .2560 | .2581 | .2602 | .2623 | .2645 | .75 | .9166 | .9200 | .9234 | .9268 | .9302 | 1.25 | 1.8625 | 1.8657 | 1.8685 | 1.8716 | 1.8744 | 1.75 | 1.3215 | 1.3142 | 1.3068 | 1.2997 | 1.2923 |
| .26 | .2667 | .2688 | .2709 | .2731 | .2753 | .76 | .9337 | .9372 | .9407 | .9443 | .9470 | 1.26 | 1.8772 | 1.8801 | 1.8829 | 1.8857 | 1.8886 | 1.76 | 1.2850 | 1.2776 | 1.2702 | 1.2628 | 1.2553 |
| .27 | .2775 | .2796 | .2818 | .2839 | .2861 | .77 | .9506 | .9542 | .9579 | .9606 | .9643 | 1.27 | 1.8914 | 1.8943 | 1.8968 | 1.8997 | 1.9022 | 1.77 | 1.2478 | 1.2404 | 1.2329 | 1.2253 | 1.2177 |
| .28 | .2884 | .2905 | .2927 | .2948 | .2971 | .78 | .9681 | .9709 | .9747 | .9785 | .9814 | 1.28 | 1.9048 | 1.9073 | 1.9102 | 1.9124 | 1.9150 | 1.78 | 1.2102 | 1.2026 | 1.1950 | 1.1874 | 1.1798 |
| .29 | .2992 | .3015 | .3037 | .3058 | .3078 | .79 | .9852 | .9891 | .9921 | .9960 | .9990 | 1.29 | 1.9175 | 1.9201 | 1.9223 | 1.9249 | 1.9272 | 1.79 | 1.1722 | 1.1644 | 1.1567 | 1.1490 | 1.1413 |
| .30 | .3103 | .3125 | .3147 | .3169 | .3191 | .80 | 1.0028 | 1.0063 | 1.0098 | 1.0134 | 1.0169 | 1.30 | 1.9298 | 1.9320 | 1.9342 | 1.9365 | 1.9387 | 1.80 | 1.1335 | 1.1257 | 1.1179 | 1.1101 | 1.1023 |
| .31 | .3213 | .3235 | .3257 | .3280 | .3303 | .81 | 1.0204 | 1.0241 | 1.0276 | 1.0311 | 1.0348 | 1.31 | 1.9406 | 1.9429 | 1.9451 | 1.9470 | 1.9489 | 1.81 | 1.0945 | 1.0866 | 1.0787 | 1.0709 | 1.0628 |
| .32 | .3324 | .3347 | .3369 | .3392 | .3414 | .82 | 1.0383 | 1.0420 | 1.0456 | 1.0491 | 1.0527 | 1.32 | 1.9512 | 1.9531 | 1.9550 | 1.9569 | 1.9589 | 1.82 | 1.0550 | 1.0470 | 1.0390 | 1.0310 | 1.0230 |
| .33 | .3436 | .3459 | .3482 | .3505 | .3527 | .83 | 1.0563 | 1.0600 | 1.0636 | 1.0672 | 1.0709 | 1.33 | 1.9604 | 1.9623 | 1.9643 | 1.9658 | 1.9673 | 1.83 | 1.0150 | 1.0070 | .9990 | .9911 | .9823 |
| .34 | .3550 | .3573 | .3595 | .3618 | .3640 | .84 | 1.0746 | 1.0783 | 1.0819 | 1.0855 | 1.0892 | 1.34 | 1.9689 | 1.9704 | 1.9724 | 1.9736 | 1.9751 | 1.84 | .9747 | .9662 | .9578 | .9497 | .9416 |
| .35 | .3663 | .3686 | .3717 | .3733 | .3755 | .85 | 1.0930 | 1.0966 | 1.1004 | 1.1041 | 1.1078 | 1.35 | 1.9767 | 1.9778 | 1.9794 | 1.9806 | 1.9822 | 1.85 | .9337 | .9251 | .9174 | .9091 | .9001 |
| .36 | .3778 | .3801 | .3824 | .3848 | .3870 | .86 | 1.1115 | 1.1152 | 1.1189 | 1.1227 | 1.1264 | 1.36 | 1.9833 | 1.9845 | 1.9857 | 1.9865 | 1.9877 | 1.86 | .8921 | .8842 | .8757 | .8673 | .8584 |
| .37 | .3894 | .3917 | .3940 | .3964 | .3986 | .87 | 1.1302 | 1.1339 | 1.1378 | 1.1414 | 1.1452 | 1.37 | 1.9889 | 1.9897 | 1.9908 | 1.9916 | 1.9924 | 1.87 | .8503 | .8418 | .8333 | .8244 | .8163 |
| .38 | .4010 | .4034 | .4057 | .4080 | .4103 | .88 | 1.1490 | 1.1529 | 1.1566 | 1.1604 | 1.1641 | 1.38 | 1.9932 | 1.9940 | 1.9948 | 1.9956 | 1.9960 | 1.88 | .8078 | .7987 | .7905 | .7819 | .7728 |
| .39 | .4127 | .4151 | .4174 | .4198 | .4221 | .89 | 1.1681 | 1.1718 | 1.1756 | 1.1795 | 1.1834 | 1.39 | 1.9968 | 1.9972 | 1.9976 | 1.9980 | 1.9984 | 1.89 | .7639 | .7553 | .7468 | .7375 | .7289 |
| .40 | .4244 | .4268 | .4292 | .4316 | .4340 | .90 | 1.1872 | 1.1910 | 1.1949 | 1.1988 | 1.2026 | 1.40 | 1.9988 | 1.9992 | 1.9996 | 1.9996 | 2.0000 | 1.90 | .7199 | .7112 | .7022 | .6930 | .6840 |
| .41 | .4365 | .4388 | .4413 | .4437 | .4460 | .91 | 1.2066 | 1.2104 | 1.2143 | 1.2182 | 1.2220 | 1.41 | 2.0000 | 2.0000 | 2.0000 | 2.0000 | 2.0000 | 1.91 | .6748 | .6658 | .6562 | .6472 | .6378 |
| .42 | .4484 | .4509 | .4533 | .4558 | .4581 | .92 | 1.2259 | 1.2299 | 1.2338 | 1.2376 | 1.2416 | 1.42 | 2.0000 | 1.9996 | 1.9996 | 1.9992 | 1.9988 | 1.92 | .6285 | .6188 | .6094 | .5999 | .5903 |
| .43 | .4606 | .4630 | .4653 | .4679 | .4704 | .93 | 1.2455 | 1.2495 | 1.2534 | 1.2574 | 1.2612 | 1.43 | 1.9984 | 1.9980 | 1.9976 | 1.9972 | 1.9968 | 1.93 | .5804 | .5708 | .5609 | .5510 | .5408 |
| .44 | .4728 | .4753 | .4778 | .4801 | .4826 | .94 | 1.2652 | 1.2692 | 1.2732 | 1.2771 | 1.2811 | 1.44 | 1.9960 | 1.9952 | 1.9948 | 1.9940 | 1.9932 | 1.94 | .5305 | .5203 | .5099 | .4995 | .4890 |
| .45 | .4852 | .4876 | .4900 | .4926 | .4950 | .95 | 1.2850 | 1.2890 | 1.2930 | 1.2970 | 1.3009 | 1.45 | 1.9924 | 1.9912 | 1.9904 | 1.9893 | 1.9881 | 1.95 | .4782 | .4673 | .4562 | .4450 | .4337 |
| .46 | .4975 | .5000 | .5025 | .5050 | .5076 | .96 | 1.3050 | 1.3091 | 1.3130 | 1.3170 | 1.3210 | 1.46 | 1.9873 | 1.9861 | 1.9849 | 1.9833 | 1.9822 | 1.96 | .4221 | .4103 | .3984 | .3861 | .3736 |
| .47 | .5099 | .5126 | .5152 | .5176 | .5203 | .97 | 1.3250 | 1.3291 | 1.3332 | 1.3371 | 1.3412 | 1.47 | 1.9810 | 1.9794 | 1.9778 | 1.9763 | 1.9747 | 1.97 | .3608 | .3476 | .3341 | .3201 | .3056 |
| .48 | .5227 | .5252 | .5277 | .5305 | .5330 | .98 | 1.3452 | 1.3492 | 1.3532 | 1.3572 | 1.3613 | 1.48 | 1.9732 | 1.9716 | 1.9697 | 1.9681 | 1.9662 | 1.98 | .2907 | .2750 | .2586 | .2412 | .2227 |
| .49 | .5356 | .5379 | .5405 | .5432 | .5459 | .99 | 1.3654 | 1.3695 | 1.3734 | 1.3776 | 1.3816 | 1.49 | 1.9643 | 1.9623 | 1.9604 | 1.9581 | 1.9562 | 1.99 | .2028 | .1808 | .1562 | .1272 | .0897 |

TABLE IV. Polarization correction, $\frac{1}{p}$

$$\left(=\frac{2}{1+\cos^2 2\theta}\right)$$

as a function of $\sigma$.

| | .000 | .002 | .004 | .006 | .008 | | .000 | .002 | .004 | .006 | .008 | | .000 | .002 | .004 | .006 | .008 | | .000 | .002 | .004 | .006 | .008 |
|---|---|---|---|---|---|---|---|---|---|---|---|---|---|---|---|---|---|---|---|---|---|---|---|
| .00 | 1.0000 | 1.0000 | 1.0000 | 1.0000 | 1.0000 | .50 | 1.1328 | 1.1339 | 1.1349 | 1.1361 | 1.1373 | 1.00 | 1.6000 | 1.6026 | 1.6051 | 1.6077 | 1.6103 | 1.50 | 1.9693 | 1.9677 | 1.9662 | 1.9646 | 1.9631 |
| .01 | 1.0001 | 1.0001 | 1.0001 | 1.0001 | 1.0002 | .51 | 1.1384 | 1.1396 | 1.1408 | 1.1419 | 1.1431 | 1.01 | 1.6129 | 1.6155 | 1.6181 | 1.6207 | 1.6231 | 1.51 | 1.9616 | 1.9600 | 1.9581 | 1.9566 | 1.9547 |
| .02 | 1.0002 | 1.0002 | 1.0003 | 1.0003 | 1.0004 | .52 | 1.1443 | 1.1455 | 1.1467 | 1.1478 | 1.1490 | 1.02 | 1.6258 | 1.6284 | 1.6308 | 1.6335 | 1.6361 | 1.52 | 1.9531 | 1.9512 | 1.9493 | 1.9474 | 1.9455 |
| .03 | 1.0004 | 1.0005 | 1.0006 | 1.0006 | 1.0007 | .53 | 1.1502 | 1.1514 | 1.1526 | 1.1538 | 1.1550 | 1.03 | 1.6388 | 1.6412 | 1.6439 | 1.6466 | 1.6491 | 1.53 | 1.9436 | 1.9417 | 1.9395 | 1.9376 | 1.9354 |
| .04 | 1.0008 | 1.0009 | 1.0010 | 1.0011 | 1.0011 | .54 | 1.1563 | 1.1575 | 1.1587 | 1.1600 | 1.1613 | 1.04 | 1.6518 | 1.6545 | 1.6570 | 1.6595 | 1.6622 | 1.54 | 1.9331 | 1.9312 | 1.9290 | 1.9268 | 1.9246 |
| .05 | 1.0012 | 1.0013 | 1.0015 | 1.0016 | 1.0017 | .55 | 1.1625 | 1.1637 | 1.1651 | 1.1663 | 1.1677 | 1.05 | 1.6650 | 1.6675 | 1.6700 | 1.6725 | 1.6753 | 1.55 | 1.9220 | 1.9198 | 1.9175 | 1.9150 | 1.9128 |
| .06 | 1.0018 | 1.0019 | 1.0020 | 1.0022 | 1.0023 | .56 | 1.1689 | 1.1703 | 1.1715 | 1.1729 | 1.1741 | 1.06 | 1.6779 | 1.6804 | 1.6829 | 1.6858 | 1.6883 | 1.56 | 1.9102 | 1.9077 | 1.9051 | 1.9026 | 1.9001 |
| .07 | 1.0024 | 1.0026 | 1.0027 | 1.0029 | 1.0030 | .57 | 1.1755 | 1.1767 | 1.1781 | 1.1794 | 1.1808 | 1.07 | 1.6909 | 1.6935 | 1.6961 | 1.6987 | 1.7013 | 1.57 | 1.8975 | 1.8947 | 1.8921 | 1.8893 | 1.8868 |
| .08 | 1.0032 | 1.0034 | 1.0035 | 1.0037 | 1.0039 | .58 | 1.1822 | 1.1834 | 1.1848 | 1.1862 | 1.1876 | 1.08 | 1.7039 | 1.7065 | 1.7091 | 1.7117 | 1.7144 | 1.58 | 1.8839 | 1.8811 | 1.8783 | 1.8755 | 1.8727 |
| .09 | 1.0040 | 1.0042 | 1.0044 | 1.0046 | 1.0048 | .59 | 1.1889 | 1.1903 | 1.1918 | 1.1930 | 1.1945 | 1.09 | 1.7170 | 1.7197 | 1.7224 | 1.7247 | 1.7274 | 1.59 | 1.8695 | 1.8667 | 1.8636 | 1.8608 | 1.8577 |
| .10 | 1.0050 | 1.0052 | 1.0054 | 1.0056 | 1.0058 | .60 | 1.1959 | 1.1973 | 1.1988 | 1.2002 | 1.2015 | 1.10 | 1.7301 | 1.7328 | 1.7352 | 1.7379 | 1.7403 | 1.60 | 1.8546 | 1.8515 | 1.8484 | 1.8454 | 1.8420 |
| .11 | 1.0060 | 1.0063 | 1.0065 | 1.0067 | 1.0069 | .61 | 1.2029 | 1.2044 | 1.2058 | 1.2073 | 1.2088 | 1.11 | 1.7431 | 1.7455 | 1.7483 | 1.7507 | 1.7535 | 1.61 | 1.8389 | 1.8355 | 1.8322 | 1.8288 | 1.8258 |
| .12 | 1.0073 | 1.0075 | 1.0078 | 1.0080 | 1.0083 | .62 | 1.2102 | 1.2117 | 1.2132 | 1.2146 | 1.2161 | 1.12 | 1.7559 | 1.7584 | 1.7612 | 1.7637 | 1.7662 | 1.62 | 1.8225 | 1.8188 | 1.8155 | 1.8123 | 1.8086 |
| .13 | 1.0085 | 1.0088 | 1.0090 | 1.0093 | 1.0096 | .63 | 1.2177 | 1.2192 | 1.2207 | 1.2222 | 1.2237 | 1.13 | 1.7687 | 1.7715 | 1.7740 | 1.7765 | 1.7790 | 1.63 | 1.8054 | 1.8018 | 1.7982 | 1.7947 | 1.7912 |
| .14 | 1.0099 | 1.0101 | 1.0104 | 1.0107 | 1.0110 | .64 | 1.2252 | 1.2267 | 1.2284 | 1.2299 | 1.2314 | 1.14 | 1.7816 | 1.7841 | 1.7867 | 1.7892 | 1.7915 | 1.64 | 1.7876 | 1.7838 | 1.7803 | 1.7765 | 1.7727 |
| .15 | 1.0113 | 1.0116 | 1.0119 | 1.0122 | 1.0126 | .65 | 1.2329 | 1.2346 | 1.2361 | 1.2376 | 1.2392 | 1.15 | 1.7940 | 1.7966 | 1.7992 | 1.8015 | 1.8041 | 1.65 | 1.7690 | 1.7655 | 1.7615 | 1.7578 | 1.7541 |
| .16 | 1.0129 | 1.0132 | 1.0136 | 1.0139 | 1.0142 | .66 | 1.2408 | 1.2424 | 1.2439 | 1.2456 | 1.2472 | 1.16 | 1.8067 | 1.8090 | 1.8116 | 1.8139 | 1.8165 | 1.66 | 1.7501 | 1.7464 | 1.7425 | 1.7385 | 1.7346 |
| .17 | 1.0145 | 1.0149 | 1.0152 | 1.0156 | 1.0160 | .67 | 1.2489 | 1.2505 | 1.2520 | 1.2538 | 1.2553 | 1.17 | 1.8188 | 1.8215 | 1.8238 | 1.8262 | 1.8285 | 1.67 | 1.7307 | 1.7268 | 1.7227 | 1.7188 | 1.7147 |
| .18 | 1.0164 | 1.0167 | 1.0171 | 1.0175 | 1.0178 | .68 | 1.2571 | 1.2588 | 1.2604 | 1.2620 | 1.2637 | 1.18 | 1.8312 | 1.8335 | 1.8359 | 1.8382 | 1.8406 | 1.68 | 1.7109 | 1.7068 | 1.7027 | 1.6987 | 1.6943 |
| .19 | 1.0182 | 1.0186 | 1.0190 | 1.0194 | 1.0198 | .69 | 1.2653 | 1.2671 | 1.2687 | 1.2705 | 1.2721 | 1.19 | 1.8430 | 1.8454 | 1.8477 | 1.8498 | 1.8522 | 1.69 | 1.6903 | 1.6861 | 1.6821 | 1.6779 | 1.6736 |
| .20 | 1.0202 | 1.0206 | 1.0210 | 1.0215 | 1.0219 | .70 | 1.2739 | 1.2755 | 1.2773 | 1.2791 | 1.2807 | 1.20 | 1.8546 | 1.8570 | 1.8591 | 1.8615 | 1.8639 | 1.70 | 1.6694 | 1.6653 | 1.6609 | 1.6567 | 1.6523 |
| .21 | 1.0223 | 1.0227 | 1.0231 | 1.0236 | 1.0241 | .71 | 1.2825 | 1.2842 | 1.2860 | 1.2878 | 1.2897 | 1.21 | 1.8660 | 1.8681 | 1.8706 | 1.8727 | 1.8751 | 1.71 | 1.6483 | 1.6439 | 1.6396 | 1.6353 | 1.6308 |
| .22 | 1.0245 | 1.0249 | 1.0254 | 1.0259 | 1.0264 | .72 | 1.2913 | 1.2932 | 1.2948 | 1.2967 | 1.2985 | 1.22 | 1.8772 | 1.8793 | 1.8815 | 1.8836 | 1.8857 | 1.72 | 1.6265 | 1.6221 | 1.6179 | 1.6134 | 1.6090 |
| .23 | 1.0268 | 1.0272 | 1.0277 | 1.0283 | 1.0287 | .73 | 1.3004 | 1.3021 | 1.3040 | 1.3058 | 1.3075 | 1.23 | 1.8879 | 1.8900 | 1.8921 | 1.8943 | 1.8965 | 1.73 | 1.6046 | 1.6000 | 1.5957 | 1.5913 | 1.5868 |
| .24 | 1.0292 | 1.0298 | 1.0302 | 1.0307 | 1.0312 | .74 | 1.3094 | 1.3113 | 1.3132 | 1.3149 | 1.3168 | 1.24 | 1.8986 | 1.9004 | 1.9026 | 1.9048 | 1.9066 | 1.74 | 1.5823 | 1.5778 | 1.5733 | 1.5689 | 1.5642 |
| .25 | 1.0318 | 1.0322 | 1.0327 | 1.0333 | 1.0338 | .75 | 1.3187 | 1.3207 | 1.3226 | 1.3243 | 1.3263 | 1.25 | 1.9088 | 1.9106 | 1.9128 | 1.9146 | 1.9164 | 1.75 | 1.5598 | 1.5552 | 1.5506 | 1.5461 | 1.5415 |
| .26 | 1.0343 | 1.0349 | 1.0354 | 1.0361 | 1.0366 | .76 | 1.3282 | 1.3301 | 1.3321 | 1.3339 | 1.3358 | 1.26 | 1.9183 | 1.9205 | 1.9223 | 1.9242 | 1.9260 | 1.76 | 1.5370 | 1.5326 | 1.5279 | 1.5235 | 1.5188 |
| .27 | 1.0371 | 1.0377 | 1.0382 | 1.0389 | 1.0394 | .77 | 1.3378 | 1.3398 | 1.3417 | 1.3437 | 1.3455 | 1.27 | 1.9279 | 1.9298 | 1.9312 | 1.9331 | 1.9350 | 1.77 | 1.5142 | 1.5097 | 1.5049 | 1.5004 | 1.4957 |
| .28 | 1.0399 | 1.0406 | 1.0411 | 1.0418 | 1.0423 | .78 | 1.3475 | 1.3495 | 1.3515 | 1.3535 | 1.3556 | 1.28 | 1.9369 | 1.9384 | 1.9402 | 1.9417 | 1.9436 | 1.78 | 1.4912 | 1.4865 | 1.4819 | 1.4771 | 1.4725 |
| .29 | 1.0430 | 1.0435 | 1.0442 | 1.0448 | 1.0454 | .79 | 1.3576 | 1.3594 | 1.3615 | 1.3635 | 1.3656 | 1.29 | 1.9451 | 1.9467 | 1.9486 | 1.9501 | 1.9516 | 1.79 | 1.4680 | 1.4633 | 1.4586 | 1.4539 | 1.4493 |
| .30 | 1.0460 | 1.0467 | 1.0472 | 1.0479 | 1.0485 | .80 | 1.3676 | 1.3697 | 1.3717 | 1.3738 | 1.3759 | 1.30 | 1.9531 | 1.9547 | 1.9562 | 1.9577 | 1.9589 | 1.80 | 1.4447 | 1.4401 | 1.4353 | 1.4306 | 1.4259 |
| .31 | 1.0492 | 1.0499 | 1.0505 | 1.0512 | 1.0519 | .81 | 1.3778 | 1.3799 | 1.3820 | 1.3841 | 1.3862 | 1.31 | 1.9604 | 1.9619 | 1.9635 | 1.9646 | 1.9662 | 1.81 | 1.4213 | 1.4166 | 1.4120 | 1.4073 | 1.4027 |
| .32 | 1.0525 | 1.0532 | 1.0539 | 1.0545 | 1.0552 | .82 | 1.3883 | 1.3904 | 1.3924 | 1.3947 | 1.3966 | 1.32 | 1.9673 | 1.9685 | 1.9701 | 1.9712 | 1.9724 | 1.82 | 1.3980 | 1.3933 | 1.3887 | 1.3841 | 1.3793 |
| .33 | 1.0560 | 1.0566 | 1.0573 | 1.0581 | 1.0588 | .83 | 1.3988 | 1.4010 | 1.4031 | 1.4053 | 1.4075 | 1.33 | 1.9736 | 1.9747 | 1.9763 | 1.9771 | 1.9782 | 1.83 | 1.3748 | 1.3701 | 1.3654 | 1.3607 | 1.3561 |
| .34 | 1.0594 | 1.0602 | 1.0609 | 1.0617 | 1.0624 | .84 | 1.4096 | 1.4118 | 1.4138 | 1.4160 | 1.4182 | 1.34 | 1.9794 | 1.9802 | 1.9814 | 1.9826 | 1.9833 | 1.84 | 1.3514 | 1.3468 | 1.3421 | 1.3374 | 1.3328 |
| .35 | 1.0632 | 1.0638 | 1.0646 | 1.0654 | 1.0661 | .85 | 1.4205 | 1.4227 | 1.4249 | 1.4271 | 1.4292 | 1.35 | 1.9845 | 1.9853 | 1.9861 | 1.9869 | 1.9881 | 1.85 | 1.3282 | 1.3235 | 1.3189 | 1.3142 | 1.3096 |
| .36 | 1.0669 | 1.0677 | 1.0684 | 1.0692 | 1.0700 | .86 | 1.4314 | 1.4337 | 1.4360 | 1.4382 | 1.4405 | 1.36 | 1.9889 | 1.9897 | 1.9904 | 1.9912 | 1.9916 | 1.86 | 1.3050 | 1.3004 | 1.2957 | 1.2912 | 1.2865 |
| .37 | 1.0708 | 1.0716 | 1.0724 | 1.0732 | 1.0740 | .87 | 1.4426 | 1.4449 | 1.4472 | 1.4495 | 1.4518 | 1.37 | 1.9924 | 1.9932 | 1.9936 | 1.9944 | 1.9948 | 1.87 | 1.2819 | 1.2773 | 1.2728 | 1.2681 | 1.2636 |
| .38 | 1.0748 | 1.0756 | 1.0764 | 1.0772 | 1.0781 | .88 | 1.4539 | 1.4562 | 1.4586 | 1.4609 | 1.4631 | 1.38 | 1.9956 | 1.9960 | 1.9964 | 1.9968 | 1.9972 | 1.88 | 1.2590 | 1.2544 | 1.2498 | 1.2453 | 1.2407 |
| .39 | 1.0789 | 1.0798 | 1.0806 | 1.0814 | 1.0824 | .89 | 1.4654 | 1.4678 | 1.4702 | 1.4723 | 1.4747 | 1.39 | 1.9976 | 1.9980 | 1.9984 | 1.9988 | 1.9988 | 1.89 | 1.2361 | 1.2317 | 1.2271 | 1.2226 | 1.2182 |
| .40 | 1.0832 | 1.0840 | 1.0850 | 1.0858 | 1.0867 | .90 | 1.4771 | 1.4795 | 1.4817 | 1.4841 | 1.4865 | 1.40 | 1.9992 | 1.9996 | 1.9996 | 1.9996 | 2.0000 | 1.90 | 1.2136 | 1.2090 | 1.2045 | 1.2000 | 1.1956 |
| .41 | 1.0875 | 1.0885 | 1.0893 | 1.0903 | 1.0912 | .91 | 1.4888 | 1.4912 | 1.4937 | 1.4959 | 1.4984 | 1.41 | 2.0000 | 2.0000 | 2.0000 | 2.0000 | 2.0000 | 1.91 | 1.1912 | 1.1867 | 1.1822 | 1.1779 | 1.1733 |
| .42 | 1.0921 | 1.0930 | 1.0939 | 1.0948 | 1.0958 | .92 | 1.5008 | 1.5031 | 1.5056 | 1.5078 | 1.5103 | 1.42 | 2.0000 | 1.9996 | 1.9996 | 1.9996 | 1.9992 | 1.92 | 1.1689 | 1.1646 | 1.1601 | 1.1557 | 1.1513 |
| .43 | 1.0967 | 1.0977 | 1.0987 | 1.0995 | 1.1005 | .93 | 1.5126 | 1.5151 | 1.5177 | 1.5200 | 1.5225 | 1.43 | 1.9988 | 1.9988 | 1.9984 | 1.9980 | 1.9976 | 1.93 | 1.1469 | 1.1426 | 1.1382 | 1.1339 | 1.1294 |
| .44 | 1.1014 | 1.1024 | 1.1034 | 1.1044 | 1.1053 | .94 | 1.5249 | 1.5274 | 1.5298 | 1.5321 | 1.5347 | 1.44 | 1.9972 | 1.9968 | 1.9964 | 1.9960 | 1.9952 | 1.94 | 1.1251 | 1.1208 | 1.1164 | 1.1122 | 1.1079 |
| .45 | 1.1063 | 1.1073 | 1.1083 | 1.1094 | 1.1104 | .95 | 1.5370 | 1.5396 | 1.5420 | 1.5446 | 1.5470 | 1.45 | 1.9948 | 1.9944 | 1.9936 | 1.9928 | 1.9920 | 1.95 | 1.1036 | 1.0994 | 1.0951 | 1.0908 | 1.0866 |
| .46 | 1.1114 | 1.1123 | 1.1135 | 1.1145 | 1.1154 | .96 | 1.5494 | 1.5521 | 1.5545 | 1.5569 | 1.5596 | 1.46 | 1.9912 | 1.9904 | 1.9897 | 1.9889 | 1.9881 | 1.96 | 1.0824 | 1.0781 | 1.0739 | 1.0697 | 1.0655 |
| .47 | 1.1166 | 1.1176 | 1.1186 | 1.1197 | 1.1207 | .97 | 1.5620 | 1.5645 | 1.5669 | 1.5696 | 1.5721 | 1.47 | 1.9873 | 1.9861 | 1.9853 | 1.9841 | 1.9829 | 1.97 | 1.0613 | 1.0572 | 1.0530 | 1.0489 | 1.0447 |
| .48 | 1.1218 | 1.1228 | 1.1240 | 1.1251 | 1.1261 | .98 | 1.5746 | 1.5770 | 1.5795 | 1.5823 | 1.5848 | 1.48 | 1.9822 | 1.9810 | 1.9798 | 1.9786 | 1.9775 | 1.98 | 1.0406 | 1.0365 | 1.0324 | 1.0283 | 1.0242 |
| .49 | 1.1271 | 1.1283 | 1.1294 | 1.1305 | 1.1316 | .99 | 1.5873 | 1.5898 | 1.5924 | 1.5949 | 1.5974 | 1.49 | 1.9759 | 1.9747 | 1.9736 | 1.9720 | 1.9708 | 1.99 | 1.0202 | 1.0161 | 1.0120 | 1.0081 | 1.0040 |

## TABLE V. Lorentz-polarization correction, $\frac{1}{L \cdot p}$

$$\left( = \sin 2\theta \frac{2\cdot}{1+\cos^2 2\theta} \right)$$

as a function of $\sin \theta$.

*Valid only for zero level when $\mu = 0$.*

| | .000 | .001 | .002 | .003 | .004 | .005 | .006 | .007 | .008 | .009 |
|---|---|---|---|---|---|---|---|---|---|---|
| .001 | .0000 | .0020 | .0040 | .0060 | .0080 | .0100 | .0120 | .0140 | .0160 | .0180 |
| .01 | .0200 | .0220 | .0240 | .0260 | .0280 | .0300 | .0320 | .0340 | .0360 | .0380 |
| .02 | .0400 | .0420 | .0440 | .0460 | .0480 | .0501 | .0521 | .0541 | .0561 | .0581 |
| .03 | .0601 | .0621 | .0641 | .0661 | .0681 | .0701 | .0722 | .0742 | .0762 | .0782 |
| .04 | .0802 | .0822 | .0842 | .0862 | .0883 | .0903 | .0923 | .0943 | .0963 | .0983 |
| .05 | .1004 | .1024 | .1044 | .1065 | .1085 | .1105 | .1125 | .1145 | .1166 | .1186 |
| .06 | .1207 | .1227 | .1247 | .1268 | .1288 | .1308 | .1329 | .1349 | .1369 | .1390 |
| .07 | .1410 | .1431 | .1451 | .1472 | .1492 | .1513 | .1533 | .1554 | .1575 | .1595 |
| .08 | .1616 | .1636 | .1657 | .1677 | .1698 | .1719 | .1739 | .1760 | .1781 | .1801 |
| .09 | .1822 | .1843 | .1863 | .1884 | .1905 | .1926 | .1947 | .1968 | .1988 | .2009 |
| .10 | .2030 | .2051 | .2072 | .2093 | .2114 | .2135 | .2156 | .2177 | .2198 | .2219 |
| .11 | .2240 | .2261 | .2283 | .2304 | .2325 | .2346 | .2367 | .2388 | .2410 | .2431 |
| .12 | .2452 | .2473 | .2495 | .2516 | .2537 | .2560 | .2581 | .2602 | .2623 | .2645 |
| .13 | .2667 | .2688 | .2709 | .2731 | .2753 | .2775 | .2796 | .2818 | .2839 | .2861 |
| .14 | .2884 | .2905 | .2927 | .2948 | .2971 | .2992 | .3015 | .3037 | .3058 | .3078 |
| .15 | .3103 | .3125 | .3147 | .3169 | .3191 | .3213 | .3235 | .3257 | .3280 | .3303 |
| .16 | .3324 | .3347 | .3369 | .3392 | .3414 | .3436 | .3459 | .3482 | .3505 | .3527 |
| .17 | .3550 | .3573 | .3595 | .3618 | .3640 | .3663 | .3686 | .3717 | .3733 | .3755 |
| .18 | .3778 | .3801 | .3824 | .3848 | .3870 | .3894 | .3917 | .3940 | .3964 | .3986 |
| .19 | .4010 | .4034 | .4057 | .4080 | .4103 | .4127 | .4151 | .4174 | .4198 | .4221 |
| .20 | .4244 | .4268 | .4292 | .4316 | .4340 | .4365 | .4388 | .4413 | .4437 | .4460 |
| .21 | .4484 | .4509 | .4533 | .4558 | .4581 | .4606 | .4630 | .4653 | .4679 | .4704 |
| .22 | .4728 | .4753 | .4778 | .4801 | .4826 | .4852 | .4876 | .4900 | .4926 | .4950 |
| .23 | .4975 | .5000 | .5025 | .5050 | .5076 | .5099 | .5126 | .5152 | .5176 | .5203 |
| .24 | .5227 | .5252 | .5277 | .5305 | .5330 | .5356 | .5379 | .5405 | .5432 | .5459 |
| .25 | .5485 | .5510 | .5537 | .5562 | .5587 | .5615 | .5640 | .5666 | .5692 | .5718 |
| .26 | .5744 | .5770 | .5797 | .5824 | .5851 | .5879 | .5903 | .5931 | .5959 | .5984 |
| .27 | .6013 | .6039 | .6064 | .6094 | .6120 | .6146 | .6173 | .6203 | .6231 | .6258 |
| .28 | .6285 | .6313 | .6341 | .6365 | .6394 | .6423 | .6452 | .6477 | .6506 | .6532 |
| .29 | .6562 | .6588 | .6618 | .6645 | .6676 | .6702 | .6729 | .6761 | .6789 | .6817 |
| .30 | .6845 | .6873 | .6901 | .6930 | .6959 | .6988 | .7017 | .7047 | .7077 | .7102 |
| .31 | .7133 | .7163 | .7194 | .7220 | .7252 | .7283 | .7310 | .7342 | .7369 | .7396 |
| .32 | .7429 | .7457 | .7491 | .7519 | .7547 | .7582 | .7610 | .7639 | .7669 | .7698 |
| .33 | .7728 | .7758 | .7794 | .7825 | .7855 | .7886 | .7911 | .7943 | .7974 | .8006 |
| .34 | .8039 | .8071 | .8104 | .8130 | .8163 | .8197 | .8224 | .8258 | .8292 | .8319 |
| .35 | .8354 | .8382 | .8418 | .8446 | .8482 | .8511 | .8547 | .8576 | .8606 | .8643 |
| .36 | .8673 | .8703 | .8741 | .8772 | .8803 | .8842 | .8873 | .8905 | .8937 | .8969 |
| .37 | .9001 | .9033 | .9066 | .9099 | .9132 | .9166 | .9200 | .9234 | .9268 | .9302 |
| .38 | .9337 | .9372 | .9407 | .9443 | .9470 | .9506 | .9542 | .9579 | .9606 | .9643 |
| .39 | .9681 | .9709 | .9747 | .9785 | .9814 | .9852 | .9891 | .9921 | .9960 | .9990 |
| .40 | 1.0028 | 1.0063 | 1.0098 | 1.0134 | 1.0169 | 1.0204 | 1.0241 | 1.0276 | 1.0311 | 1.0348 |
| .41 | 1.0383 | 1.0420 | 1.0456 | 1.0491 | 1.0527 | 1.0563 | 1.0600 | 1.0636 | 1.0672 | 1.0709 |
| .42 | 1.0746 | 1.0783 | 1.0819 | 1.0855 | 1.0892 | 1.0930 | 1.0966 | 1.1004 | 1.1041 | 1.1078 |
| .43 | 1.1115 | 1.1152 | 1.1189 | 1.1227 | 1.1264 | 1.1302 | 1.1339 | 1.1378 | 1.1414 | 1.1452 |
| .44 | 1.1490 | 1.1529 | 1.1566 | 1.1604 | 1.1641 | 1.1681 | 1.1718 | 1.1756 | 1.1795 | 1.1834 |
| .45 | 1.1872 | 1.1910 | 1.1949 | 1.1988 | 1.2026 | 1.2066 | 1.2104 | 1.2143 | 1.2182 | 1.2220 |
| .46 | 1.2259 | 1.2299 | 1.2338 | 1.2376 | 1.2416 | 1.2455 | 1.2495 | 1.2534 | 1.2574 | 1.2612 |
| .47 | 1.2652 | 1.2692 | 1.2732 | 1.2771 | 1.2811 | 1.2850 | 1.2890 | 1.2930 | 1.2970 | 1.3009 |
| .48 | 1.3050 | 1.3091 | 1.3130 | 1.3170 | 1.3210 | 1.3250 | 1.3291 | 1.3332 | 1.3371 | 1.3412 |
| .49 | 1.3452 | 1.3492 | 1.3532 | 1.3572 | 1.3613 | 1.3654 | 1.3695 | 1.3734 | 1.3776 | 1.3816 |

| | .000 | .001 | .002 | .003 | .004 | .005 | .006 | .007 | .008 | .009 |
|---|---|---|---|---|---|---|---|---|---|---|
| .50 | 1.3856 | 1.3899 | 1.3937 | 1.3980 | 1.4019 | 1.4061 | 1.4102 | 1.4142 | 1.4182 | 1.4223 |
| .51 | 1.4265 | 1.4304 | 1.4345 | 1.4386 | 1.4428 | 1.4468 | 1.4510 | 1.4550 | 1.4592 | 1.4633 |
| .52 | 1.4674 | 1.4715 | 1.4756 | 1.4797 | 1.4837 | 1.4877 | 1.4919 | 1.4959 | 1.4999 | 1.5042 |
| .53 | 1.5083 | 1.5124 | 1.5163 | 1.5205 | 1.5246 | 1.5286 | 1.5328 | 1.5368 | 1.5408 | 1.5449 |
| .54 | 1.5489 | 1.5530 | 1.5571 | 1.5610 | 1.5652 | 1.5694 | 1.5733 | 1.5773 | 1.5813 | 1.5853 |
| .55 | 1.5893 | 1.5934 | 1.5974 | 1.6003 | 1.6054 | 1.6095 | 1.6134 | 1.6176 | 1.6215 | 1.6255 |
| .56 | 1.6295 | 1.6335 | 1.6375 | 1.6415 | 1.6453 | 1.6491 | 1.6532 | 1.6570 | 1.6609 | 1.6650 |
| .57 | 1.6686 | 1.6728 | 1.6764 | 1.6804 | 1.6844 | 1.6880 | 1.6920 | 1.6958 | 1.6995 | 1.7033 |
| .58 | 1.7074 | 1.7112 | 1.7147 | 1.7185 | 1.7224 | 1.7259 | 1.7298 | 1.7334 | 1.7373 | 1.7409 |
| .59 | 1.7446 | 1.7483 | 1.7519 | 1.7556 | 1.7590 | 1.7627 | 1.7665 | 1.7699 | 1.7734 | 1.7768 |
| .60 | 1.7806 | 1.7841 | 1.7876 | 1.7912 | 1.7944 | 1.7979 | 1.8012 | 1.8047 | 1.8080 | 1.8116 |
| .61 | 1.8149 | 1.8182 | 1.8215 | 1.8248 | 1.8282 | 1.8312 | 1.8345 | 1.8376 | 1.8409 | 1.8440 |
| .62 | 1.8471 | 1.8501 | 1.8532 | 1.8563 | 1.8594 | 1.8625 | 1.8657 | 1.8685 | 1.8716 | 1.8744 |
| .63 | 1.8772 | 1.8801 | 1.8829 | 1.8857 | 1.8886 | 1.8914 | 1.8943 | 1.8968 | 1.8997 | 1.9022 |
| .64 | 1.9048 | 1.9073 | 1.9102 | 1.9124 | 1.9150 | 1.9175 | 1.9201 | 1.9223 | 1.9249 | 1.9272 |
| .65 | 1.9298 | 1.9320 | 1.9342 | 1.9365 | 1.9387 | 1.9406 | 1.9429 | 1.9451 | 1.9470 | 1.9489 |
| .66 | 1.9512 | 1.9531 | 1.9550 | 1.9569 | 1.9589 | 1.9604 | 1.9623 | 1.9643 | 1.9658 | 1.9673 |
| .67 | 1.9689 | 1.9704 | 1.9724 | 1.9736 | 1.9751 | 1.9767 | 1.9778 | 1.9794 | 1.9806 | 1.9822 |
| .68 | 1.9833 | 1.9845 | 1.9857 | 1.9865 | 1.9877 | 1.9889 | 1.9897 | 1.9908 | 1.9916 | 1.9924 |
| .69 | 1.9932 | 1.9940 | 1.9948 | 1.9956 | 1.9960 | 1.9968 | 1.9972 | 1.9976 | 1.9980 | 1.9984 |
| .70 | 1.9988 | 1.9992 | 1.9996 | 1.9996 | 2.0000 | 2.0000 | 2.0000 | 2.0000 | 2.0000 | 2.0000 |
| .71 | 2.0000 | 1.9996 | 1.9996 | 1.9992 | 1.9988 | 1.9984 | 1.9980 | 1.9976 | 1.9972 | 1.9968 |
| .72 | 1.9960 | 1.9952 | 1.9948 | 1.9940 | 1.9932 | 1.9924 | 1.9912 | 1.9904 | 1.9893 | 1.9881 |
| .73 | 1.9873 | 1.9861 | 1.9849 | 1.9833 | 1.9822 | 1.9810 | 1.9794 | 1.9778 | 1.9763 | 1.9747 |
| .74 | 1.9732 | 1.9716 | 1.9697 | 1.9681 | 1.9662 | 1.9643 | 1.9623 | 1.9604 | 1.9581 | 1.9562 |
| .75 | 1.9539 | 1.9516 | 1.9493 | 1.9470 | 1.9448 | 1.9425 | 1.9399 | 1.9372 | 1.9346 | 1.9320 |
| .76 | 1.9294 | 1.9268 | 1.9238 | 1.9212 | 1.9183 | 1.9153 | 1.9120 | 1.9091 | 1.9059 | 1.9030 |
| .77 | 1.8997 | 1.8965 | 1.8932 | 1.8896 | 1.8864 | 1.8829 | 1.8793 | 1.8758 | 1.8723 | 1.8685 |
| .78 | 1.8650 | 1.8612 | 1.8574 | 1.8532 | 1.8495 | 1.8457 | 1.8416 | 1.8376 | 1.8335 | 1.8292 |
| .79 | 1.8252 | 1.8208 | 1.8165 | 1.8123 | 1.8077 | 1.8034 | 1.7989 | 1.7944 | 1.7899 | 1.7851 |
| .80 | 1.7806 | 1.7759 | 1.7709 | 1.7662 | 1.7615 | 1.7565 | 1.7516 | 1.7464 | 1.7416 | 1.7364 |
| .81 | 1.7313 | 1.7262 | 1.7209 | 1.7159 | 1.7106 | 1.7053 | 1.6998 | 1.6943 | 1.6889 | 1.6835 |
| .82 | 1.6779 | 1.6722 | 1.6667 | 1.6611 | 1.6554 | 1.6499 | 1.6439 | 1.6383 | 1.6324 | 1.6265 |
| .83 | 1.6205 | 1.6145 | 1.6085 | 1.6026 | 1.5964 | 1.5903 | 1.5843 | 1.5780 | 1.5718 | 1.5657 |
| .85 | 1.5596 | 1.5533 | 1.5468 | 1.5406 | 1.5342 | 1.5377 | 1.5211 | 1.5147 | 1.5083 | 1.5017 |
| .85 | 1.4952 | 1.4885 | 1.4817 | 1.4751 | 1.4684 | 1.4618 | 1.4550 | 1.4482 | 1.4413 | 1.4345 |
| .86 | 1.4276 | 1.4207 | 1.4138 | 1.4069 | 1.4000 | 1.3930 | 1.3858 | 1.3787 | 1.3717 | 1.3646 |
| .87 | 1.3574 | 1.3504 | 1.3432 | 1.3360 | 1.3287 | 1.3215 | 1.3142 | 1.3068 | 1.2997 | 1.2923 |
| .88 | 1.2850 | 1.2776 | 1.2702 | 1.2628 | 1.2553 | 1.2478 | 1.2404 | 1.2329 | 1.2253 | 1.2177 |
| .89 | 1.2102 | 1.2026 | 1.1950 | 1.1874 | 1.1798 | 1.1722 | 1.1644 | 1.1567 | 1.1490 | 1.1413 |
| .90 | 1.1335 | 1.1257 | 1.1179 | 1.1101 | 1.1023 | 1.0945 | 1.0866 | 1.0787 | 1.0709 | 1.0628 |
| .91 | 1.0550 | 1.0470 | 1.0390 | 1.0310 | 1.0230 | 1.0150 | 1.0070 | .9990 | .9911 | .9823 |
| .92 | .9747 | .9662 | .9578 | .9497 | .9416 | .9337 | .9251 | .9174 | .9091 | .9001 |
| .93 | .8921 | .8842 | .8757 | .8673 | .8584 | .8503 | .8418 | .8333 | .8244 | .8163 |
| .94 | .8078 | .7987 | .7905 | .7819 | .7728 | .7639 | .7553 | .7468 | .7375 | .7289 |
| .95 | .7199 | .7112 | .7022 | .6930 | .6840 | .6748 | .6658 | .6562 | .6472 | .6378 |
| .96 | .6285 | .6188 | .6094 | .5999 | .5903 | .5804 | .5708 | .5609 | .5510 | .5408 |
| .97 | .5305 | .5203 | .5099 | .4995 | .4890 | .4782 | .4673 | .4562 | .4450 | .4337 |
| .98 | .4221 | .4103 | .3984 | .3861 | .3736 | .3608 | .3476 | .3341 | .3201 | .3056 |
| .99 | .2907 | .2750 | .2586 | .2412 | .2227 | .2028 | .1808 | .1562 | .1272 | .0897 |

## TABLE VI. Polarization correction, $\frac{1}{p}$

$$\left(=\frac{2}{1+\cos^2 2\theta}\right)$$

as a function of $\sin\theta$.

| | .000 | .001 | .002 | .003 | .004 | .005 | .006 | .007 | .008 | .009 |
|---|---|---|---|---|---|---|---|---|---|---|
| .00 | 1.0000 | 1.0000 | 1.0000 | 1.0000 | 1.0000 | 1.0001 | 1.0001 | 1.0001 | 1.0001 | 1.0002 |
| .01 | 1.0002 | 1.0002 | 1.0003 | 1.0003 | 1.0004 | 1.0004 | 1.0005 | 1.0006 | 1.0006 | 1.0007 |
| .02 | 1.0008 | 1.0009 | 1.0010 | 1.0011 | 1.0011 | 1.0012 | 1.0013 | 1.0015 | 1.0016 | 1.0017 |
| .03 | 1.0018 | 1.0019 | 1.0020 | 1.0022 | 1.0023 | 1.0024 | 1.0026 | 1.0027 | 1.0029 | 1.0030 |
| .04 | 1.0032 | 1.0034 | 1.0035 | 1.0037 | 1.0039 | 1.0040 | 1.0042 | 1.0044 | 1.0046 | 1.0048 |
| .05 | 1.0050 | 1.0052 | 1.0054 | 1.0056 | 1.0058 | 1.0060 | 1.0063 | 1.0065 | 1.0067 | 1.0069 |
| .06 | 1.0073 | 1.0075 | 1.0078 | 1.0080 | 1.0083 | 1.0085 | 1.0088 | 1.0090 | 1.0093 | 1.0096 |
| .07 | 1.0099 | 1.0101 | 1.0104 | 1.0107 | 1.0110 | 1.0113 | 1.0116 | 1.0119 | 1.0122 | 1.0126 |
| .08 | 1.0129 | 1.0132 | 1.0136 | 1.0139 | 1.0142 | 1.0145 | 1.0149 | 1.0152 | 1.0156 | 1.0160 |
| .09 | 1.0164 | 1.0167 | 1.0171 | 1.0175 | 1.0178 | 1.0182 | 1.0186 | 1.0190 | 1.0194 | 1.0198 |
| .10 | 1.0202 | 1.0206 | 1.0210 | 1.0215 | 1.0219 | 1.0223 | 1.0227 | 1.0231 | 1.0236 | 1.0241 |
| .11 | 1.0245 | 1.0249 | 1.0254 | 1.0259 | 1.0264 | 1.0268 | 1.0272 | 1.0277 | 1.0283 | 1.0287 |
| .12 | 1.0292 | 1.0298 | 1.0302 | 1.0307 | 1.0312 | 1.0318 | 1.0322 | 1.0327 | 1.0333 | 1.0338 |
| .13 | 1.0343 | 1.0349 | 1.0354 | 1.0361 | 1.0366 | 1.0371 | 1.0377 | 1.0382 | 1.0389 | 1.0394 |
| .14 | 1.0399 | 1.0406 | 1.0411 | 1.0418 | 1.0423 | 1.0430 | 1.0435 | 1.0442 | 1.0448 | 1.0454 |
| .15 | 1.0460 | 1.0467 | 1.0472 | 1.0479 | 1.0485 | 1.0492 | 1.0499 | 1.0505 | 1.0512 | 1.0519 |
| .16 | 1.0525 | 1.0532 | 1.0539 | 1.0545 | 1.0552 | 1.0560 | 1.0566 | 1.0573 | 1.0581 | 1.0588 |
| .17 | 1.0594 | 1.0602 | 1.0609 | 1.0617 | 1.0624 | 1.0632 | 1.0638 | 1.0646 | 1.0654 | 1.0661 |
| .18 | 1.0669 | 1.0677 | 1.0684 | 1.0692 | 1.0700 | 1.0708 | 1.0716 | 1.0724 | 1.0732 | 1.0740 |
| .19 | 1.0748 | 1.0756 | 1.0764 | 1.0772 | 1.0781 | 1.0789 | 1.0798 | 1.0806 | 1.0814 | 1.0824 |
| .20 | 1.0832 | 1.0840 | 1.0850 | 1.0858 | 1.0867 | 1.0875 | 1.0885 | 1.0893 | 1.0903 | 1.0912 |
| .21 | 1.0921 | 1.0930 | 1.0939 | 1.0948 | 1.0958 | 1.0967 | 1.0977 | 1.0987 | 1.0995 | 1.1005 |
| .22 | 1.1014 | 1.1024 | 1.1034 | 1.1044 | 1.1053 | 1.1063 | 1.1073 | 1.1083 | 1.1094 | 1.1104 |
| .23 | 1.1114 | 1.1123 | 1.1135 | 1.1145 | 1.1154 | 1.1166 | 1.1176 | 1.1186 | 1.1197 | 1.1207 |
| .24 | 1.1218 | 1.1228 | 1.1240 | 1.1251 | 1.1261 | 1.1271 | 1.1283 | 1.1294 | 1.1305 | 1.1316 |
| .25 | 1.1328 | 1.1339 | 1.1349 | 1.1361 | 1.1373 | 1.1384 | 1.1396 | 1.1408 | 1.1419 | 1.1431 |
| .26 | 1.1443 | 1.1455 | 1.1467 | 1.1478 | 1.1490 | 1.1502 | 1.1514 | 1.1526 | 1.1538 | 1.1550 |
| .27 | 1.1563 | 1.1575 | 1.1587 | 1.1600 | 1.1613 | 1.1625 | 1.1637 | 1.1651 | 1.1663 | 1.1677 |
| .28 | 1.1689 | 1.1703 | 1.1715 | 1.1729 | 1.1741 | 1.1755 | 1.1767 | 1.1781 | 1.1794 | 1.1808 |
| .29 | 1.1822 | 1.1834 | 1.1848 | 1.1862 | 1.1876 | 1.1889 | 1.1903 | 1.1918 | 1.1930 | 1.1945 |
| .30 | 1.1959 | 1.1973 | 1.1988 | 1.2002 | 1.2015 | 1.2029 | 1.2044 | 1.2058 | 1.2073 | 1.2088 |
| .31 | 1.2102 | 1.2117 | 1.2132 | 1.2146 | 1.2161 | 1.2177 | 1.2192 | 1.2207 | 1.2222 | 1.2237 |
| .32 | 1.2252 | 1.2267 | 1.2284 | 1.2299 | 1.2314 | 1.2329 | 1.2346 | 1.2361 | 1.2376 | 1.2392 |
| .33 | 1.2408 | 1.2424 | 1.2439 | 1.2456 | 1.2472 | 1.2489 | 1.2505 | 1.2520 | 1.2538 | 1.2553 |
| .34 | 1.2571 | 1.2588 | 1.2604 | 1.2620 | 1.2637 | 1.2653 | 1.2671 | 1.2687 | 1.2705 | 1.2721 |
| .35 | 1.2739 | 1.2755 | 1.2773 | 1.2791 | 1.2807 | 1.2825 | 1.2842 | 1.2860 | 1.2878 | 1.2897 |
| .36 | 1.2913 | 1.2932 | 1.2948 | 1.2967 | 1.2985 | 1.3004 | 1.3021 | 1.3040 | 1.3058 | 1.3075 |
| .37 | 1.3094 | 1.3113 | 1.3132 | 1.3149 | 1.3168 | 1.3187 | 1.3207 | 1.3226 | 1.3243 | 1.3263 |
| .38 | 1.3282 | 1.3301 | 1.3321 | 1.3339 | 1.3358 | 1.3378 | 1.3398 | 1.3417 | 1.3437 | 1.3455 |
| .39 | 1.3475 | 1.3495 | 1.3515 | 1.3535 | 1.3556 | 1.3576 | 1.3594 | 1.3615 | 1.3635 | 1.3656 |
| .40 | 1.3676 | 1.3697 | 1.3717 | 1.3738 | 1.3759 | 1.3778 | 1.3799 | 1.3820 | 1.3841 | 1.3862 |
| .41 | 1.3883 | 1.3904 | 1.3924 | 1.3947 | 1.3966 | 1.3988 | 1.4010 | 1.4031 | 1.4053 | 1.4075 |
| .42 | 1.4096 | 1.4118 | 1.4138 | 1.4160 | 1.4182 | 1.4205 | 1.4227 | 1.4249 | 1.4271 | 1.4292 |
| .43 | 1.4314 | 1.4337 | 1.4360 | 1.4382 | 1.4405 | 1.4426 | 1.4449 | 1.4472 | 1.4495 | 1.4518 |
| .44 | 1.4539 | 1.4562 | 1.4586 | 1.4609 | 1.4631 | 1.4654 | 1.4678 | 1.4702 | 1.4723 | 1.4747 |
| .45 | 1.4771 | 1.4795 | 1.4817 | 1.4841 | 1.4865 | 1.4888 | 1.4912 | 1.4937 | 1.4959 | 1.4984 |
| .46 | 1.5008 | 1.5031 | 1.5056 | 1.5078 | 1.5103 | 1.5126 | 1.5151 | 1.5177 | 1.5200 | 1.5225 |
| .47 | 1.5249 | 1.5274 | 1.5298 | 1.5321 | 1.5347 | 1.5370 | 1.5396 | 1.5420 | 1.5446 | 1.5470 |
| .48 | 1.5494 | 1.5521 | 1.5545 | 1.5569 | 1.5596 | 1.5620 | 1.5645 | 1.5669 | 1.5696 | 1.5721 |
| .49 | 1.5746 | 1.5770 | 1.5795 | 1.5823 | 1.5848 | 1.5873 | 1.5898 | 1.5924 | 1.5949 | 1.5974 |

| | .000 | .001 | .002 | .003 | .004 | .005 | .006 | .007 | .008 | .009 |
|---|---|---|---|---|---|---|---|---|---|---|
| .50 | 1.6000 | 1.6026 | 1.6051 | 1.6077 | 1.6103 | 1.6129 | 1.6155 | 1.6181 | 1.6207 | 1.6231 |
| .51 | 1.6258 | 1.6284 | 1.6308 | 1.6335 | 1.6361 | 1.6388 | 1.6412 | 1.6439 | 1.6466 | 1.6491 |
| .52 | 1.6518 | 1.6545 | 1.6570 | 1.6595 | 1.6622 | 1.6650 | 1.6675 | 1.6700 | 1.6725 | 1.6753 |
| .53 | 1.6779 | 1.6804 | 1.6829 | 1.6858 | 1.6883 | 1.6909 | 1.6935 | 1.6961 | 1.6987 | 1.7013 |
| .54 | 1.7039 | 1.7065 | 1.7091 | 1.7117 | 1.7144 | 1.7170 | 1.7197 | 1.7224 | 1.7247 | 1.7274 |
| .55 | 1.7301 | 1.7328 | 1.7352 | 1.7379 | 1.7403 | 1.7431 | 1.7455 | 1.7483 | 1.7507 | 1.7535 |
| .56 | 1.7559 | 1.7584 | 1.7612 | 1.7637 | 1.7662 | 1.7687 | 1.7715 | 1.7740 | 1.7765 | 1.7790 |
| .57 | 1.7816 | 1.7841 | 1.7867 | 1.7892 | 1.7915 | 1.7940 | 1.7966 | 1.7992 | 1.8015 | 1.8041 |
| .58 | 1.8067 | 1.8090 | 1.8116 | 1.8139 | 1.8165 | 1.8188 | 1.8215 | 1.8238 | 1.8262 | 1.8285 |
| .59 | 1.8312 | 1.8335 | 1.8359 | 1.8382 | 1.8406 | 1.8430 | 1.8454 | 1.8477 | 1.8498 | 1.8522 |
| .60 | 1.8546 | 1.8570 | 1.8591 | 1.8615 | 1.8639 | 1.8660 | 1.8681 | 1.8706 | 1.8727 | 1.8751 |
| .61 | 1.8772 | 1.8793 | 1.8815 | 1.8836 | 1.8857 | 1.8879 | 1.8900 | 1.8921 | 1.8943 | 1.8965 |
| .62 | 1.8986 | 1.9004 | 1.9026 | 1.9048 | 1.9066 | 1.9088 | 1.9106 | 1.9128 | 1.9146 | 1.9164 |
| .63 | 1.9183 | 1.9205 | 1.9223 | 1.9242 | 1.9260 | 1.9279 | 1.9298 | 1.9312 | 1.9331 | 1.9350 |
| .64 | 1.9369 | 1.9384 | 1.9402 | 1.9417 | 1.9436 | 1.9451 | 1.9467 | 1.9486 | 1.9501 | 1.9516 |
| .65 | 1.9531 | 1.9547 | 1.9562 | 1.9577 | 1.9589 | 1.9604 | 1.9619 | 1.9635 | 1.9646 | 1.9662 |
| .66 | 1.9673 | 1.9685 | 1.9701 | 1.9712 | 1.9724 | 1.9736 | 1.9747 | 1.9763 | 1.9771 | 1.9782 |
| .67 | 1.9794 | 1.9802 | 1.9814 | 1.9826 | 1.9833 | 1.9845 | 1.9853 | 1.9861 | 1.9869 | 1.9881 |
| .68 | 1.9889 | 1.9897 | 1.9904 | 1.9912 | 1.9916 | 1.9924 | 1.9932 | 1.9936 | 1.9944 | 1.9948 |
| .69 | 1.9956 | 1.9960 | 1.9964 | 1.9968 | 1.9972 | 1.9976 | 1.9980 | 1.9984 | 1.9988 | 1.9988 |
| .70 | 1.9992 | 1.9996 | 1.9996 | 1.9996 | 2.0000 | 2.0000 | 2.0000 | 2.0000 | 2.0000 | 2.0000 |
| .71 | 2.0000 | 1.9996 | 1.9996 | 1.9996 | 1.9992 | 1.9988 | 1.9988 | 1.9984 | 1.9980 | 1.9976 |
| .72 | 1.9972 | 1.9968 | 1.9964 | 1.9960 | 1.9952 | 1.9948 | 1.9944 | 1.9936 | 1.9928 | 1.9920 |
| .73 | 1.9912 | 1.9904 | 1.9897 | 1.9889 | 1.9881 | 1.9873 | 1.9861 | 1.9853 | 1.9841 | 1.9829 |
| .74 | 1.9822 | 1.9810 | 1.9798 | 1.9786 | 1.9775 | 1.9759 | 1.9747 | 1.9736 | 1.9720 | 1.9708 |
| .75 | 1.9693 | 1.9677 | 1.9662 | 1.9646 | 1.9631 | 1.9616 | 1.9600 | 1.9581 | 1.9566 | 1.9547 |
| .76 | 1.9531 | 1.9512 | 1.9493 | 1.9474 | 1.9455 | 1.9436 | 1.9417 | 1.9395 | 1.9376 | 1.9354 |
| .77 | 1.9331 | 1.9312 | 1.9290 | 1.9268 | 1.9246 | 1.9220 | 1.9198 | 1.9175 | 1.9150 | 1.9128 |
| .78 | 1.9102 | 1.9077 | 1.9051 | 1.9026 | 1.9001 | 1.8975 | 1.8947 | 1.8921 | 1.8893 | 1.8868 |
| .79 | 1.8839 | 1.8811 | 1.8783 | 1.8755 | 1.8727 | 1.8695 | 1.8667 | 1.8636 | 1.8608 | 1.8577 |
| .80 | 1.8546 | 1.8515 | 1.8484 | 1.8454 | 1.8420 | 1.8389 | 1.8355 | 1.8322 | 1.8288 | 1.8258 |
| .81 | 1.8225 | 1.8188 | 1.8155 | 1.8123 | 1.8086 | 1.8054 | 1.8018 | 1.7982 | 1.7947 | 1.7912 |
| .82 | 1.7876 | 1.7838 | 1.7803 | 1.7765 | 1.7727 | 1.7690 | 1.7655 | 1.7615 | 1.7578 | 1.7541 |
| .83 | 1.7501 | 1.7464 | 1.7425 | 1.7385 | 1.7346 | 1.7307 | 1.7268 | 1.7227 | 1.7188 | 1.7147 |
| .84 | 1.7109 | 1.7068 | 1.7027 | 1.6987 | 1.6943 | 1.6903 | 1.6861 | 1.6821 | 1.6779 | 1.6736 |
| .85 | 1.6694 | 1.6653 | 1.6609 | 1.6567 | 1.6523 | 1.6483 | 1.6439 | 1.6396 | 1.6353 | 1.6308 |
| .86 | 1.6265 | 1.6221 | 1.6179 | 1.6134 | 1.6090 | 1.6046 | 1.6000 | 1.5957 | 1.5913 | 1.5868 |
| .87 | 1.5823 | 1.5778 | 1.5733 | 1.5689 | 1.5642 | 1.5598 | 1.5552 | 1.5506 | 1.5461 | 1.5415 |
| .88 | 1.5370 | 1.5326 | 1.5279 | 1.5235 | 1.5188 | 1.5142 | 1.5097 | 1.5049 | 1.5004 | 1.4957 |
| .89 | 1.4912 | 1.4865 | 1.4819 | 1.4771 | 1.4725 | 1.4680 | 1.4633 | 1.4586 | 1.4539 | 1.4493 |
| .90 | 1.4447 | 1.4401 | 1.4353 | 1.4306 | 1.4259 | 1.4213 | 1.4166 | 1.4120 | 1.4073 | 1.4027 |
| .91 | 1.3980 | 1.3933 | 1.3887 | 1.3841 | 1.3793 | 1.3748 | 1.3701 | 1.3654 | 1.3607 | 1.3561 |
| .92 | 1.3514 | 1.3468 | 1.3421 | 1.3374 | 1.3328 | 1.3282 | 1.3235 | 1.3189 | 1.3142 | 1.3096 |
| .93 | 1.3050 | 1.3004 | 1.2957 | 1.2912 | 1.2865 | 1.2819 | 1.2773 | 1.2728 | 1.2681 | 1.2636 |
| .94 | 1.2590 | 1.2544 | 1.2498 | 1.2453 | 1.2407 | 1.2361 | 1.2317 | 1.2271 | 1.2226 | 1.2182 |
| .95 | 1.2136 | 1.2090 | 1.2045 | 1.2000 | 1.1956 | 1.1912 | 1.1867 | 1.1822 | 1.1779 | 1.1733 |
| .96 | 1.1689 | 1.1646 | 1.1601 | 1.1557 | 1.1513 | 1.1469 | 1.1426 | 1.1382 | 1.1339 | 1.1294 |
| .97 | 1.1251 | 1.1208 | 1.1164 | 1.1122 | 1.1079 | 1.1036 | 1.0994 | 1.0951 | 1.0908 | 1.0866 |
| .98 | 1.0824 | 1.0781 | 1.0739 | 1.0697 | 1.0655 | 1.0613 | 1.0572 | 1.0530 | 1.0489 | 1.0447 |
| .99 | 1.0406 | 1.0365 | 1.0324 | 1.0283 | 1.0242 | 1.0202 | 1.0161 | 1.0120 | 1.0081 | 1.0040 |

TABLE VII. Example of computation of timing of exposures of the photographs of the several levels.

*Case: equi-inclination Weissenberg.* Varies with method according to (15)–(17)

| I | II | III | IV | V | VI | VII |
|---|---|---|---|---|---|---|
| Level number | coordinate of level, $\xi$ | inclination angle,[a] $\mu$ | layer-screen setting,[a] $s$ | $\cos\mu$ | $S=\cos^2\mu$ | $t=T_0S$ |
| 0 | 0.000 | 0.0° | 0.0 mm | 1.000 | 1.000 | 20.00 hrs. |
| 1 | .178 | 5.1 | 2.2 | .996 | .992 | 19.84 |
| 2 | .356 | 10.3 | 4.7 | .984 | .966 | 19.32 |
| 3 | .534 | 15.5 | 7.1 | .964 | .930 | 18.60 |

[a] From *X-Ray Crystallography*, see reference 3, Figs. 155 and 156.

TABLE VIII. Example of computation of $F^2$ from $I$, hexagonal crystal.

*Case: zero level, $\mu=0$. $a^{*2}=0.0316$. $\zeta=0$.*

| I | II | III | IV | V | VI | VII |
|---|---|---|---|---|---|---|
| Reflection *hkl* | $h^2+k^2+hk$ (from Table II) | $a^{*2}(h^2+k^2+hk)$ | $\sigma=[a^{*2}(h^2+k^2+hk)]^{\frac{1}{2}}$ | $1/L\cdot p$ (from Table III) | $I$ (experimental data) | $F^2$ (V×VI) |
| 130 | 13 | 0.411 | 0.641 | 0.7457 | 2.4 | 1.8 |
| 200 | 4 | .126 | .355 | .3733 | 7.1 | 2.7 |
| 220 | 12 | .379 | .615 | .7077 | 11.6 | 8.2 |
| 350 | 49 | 1.548 | 1.244 | 1.8532 | 1.5 | 2.8 |
| 600 | 36 | 1.138 | 1.063 | 1.5163 | 1.5 | 2.3 |

TABLE IX. Example of computation of $F^2$ from $I$, hexagonal crystal.

*Case: n-level, equi-inclination.* $a^{*2}=0.0316$. $c^{*2}=0.0336$. $l=2$. $l^2c^{*2}=0.134$.

| I | II | III | IV | V | VI | VII | VIII | IX | X |
|---|---|---|---|---|---|---|---|---|---|
| Reflection *hkl* | $h^2+k^2+hk$ (from Table II) | $a^{*2}(h^2+k^2+hk)$ | III+$l^2c^2$ | $\sigma=$(IV)$^{\frac{1}{2}}$ | $1/p$ (from Table IV) | $\tau$ (from film measurement) | sin $\tau$ | $I$ (experimental data) | $F^2$ =VI·VIII·IX |
| 122 | 7 | 0.221 | 0.355 | 0.596 | 1.1930 | 28.40 mm | 0.4756 | 5.1 | 2.9 |
| 252 | 39 | 1.232 | 1.366 | 1.170 | 1.8188 | 69.00 | .9336 | 0.2 | 0.3 |
| 302 | 9 | 0.284 | 0.418 | 0.647 | 1.2314 | 31.90 | .5284 | 1.0 | 0.7 |
| 332 | 27 | .853 | .987 | .993 | 1.5924 | 56.40 | .8329 | 0.7 | 0.9 |
| 512 | 31 | .980 | 1.114 | 1.055 | 1.6725 | 60.80 | .8729 | 0.5 | 0.7 |

TABLE X. Example of computation of $F^2$ from $I$, hexagonal crystal.

*Case: zero level, $\mu\neq0$ (de Jong-Bouman)* $a^{*2}=0.0316$. $\zeta=0$. $\mu=45°$.

| I | II | III | IV | V | VI | VII | VIII |
|---|---|---|---|---|---|---|---|
| Reflection *hkl* | $h^2+k^2+hk$ (from Table II) | $a^{*2}(h^2+k^2+hk)$ | $\sigma=[a^{*2}(h^2+k^2+hk)]^{\frac{1}{2}}$ | $1/p$ (from Table IV) | sin $\tau$ (from Fig. 1) | $I$ (experimental data) | $F^2$ V·VI·VII |
| 130 | 13 | 0.411 | 0.641 | 1.2267 | 0.81 | 1.8 | 1.8 |
| 200 | 4 | .126 | .355 | 1.0654 | .49 | 5.1 | 2.7 |
| 220 | 12 | .379 | .615 | 1.2073 | .78 | 8.7 | 8.2 |
| 350 | 49 | 1.548 | 1.244 | 1.9026 | .84 | 1.7 | 2.7 |
| 600 | 36 | 1.138 | 1.063 | 1.6829 | .99 | 1.4 | 2.3 |

# The Determination of Molecular-Weight Distribution in High Polymers by Means of Solubility Limits*†

D. R. Morey and J. W. Tamblyn
*Kodak Research Laboratories, Rochester, New York*

(Received March 20, 1945)

By means of polymer fractions of known molecular weight, dissolved in solutions of known compositions, it is possible to determine the solubility law which relates the point of solution saturation to the molecular weight and concentration of the dissolved polymer. Having established such a calibration, it is possible to determine the molecular-weight distribution in a heterogeneous sample of the polymer by suitable operation on a curve relating the mass of polymer precipitated to the amount of precipitant added to the solution. Optical means, making use of scattering from the precipitate, are used to obtain this latter curve. The method is applied to cellulose acetate butyrate and is shown to give results in agreement with gravimetrically obtained distribution curves.

## INTRODUCTION

With the increasing use of high polymers, it has become more and more evident that the molecular sizes in a heterogeneous polymer are not sufficiently characterized by an average value only. For more precise knowledge of the basis of solubility, swelling, and mechanical properties, a knowledge of the distribution function of the molecules with respect to weight is necessary. The standard method of determining such a distribution function is to effect by physical means a separation or fractionation of the polymer into relatively homogeneous parts, and obtain both the average molecular weight and the weight fraction in each of these parts. The difficulties and the time required for such a procedure are so great that it is not often carried out. The need for a simpler or more rapid method of obtaining the chain-length distribution function has stimulated research, and two new methods are now coming to fruition.

The first of these is based on the work of Debye,[1] the second was reported by us recently.[2] It is interesting that both these methods make use of scattered light, although in quite different ways. Debye's method measures the light scattered from dilute solutions of the polymer; this scattering arises from the random thermally-induced local variations in solution density and polymer concentration. This latter contribution is related to the molecular weight, and for a heterogeneous distribution, leads to a weight average.[3] The possibility of extending this method to yield information about the molecular-weight distribution was recently discussed by Zimm and Doty,[4] and by Debye,[5] and it appears that while the distribution curve itself cannot (at the present state of development) be obtained, accurate measurements of the turbidity should lead to other weighted averages. A measure of the distribution curve width is then obtained from these different averages.

A valuable feature of Debye's method, applied to the derivation of an average molecular weight, is that it is a fundamental or absolute one; it derives the answer from measurable basic quantities without recourse to calibration from the osmotic pressure method. In view of the limitations and difficulties of the osmotic pressure and ultracentrifuge methods for measuring very high molecular weights, another independent method is most welcome.

In contrast to this use of light scattered from polymer molecules while in the dissolved state, the second method makes use of the light scattered from particles or aggregates of the polymer precipitated out of solution by the addition of non-solvent. By making properly verified corrections, this scattered light is a measure of the increment of polymer which precipitates out, for

* Presented to the Division of High-Polymer Physics, Rochester, New York, June, 1944. In the schedule of papers presented in the symposium at this meeting, which was published in the January, 1945, issue of this Journal, it was stated incorrectly that this paper was to be published in *Industrial and Engineering Chemistry*. This error occurred because a paper by the present authors having a somewhat similar title was scheduled for *Industrial and Engineering Chemistry*.

† Communication No. 1024 from the Kodak Research Laboratories.

[1] P. Debye, J. App. Phys. 15, 338 (1944).

[2] D. R. Morey and J. W. Tamblyn, Meeting, High-Polymer Physics Division, Rochester, N. Y., June, 1944.

[3] P. M. Doty, B. H. Zimm, and H. Mark, J. Chem. Phys. 12, 144 (1944).

[4] B. H. Zimm and P. M. Doty, J. Chem. Phys. 12, 203 (1944).

[5] P. Debye, Meeting, High-Polymer Physics Division, Rochester, N. Y., June, 1944.

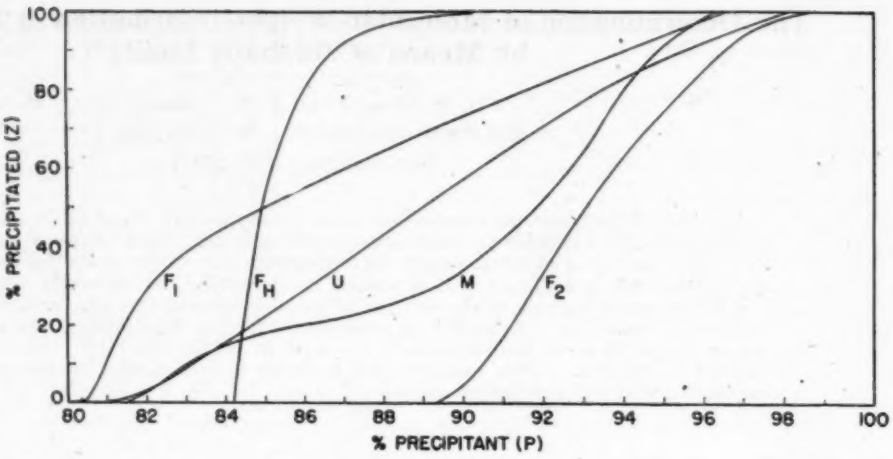


FIG. 1. Precipitation curves for cellulose acetate butyrate.

$U$—Unfractionated ($M$ =71,000)
$F_1$—Fraction ($M$ =183,000)
$F_2$—Fraction ($M$ =33,000)
$M$—1 part by weight fraction $F_1$ 2 parts by weight fraction $F_2$
$F_H$—Calculated curve for a fraction of perfect homogeneity ($M$=100,000)

each increment of non-solvent added. Scattered light in this method is a means of "weighing" the precipitates without the actual physical steps of filtration, washing, drying, and weighing.

## EXPERIMENTAL PROCEDURE

The apparatus centers about a square glass cell, which is illuminated by a parallel beam of light. A barrier-layer type of photo-cell receives the directly transmitted horizontal beam, while two other photo-cells are mounted to pick up light which is scattered transversely to the direct beam. The polymer to be studied is dissolved in a suitable solvent, and diluted to the appropriate value. Best optical results are obtained with quite dilute solutions; the standard value used in our case was 0.1786 g per 100 cc of acetone. In order to bring the solution closer to the precipitation point before starting the mechanical addition of precipitant, the solution was further diluted with precipitant (a 3:1-by-volume mixture of ethyl alcohol-water in this case) to a value of 0.05 g per 100 cc. A sufficient amount of this solution (125 cc) is then placed in the cell, so that the incident beam is completely within the solution. A mechanical pump delivers additional precipitant at a slow rate (18 cc per minute) to the solution, which is continuously and rapidly stirred during this pumping. The development of turbidity is followed either with a drop in transmission or with an increase in right-angled scatter, the photo-cell output being recorded on a galvanometer-type recorder. It is necessary, in order to achieve reproducibility in such solution phenomena, to maintain controlled temperatures. Heats of mixing will cause temperature changes but by control of initial temperatures, and by immersion of the glass cell in a water bath (with appropriate windows for optical illumination and photo-cells), consistent results may be obtained. There is thus obtained a curve relating the intensity of the transmitted (or scattered) light as a function of the amount of precipitant added.

Since the purpose of such optical readings is to furnish a number proportional to the amount of material precipitated, the curves as taken from the recording chart are replotted, making the abscissa the percentage of precipitant added (denoted by $P$), and the ordinate a percentage of the maximum optical density obtained when all of the material has been thrown out of solution. With the addition of diluent, that material already precipitated is progressively diluted, so that it is necessary to correct the density readings to some fixed value of concentration. This assumes Beer's law, which can be tested in a subsidiary experiment. This type of curve has already been used as a relative and approximate measure of the molecular-weight spread in heterogeneous polymers.[6,7] Examples of such a curve, obtained by the above procedure are shown in Fig. 1.

## EXPERIMENTAL PRECAUTIONS

It is advisable, although not necessary, to choose a solvent and a precipitant of nearly the same refractive index. By so doing, there is little change of index of the solution as precipitation proceeds and no need to apply a Rayleigh index correction to the observed scattering from the particles of the precipitate. The solvent-precipitant system must also have an index different from that of the polymer. Marked heat of mixing, in cases of rapid pumping, leads to

[6] H. E. Adams, and P. O. Powers, Ind. Eng. Chem., Anal. Ed. **15**, 711 (1943).
[7] J. G. McNally, Lecture at the Gibson Island Conference on High Polymers, 1942.

spurious results, and this is another point to keep in mind in choosing the liquid system.

There may be further complications because of aging of the precipitate and agglomeration to large particles, thus changing the optical effects without necessarily producing a change in the amount precipitated out. We have observed such aging phenomena particularly in the case of polyvinyl acetate resins. For the cellulose esters, these effects are fortunately not pronounced. By judicious selection of the solvent and precipitant, it is possible to minimize such effects.

It may also be necessary to make corrections in case the scattering power of a precipitate is itself a function of molecular weight. This latter possibility can come about because of the different degrees to which a precipitate is swollen with liquid, according to the length of the polymer chain. Different states of swelling mean a different particle size and refractive index—two variables which influence the scatter. Fortunately, for cellulose acetate and acetate butyrate, as they are precipitated from acetone by ethyl alcohol and water, the scattering power per gram of precipitate does not vary much with molecular weight. As an illustration, however, of how markedly the precipitate scatter can depend on the molecular weight, Fig. 2 is shown. The test tubes contained equal masses, each fully precipitated, of fractions of a polymer (the butyl ester of the lactonized copolymer of maleic anhydride and vinyl acetate), fraction I being the highest molecular weight and IX, the lowest. It is readily seen how much greater is the scatter from the lower fractions.

Still another precaution is to choose a solvent-precipitant system which will result in good separations on a basis of molecular weight. Systems exist which produce precipitates with practically no dependence of the precipitation point upon polymer molecular weight.[8]

## CALCULATION OF THE DISTRIBUTION CURVE

A specific value of $P$ at which a precipitate appears is determined by five factors: (1) The molecular weights $M_i$ present in solution, (2) the concentration $C_i$ of each species of molecular weight in solution at the time of precipitation, (3) the type of polymer, (4) the temperature of the system, and (5) the solvent-precipitant system used.

[8] D. R. Morey and J. W. Tamblyn, "Experimental Studies on the Fractionation of High Polymers" (to appear in J. Phys. Chem.)

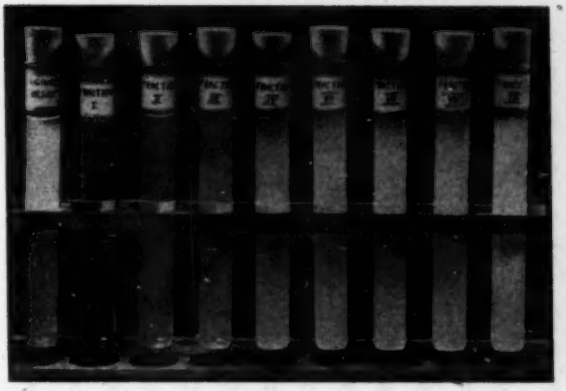

FIG. 2. Variation of scattering power with molecular weight.

In a given experiment, the last three of these are experimentally controlled, so that $P=F(M, C)$ at saturation. Thus, any solvent-precipitant composition, denoted by $P$, is a saturation state for some value of molecular weight and concentration of the molecular-weight species. This view of $P$ as a parameter denoting a saturated state is used in the following development. It is necessary to determine by experiment the function $F(M, C)$, by the use of homogeneous fractions of known molecular weight, and at known concentrations.*

### A. The Determination of the Saturation Limit Law

The fractionation procedure is described elsewhere,[9] together with the actual values for the cellulose acetate butyrate fractions used in these experiments. The effect of concentration on the saturation limit is studied by precipitating these known fractions, using different starting concentrations, and noting the percent of precipitant at which precipitation starts.** It is then

* Since a fractionation is required to obtain such fractions, the query arises as to why continue with an optical method, since the standard gravimetric distribution curve is readily obtained if the amounts of the fractions are known. Indeed there is no point to establishing this optical method if the polymer always exists with only one and the same distribution, or if it is of little future interest. The utility of this method is that once the calibration for a given type of polymer is established, it is a relatively rapid means for deducing any new distribution which may occur as a result of different methods of synthesis, blending, or degradation.

[9] J. W. Tamblyn, D. R. Morey, and R. H. Wagner, "Viscosity-Molecular Weight Relationships for Cellulose Acetate Butyrate," Ind. Eng. Chem., Ind. Ed. **37**, 573–77 (June, 1945).

** If saturation, and the corresponding $P$ value, are defined by the point at which a precipitate just appears, the exact value will depend upon the sensitivity of the

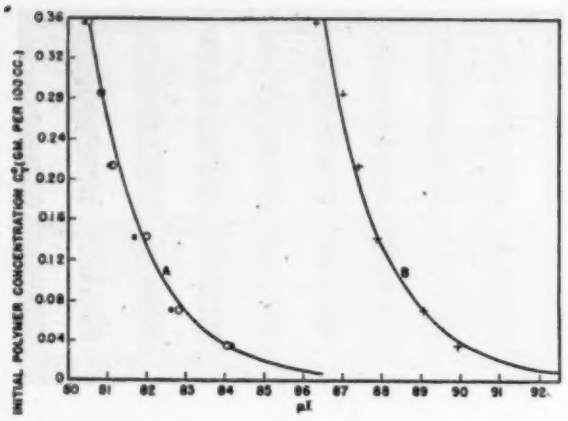


FIG. 3. Effect of concentration on precipitation point.

• • • Unfractionated cellulose acetate butyrate ($M$ =71,000)
○○○ Fraction $B_2$ ($M$ =137,500)
+++ Fraction $D_2$ ($M$ =50,000)
Curve $A$: $P^\gamma+3.2 \log [C_T^0(1-(P^\gamma/100))] = f(M_i) = 76.8$
Curve $B$: $P^\gamma+3.2 \log [C_T^0(1-(P^\gamma/100))] = f(M_i) = 82.3$

possible to plot curves such as those shown in Fig. 3 and to establish the law governing concentration as a variable. If this law is the same for different fractions, then $M$ and $C$ appear in separate terms, and the analytical procedure is simpler. This turned out to be the case for our system, the law being

$$P^\gamma = -3.2 \log C^\gamma + f(M). \quad (1)$$

It is of interest to note that Schulz[10, 11] has derived a form of the function $F(M, C)$ as follows:

$$P^\gamma = K_0 + K_1 \log C^\gamma/M_i + K_2/M_i, \quad (2)$$

where $K_0$, $K_1$, and $K_2$ take on specific values for each polymer and solvent-precipitant system, and $C^\gamma$ is the actual concentration of the molecular-weight species $M_i$ at its point of precipitation, corresponding to the value $P^\gamma$.

The concentration $C^\gamma$ may be expressed in terms of its initial value $C^0$ in pure solvent ($P=0$) by the relation:

$$C^\gamma = C^0(1-P^\gamma/100). \quad (3)$$

(The superscripts designate the corresponding values of $C$ and $P$, paired together by some relation $P=F(M, C)$. Subscripts are used to denote particular $M$ values.) In Eq. (3) it is assumed that no precipitation occurs until the value $P^\gamma$ is reached, and the equation represents a concentration change caused by dilution only. Concentration changes caused by precipitation are calculated with the aid of the function $F(M, C)$.

Next, by precipitating fractions of varying molecular weight and applying the dilution Eq. (3) to the results, we determine the effect of $M$ as a variable. Figure 4 shows the precipitation curves of a number of fractions, and Fig. 5 the $f(M)$ plotted against $M$, obtained by putting the observed paired values of $P$ and $C$ into (1).

### B. Application of the Saturation Limit Law

Let us suppose that a polymer of unknown distribution, but for which Eq. (1) holds, is precipitated by the gradual addition of precipitant. From the light-scattering data, as will be shown later, it is possible to calculate the mass precipitated as a function of the percent of precipitant. Let $Z$ be the percentage of the dissolved polymer which has precipitated out. Then from the optical data we can draw a graph of the function:

$$Z = G(P), \quad (4)$$

and can read off the corresponding increments of:

$$\Delta Z = G'(P)\Delta P. \quad (5)$$

Any given increment $\Delta Z$ does not consist entirely of one molecular-weight species, but contains a distribution around a most probable value, just as relatively homogeneous fractions but never perfect fractions can be separated from a heterogeneous mixture.

It has been our experience, however, in working with cellulose acetate butyrate, that we can assign to each $\Delta Z$ some representative value and assume that all of the $\Delta Z$ is of this single value only. Results obtained with this assumption are in accord with experiment, but it may be that for other materials and systems, better accord may be obtained if some account is taken of the molecular-weight spread in each $\Delta Z$.

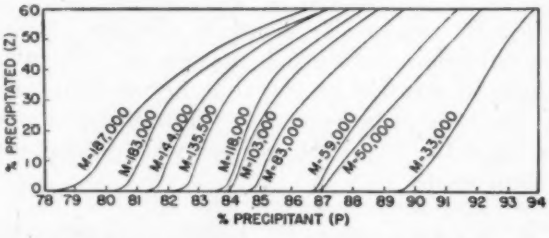


FIG. 4. Precipitation curves for a series of molecular-weight fractions.

turbidity measuring system and the constancy of initial haze. A more accurate parameter is the point at which 1 percent of the maximum turbidity is developed. This necessitates completing the precipitation.

[10] G. V. Schulz, Zeits. f. physik. Chemie **A179**, 321 (1937).

[11] G. V. Schulz and B. Jirgensons, Zeits. f. physik. Chemie **B46**, 105 (1940).

Suppose that in $W_T$ grams of the polymer there are $W_1$, $W_2$, $W_3$, $\cdots$ grams of molecular weight species $M_1$, $M_2$, $M_3$, $\cdots$. The ratios $W_1/W_T$, $W_2/W_T$, $W_3/W_T$, $\cdots$, when plotted against $M$, will form the desired distribution curve. For any species $M_i$ we have:

$$\frac{W_i}{W_T}=\frac{C_i^0}{C_T^0}=\frac{C_i^\gamma}{C_T^\gamma}. \tag{6}$$

Now, suppose that species $M_i$ is present in such an amount that the solution becomes saturated (for species $M_i$) at a value of $P=P^\gamma$. If $P^\gamma$ is increased by $\Delta P$, a percentage $(\Delta Z)^\gamma$ of the total mass comes out of solution, and this $(\Delta Z)^\gamma$ we take to be of the species $M_i$. Then,

$$(\Delta Z)_i^\gamma=\delta_i(C_i^0/C_T^0)100,$$

where $\delta_i$ is the fraction of species $M_i$ precipitated in the interval $P^\gamma$ to $P^\gamma+\Delta P$.

$$\delta_i=(C_T^0/C_i^0)((\Delta Z)_i^\gamma)/100. \tag{7}$$

The concentration of species $M_i$ now remaining in solution at the end of this interval is, from Eqs. (3) and (7).

$$\begin{aligned}C_i^{\gamma+\Delta}&=C_i^0(1-\delta_i)\left(1-\frac{P^\gamma+\Delta P}{100}\right)\\&=\left[C_i^0-\frac{C_T^0(\Delta Z)_i^\gamma}{100}\right]\left[1-\frac{P^\gamma+\Delta P}{100}\right].\end{aligned} \tag{8}$$

At both the dilution $P^\gamma$ and at $P^\gamma+\Delta P$, the solution is saturated with respect to species $M_i$, and therefore the saturation limit law (1) holds.

Rewriting (1) as:

$$C_i^\gamma=10^{P^\gamma/K}10^{-f(M_i)/K}, \tag{9}$$

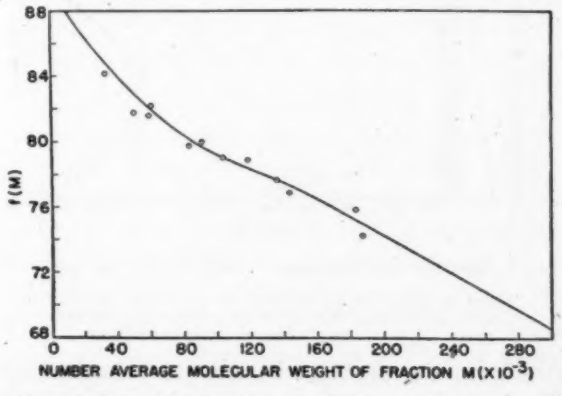


FIG. 5. Determination of the molecular-weight term in the expression for $P$

$$f(M_i)=P^\gamma+3.2\log 0.1786(1-(P^\gamma/100)).$$

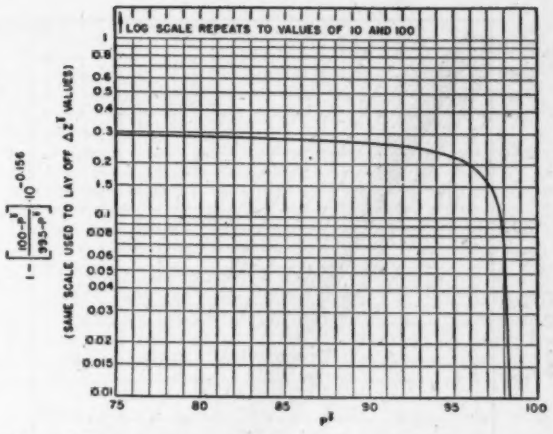


FIG. 6. Nomogram for obtaining the percentage of a given molecular-weight species.

and applying (9) to the two cases, we get:

$$\frac{C_i^0}{C_T^0}\left(1-\frac{P^\gamma}{100}\right)=\frac{1}{C_T^0}10^{P^\gamma/K}10^{-f(M_i)/K}, \tag{10}$$

$$\left[C_i^0-\frac{C_T^0(\Delta Z)_i^\gamma}{100}\right]\left[1-\frac{P^\gamma+\Delta P}{100}\right]=10^{(P^\gamma+\Delta P)/K}10^{-f(M_i)/K}. \tag{11}$$

Eliminating $f(M_i)$, we obtain:

$$100\frac{C_i^0}{C_T^0}=\frac{(\Delta Z)_i^\gamma}{1-10^{\Delta P/K}\left(\dfrac{100-P^\gamma}{100-P^\gamma-\Delta P}\right)}. \tag{12}$$

The ratio $C_i^0/C_T^0$ is the key to the distribution curve. The right-hand side of (12) can be completely evaluated, since a constant interval $\Delta P$ can be assigned, and corresponding values of $(\Delta Z)^\gamma$ and $P^\gamma$ read directly from the optical precipitation curve of the polymer. (Examples of such curves appear in Fig. 1.)

The actual evaluation of Eq. (12) for the ratio $C_i^0/C_T^0$ is accomplished most easily by keeping $\Delta P$ fixed, at, say, 0.5, and using the nomogram of Fig. 6 in which the denominator of the right-hand side of Eq. (12) (for $\Delta P=0.5$ and $K=-3.2$) has been plotted as ordinate against $P^\gamma$ as abscissa. Since the ordinate is on a logarithmic scale, the linear difference between the value for $(\Delta Z)^\gamma$ (the numerator of (12)) and the corresponding value of the denominator (determined by the particular $P^\gamma$), represents in length the log of $(100C_i^0/C_T^0)$. The procedure is then to set dividers to the distance from the curve to the value of $(\Delta Z)^\gamma$, measured along the

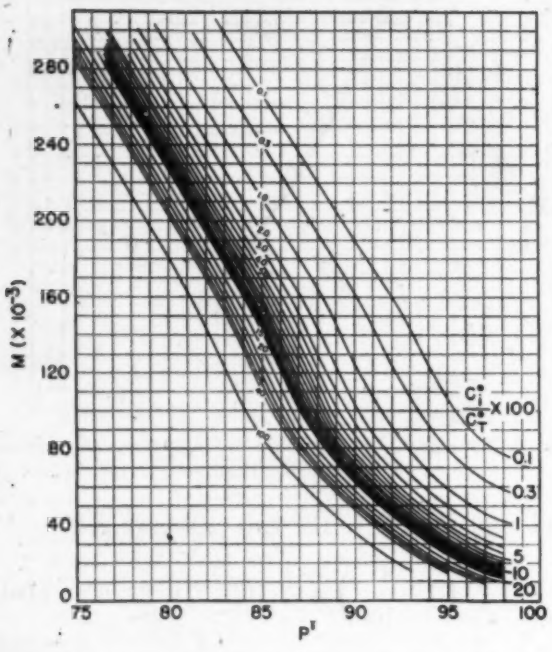


FIG. 7. Nomogram for assigning molecular weights.

vertical line corresponding to the proper $P'$. This distance is laid off from the ordinate 1. The ordinate reading at the other end of the dividers is $(100C_i^0/C_T^0)$.

There remains the assignment of the actual molecular weight corresponding to the ratio $C_i^0/C_T^0$. This is done by putting back into (10) each value of the ratio and its corresponding $P$ value. The molecular weight $M$ is then the only unknown and is obtained from a suitably constructed nomogram which is based on Eq. (10) and a knowledge of $f(M)$. (The function $f(M)$ is determined by experiment on the fractions (whose osmotic molecular weights have been measured) as has been shown in Fig. 5.) The value of $M$ associated with the distribution ratio obtained from Fig. 6 is found from the nomogram shown in Fig. 7. In using this nomogram, we select the curve for this distribution ratio, note its intersection with the proper value, and read off the corresponding $M$.

According to this procedure, a tabulation of distribution ratios and corresponding molecular weights is made, covering the $P$ range of the whole precipitation curve. Since $\sum(100C_i^0/C_T^0)$ must equal 100, the values of the distribution ratios should be "normalized," so to speak, before they are plotted against $M$ to make the final distribution curve.

The values of the ratios, in suitable class intervals of $\Delta M$ (usually, $\Delta M = 10{,}000$) are then added to form the final distribution curve. Figure 8 shows the distribution curve obtained optically, and the gravimetric distribution curve for the same sample of cellulose acetate butyrate. The agreement is most satisfactory.

Figure 9 illustrates how well this optical method analyzes a synthetic mixture of one part by weight of a fraction of molecular weight 183,000 and two parts by weight of a fraction of molecular weight 33,000. (The precipitation curve for this mixture is shown in Fig. 1.) The peaks are seen to agree closely with the molecular weights of the component fractions.

In applying this method to other polymers, the specific details may be different from those given here, because of a different form of the saturation limit law or because of necessary corrections in the conversion of light-scattering data to mass precipitated. The general mode of

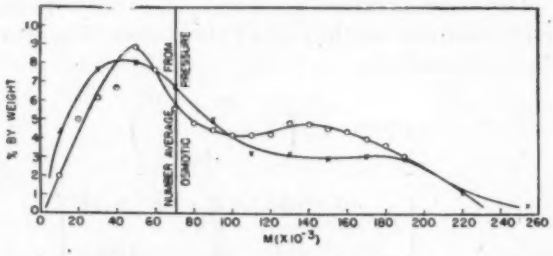


FIG. 8. Distribution curves of a heterogeneous cellulose acetate butyrate obtained by gravimetric and by optical-solubility procedures.

O——O Gravimetric data
X——X Optical data

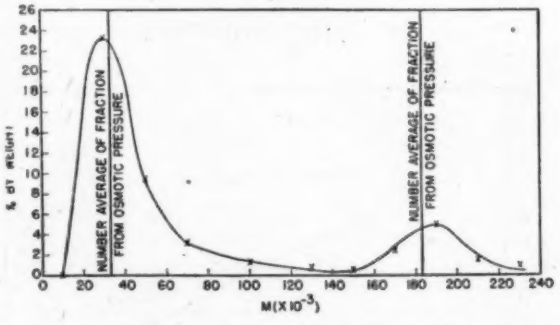


FIG. 9. Distribution curves of a mixture of two fractions.

1 part by weight of fraction of molecular weight 183,000.
2 parts by weight of fraction of molecular weight 33,000.

attack on the problem is, however, unchanged. The procedure requires considerable initial labor in calibration but is capable of yielding detailed and accurate results.

# Techniques for Evaporation of Metals*

LEONARD O. OLSEN, CHARLES S. SMITH, AND E. C. CRITTENDEN, JR.
*Case School of Applied Science, Cleveland, Ohio*

(Received March 23, 1945)

Thirty-four elements have been observed for evaporation behavior, the results being summarized for each element and the best techniques then listed in Table I. Heaters studied fall into two general classes, wires and crucibles. Tungsten, iron, nickel, and chromel wires were used and these were formed into close wound conical baskets and helical coils. Each element was studied for evaporation behavior from as many of these forms as was possible. Alundum and BeO crucibles formed by painting suspensions of these materials on a tungsten conical basket followed by baking at a high temperature were exceptionally satisfactory heaters for almost all of the elements studied. These crucibles served well for the evaporation of metals whose evaporation temperatures approached 2000°C as well as for those with lower evaporation temperatures.

The 18-inch evaporation system was designed and constructed along fairly standard lines. An externally operated, four-inch vacuum valve between the diffusion pump and the bell jar allowed air to be admitted to the bell jar without cooling the diffusion pump. This valve was an especially useful feature of the equipment.

## INTRODUCTION

EVAPORATION techniques have long been used in the preparation of astronomical mirrors and more recently in the preparation of reflecting and non-reflecting surfaces for many uses. Such techniques, particularly those for evaporating metals, have recently assumed considerable importance because of the scientific utility of thin metallic films and because of the scientific interest in the properties of such films.

Strong's *Procedures in Experimental Physics*[1] contains considerable valuable information on evaporation. However, it is primarily concerned with aluminum evaporation and successful techniques for aluminum are unsatisfactory for some other materials. Caldwell's[2] article on evaporation of metals contains much specific information which this article supplements and in some cases corrects.

The literature contains many other references to studies made on the properties of evaporated surfaces but there is little in these sources that is detailed and up to date in regard to the actual technique of preparing the surfaces.

## APPARATUS

An evaporation system consisting of an 18-inch diameter bell jar, pumping system, and vacuum gauges was constructed along fairly standard lines. Twelve electrical terminals were brought into the jar and served to mount a number of independent filaments, allowing several evaporations to be done with one evacuation of the system. These electrical leads were quarter-inch rods which passed through larger holes in the metal base plate. They were held firmly by tightening nuts on washers, both on top and bottom of the base plate. Rubber washers cut from a roll of tire patch material and attached to the metal washers furnished the necessary electrical insulation and made good vacuum seals.

A vacuum valve between the bell jar and diffusion pump allowed air to be admitted to the bell jar without admitting it to the pumps. This convenience saved a great deal of time when successive evaporations were conducted. The valve was built up by brazing two sections of four-inch pipe in the shape of a tee, with flanges brazed on the three ends. A right-angle vacuum path consisting of the stem and half of the tee head was used. The valve stem was mounted axially in the other half of the tee head and carried a hinged flat valve head provided with a koroseal gasket. The hinging arrangement provided maximum clearance with minimum throw of the valve stem. An external sylphon vacuum seal was provided.

A Pirani gauge in the fore-pumping line was used to follow the operation of the pumping system and an ion gauge connected to the system through the base plate was used to observe the absolute pressure in the system during evaporation. Evaporations were carried out at pressures below $5\times10^{-5}$ mm of mercury.

## EVAPORATION HEATERS

Three distinct types of heaters for evaporation were used in this study: open helical wire coils,

* The desirability of carrying out the work described in this paper was suggested to the authors by prior work conducted for the Brush Development Company of Cleveland, Ohio, under subcontract with National Defense Research Council. The Council and the Office of Scientific Research and Development have granted permission to publish this paper.

[1] J. Strong, *Procedures in Experimental Physics* (Prentice-Hall, Inc., New York, 1943) p. 168.

[2] W. C. Caldwell, J. App. Phys. 12, 779–781 (1941).

close wound conical wire baskets, and ceramic crucibles formed on wire baskets. Four metals, tungsten, iron, nickel, and chromel, were used as bare wire coils and baskets and the performance of two ceramics, alundum and BeO, was studied in the form of crucibles. Several major considerations govern the choice of heater type and material when evaporating a given metal. Open helical coils are obviously not suitable for the many metals which are not available in wire or strip form. Crucibles must be used with those metals which either dissolve or react with the metals named above to a serious degree. Again, if quantity evaporation is desired, the tendency will be toward the use of crucibles which can be made with relatively large capacity. Open helical coils possess the advantage of showing less directional effect than close wound conical baskets. The relation between the melting temperature of the heater wire and the evaporation temperature of the metal governs in part the choice of bare wire material. (Evaporation temperature is defined as the temperature at which the vapor pressure is $10^{-2}$ mm Hg. A list of such temperatures is given in Strong.[1]) Other considerations determining the choice of bare heater metal are metallurgical factors, cost, and availability, these considerations suggesting the inclusion of iron, nickel, and chromel in the present survey. Temperature and chemical factors are first considerations in the choice of crucible ceramic.

The helical coils are formed by winding the wire on a cylindrical mandrel of the required size, while the close wound baskets are easily formed on a wood screw. A very useful suggestion was given to the authors by Dr. Robley Williams concerning the forming of tungsten. Even large diameter tungsten wire can be coiled on a mandrel or wood screw of small diameter, with ease and without cracking or breaking, if the forming device has been previously heated to somewhere around 100°C. This temperature is not at all critical, it being sufficient to hold the mandrel in a vise and heat it briefly with a bunsen burner. A clue to this peculiar behavior is to be found in Figure 11, page 544, of Strong's book which displays experimental results on percent elongation at breaking point for nonrecrystallized tungsten which indicate a maximum for this particular property in the neighborhood of 100°C.

## ALUNDUM AND BeO CRUCIBLES

Remarkable success has been experienced in the evaporation of numerous metals from crucibles. A number of ceramics were tried and various heating methods were investigated. The best results were secured with alundum and BeO suspensions painted on tungsten baskets and then baked. Heating was accomplished by passing current through the baskets.

The alundum crucibles are made by painting a close wound conical coil of tungsten with a water suspension of $Al_2O_3$. This should dry in air to form a white shell barely covering the wire and filling the spaces between the wire. It is preferable to have a somewhat thicker coating of ceramic and two procedures may be followed. When dry, the crucible can be repainted with the water suspension, inside and out, thus building up the wall thickness, or the crucible may be baked and then repainted, followed by another baking. Baking consists of heating the crucible slowly in a vacuum by passing current through the tungsten forming basket until a temperature of 1200°C to 1500°C is attained. After holding the crucible at this temperature for five to ten minutes, it may be cooled slowly. Considerable gas is driven out of the crucible during the baking process but its vacuum characteristics are excellent after this initial heating. If any blow holes or cracks should develop during baking they should be painted over and the heating process repeated. These crucibles will be found to be very hard and they can be used for repeated evaporations of those metals which melt below 1600°C and which do not react with alundum. Only one metal was observed to react appreciably with alundum.

BeO crucibles are quite satisfactory and will withstand somewhat higher temperatures than those of alundum. These crucibles are made by painting conical tungsten baskets with an acidulated water suspension of fine BeO powder. The water should contain sufficient HCl to give it a *p*H of between one and two. Heat treatment is the same as for alundum crucibles. Again, cracks which develop will necessitate repainting the crucible with the suspension followed by another baking. Such crucibles have been used for repeated evaporations of materials such as nickel, iron, and cobalt.

Considerable experience with both types of crucible was gained in the work reported below and from this experience a few conclusions may be drawn about the relative merits of alundum

and BeO. Alundum crucibles are much the easier to construct and are greatly superior from a mechanical point of view, being harder, stronger, and showing less tendency to crack at high temperatures. The latter consideration is of importance since a cracked crucible allows contact between the tungsten and the evaporating metal, causing failure in those cases where the two metals react. The alundum used here was supposed to be useful up to 1800°C, while BeO is used as a refractory at much higher temperatures. Presumably then BeO might be effective at temperatures beyond 1800°C when formed into a non-cracking crucible. No evaporations were attempted, however, using alundum at temperatures higher than 1600°C, and while some fast, quantity evaporations of iron were carried out from BeO crucibles at 1750°C, the crucible life was found to be quite short. As far as these studies are concerned alundum appears to be by far superior to BeO, the latter being useful in the case of alundum failure or, presumably, at high temperatures. Alundum was found to fail in certain cases on what were apparently chemical grounds, e.g., in the case of aluminum evaporation.

The vacuum properties of both types of crucibles, constructed according to the above outlined methods, are excellent. Evaporating pressures of $5\times10^{-5}$ mm Hg were readily secured for even high melting point metals.

A few of the crucibles used for these experiments are displayed in Fig. 1.

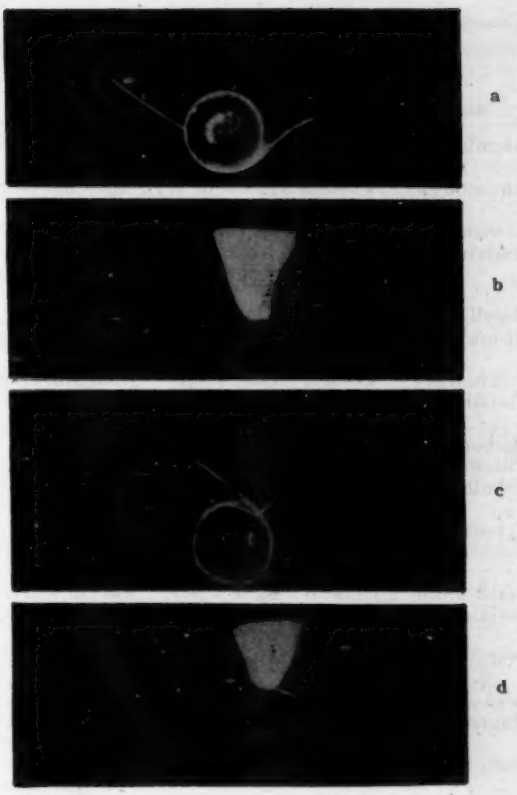


FIG. 1. Alundum (a, b, c) and BeO (d) crucibles used successfully for evaporation of iron, nickel and cobalt. These crucibles are about 1.5 cm in diameter at the base of the cone and are formed on 25-mil tungsten. The interior views show some metal remaining in the crucibles.

## RESULTS

The experience with each material evaporated will be described briefly in the following section. In addition a table (see Table I) is used to indicate the recommended method of evaporating a given material in either small or large quantities. In some cases the best method produced through these experiments is the same as that suggested by Strong or Caldwell. It was thought best to present all of the results regardless of agreement or lack of agreement with other published work. It might be well to point out here that a number of the materials evaporated by sublimation.

## ALUMINUM

A helical tungsten filament is most satisfactory for aluminum evaporation. Heavy aluminum wire cut in short lengths and clipped over the coils of the filament is readily melted. The molten aluminum draws up around the filament, spreads slightly and reacts mildly with the tungsten. For evaporation of large amounts it is only necessary to use a moderately large gauge tungsten wire.

Small quantities of aluminum were evaporated from iron filaments. A small amount of twenty mil aluminum wire was wound around the bottom portion of several coils of a 36 mil iron helical filament. Slow evaporation occurred when the filament was near its melting point. Limited reaction of the aluminum with iron was enough to cause failure of the filament after a short time.

Violet reaction of aluminum with nickel filaments made it impossible for any evaporation to occur.

An alundum crucible behaved peculiarly. The molten aluminum seemed to migrate rapidly through the crucible, making it conducting. The principal resistance was then in the leads causing the aluminum to cool and solidify shortly after melting.

TABLE I. Suggested methods for evaporation of various metals.

| Metal | Method for small quantities | Method for large quantities |
|---|---|---|
| Aluminum | Helical coil of W | Helical tungsten coil |
| Antimony | Conical baskets of W, Ni or chromel | Alundum crucible |
| Arsenic | Alundum crucible | Alundum crucible |
| Barium | Conical baskets of W, Ni, Fe or chromel | Conical baskets of W, Ni, Fe or chromel |
| Beryllium | Conical basket of W | —— |
| Bismuth | Conical baskets of W, Fe, Ni, or chromel | Alundum crucible |
| Calcium | Conical basket of W | Alundum crucible |
| Cadmium | Conical baskets of W, Ni, Fe, or chromel | Alundum crucible |
| Carbon | Unsuccessful | Unsuccessful |
| Chromium | Conical basket of W | —— |
| Cobalt | Helical coil of W | Alundum or BeO crucible |
| Columbium | Helical coil of W | —— |
| Copper | Helical coil of W or conical basket of W | Alundum crucible |
| Germanium | Conical basket of W | Alundum crucible |
| Indium | Conical baskets of W or Fe | Alundum crucible |
| Iron | Helical coil of W | Alundum or BeO crucible |
| Lead | Conical basket of Fe | Alundum crucible |
| Magnesium | Conical baskets of W, Ni, Fe, or chromel | Alundum crucible |
| Manganese | Conical basket of W | Conical basket of W or Alundum crucible |
| Molybdenum | Melting of molybdenum filament | —— |
| Nickel | Helical coil of W | Alundum or BeO crucible |
| Palladium | Helical coil of W | —— |
| Phosphorus (red) | Unsuccessful | Unsuccessful |
| Platinum | Helical coil of W | —— |
| Selenium | Conical baskets of W, Ni, Fe or chromel | Alundum crucible |
| Silicon | BeO crucible | BeO crucible |
| Silver | Helical coil or conical basket of W | Alundum crucible |
| Strontium | Conical basket of W | Large conical basket of W |
| Tellurium | Conical baskets of W, Ni, Fe, or chromel | Alundum crucible |
| Thorium | Conical basket of W | Conical basket of W |
| Tin | Conical basket of W | Alundum crucible |
| Uranium | Conical basket of W | —— |
| Vanadium | Conical basket of W | Conical basket of W |
| Zinc | Conical baskets of W, Ni, Fe, or chromel | Alundum crucible |
| Zirconium | Conical basket of W | —— |

A BeO crucible was somewhat more useful. Migration of aluminum through the crucible occurred, but rather slowly. Considerable evaporation occurred from the crucible in the expected manner but some also occurred from its outside walls. As time progressed the crucible current increased, showing that aluminum migration was shorting out the turns.

The evaporation of aluminum from a tungsten helical filament may be considered as an example of the ideal evaporation of metal from a filament.

### ANTIMONY

As antimony was not available in sheets or wires, only conical, close wound baskets were used. Tungsten, nickel, and chromel were good materials for these baskets, as evaporation proceeded nicely from all of them. In each case the charge melted and wetted the baskets. In some cases the molten charge remained suspended at the central turns of the basket. Iron did not prove satisfactory for the evaporation of antimony. As soon as the antimony melted it was absorbed by the iron, the result being a solid wire from which antimony evaporation did not occur. The basket burned out at a temperature considerably in excess of that at which evaporation of antimony took place from, for instance, the tungsten basket.

Antimony evaporated very satisfactorily from an alundum crucible. If quantity evaporation is desired the crucible is probably the best source. For moderate amounts, the conical baskets of tungsten, nickel and chromel are good heaters.

### ARSENIC

Arsenic was available in powder form. Attempts to evaporate the briquetted arsenic powder from tungsten, iron, nickel, and chromel baskets failed because the briquets fell apart at high temperatures.

Very satisfactory evaporation of arsenic occurred from the alundum crucible. The material sublimed rapidly at low temperatures and therefore heating had to be done slowly so that the charge did not "jump" out of the crucible.

### BARIUM

Barium was evaporated successfully from close wound baskets of tungsten, iron, nickel, and chromel. The barium chips were placed in the baskets without removing the kerosene. Pumping and the initial heatings served to clean up the barium. In all cases the metal melted, wetted the wires nicely and evaporated rapidly.

The deposited barium was metallic and shiny until exposed to air. Rapid oxidation occurred as soon as air was introduced in the system.

The alundum crucible was unsatisfactory. As soon as the barium melted it migrated through-

out the $Al_2O_3$ and reacted with it. Upon exposure to air the walls crumbled away from the tungsten in fine powder.

### BERYLLIUM

Beryllium chips were evaporated successfully from a 25-mil close wound conical tungsten basket. No evaporation was secured from either iron or nickel. Although baskets of the latter materials were slowly heated, they burned out before the beryllium melted.

### BISMUTH

Bismuth was evaporated with equal ease from all the close wound conical baskets which were tried, namely, tungsten, iron, nickel, and chromel. The molten bismuth does not short out the baskets as much as some of the other metals do and evaporation thus proceeds rapidly. This behavior is probably due to the fact that the bismuth is supported chiefly by surface tension and also to the fact that the resistivity of bismuth is roughly 10 times as great as for other metals.

Very satisfactory evaporation of bismuth was secured from an alundum crucible. The molten bismuth pulled up in a bright sphere and evaporated rapidly.

### CADMIUM

Tungsten, iron, and chromel helical filaments were loaded with 40-mg cadmium clips. When these filaments were heated, most of the Cd clips melted and fell off. No Cd remained on the tungsten or iron filaments long enough to observe any evaporation. A small portion of the charge did remain on the chromel filament and was evaporated. It cannot be said that this method was successful, however.

Tungsten, iron, nickel, and chromel conical, close wound baskets were all successful when used to evaporate cadmium. The charge melted readily and stayed in the basket, provided the inverted cone did not have too large an opening at its apex.

The alundum crucible was also a very satisfactory source. This method is probably the best for quantity evaporation and there is no chance of losing the charge by its dropping out of the bottom.

### CALCIUM

Calcium turnings were used for these studies. Of the four close wound baskets used, best evaporation occurred from the tungsten, the lower melting point baskets requiring excessive care to prevent failure. Heating sufficient to produce rapid evaporation caused the remaining calcium to "jump" out of the basket, which effect was frequently encountered with materials which sublime readily. A non-volatile portion remained after completion of the evaporation. This ash-like substance was probably CaO present in the calcium with which the baskets were charged.

An alundum crucible was also satisfactory for calcium evaporation. The high vapor pressure at the bottom of the crucible tended to blow the charge out over the top. However, if evaporation was allowed to proceed slowly, no trouble was encountered.

### CARBON

Small pellets of carbon, broken from a spectroscopically pure graphite rod, were placed in a tungsten basket. Intense heating caused some tungsten evaporation but apparently little, if any, carbon evaporation.

### CHROMIUM

Chromium pellets can be evaporated with ease from a tungsten basket. Because of the high melting temperature of chromium, no other material is satisfactory for its evaporation. No evaporations were tried in atmospheres of helium or hydrogen as suggested in Strong,[1] because the vacuum evaporation was successful.

### COBALT

Some metals react seriously with tungsten near their evaporation temperature, which is usually but not always above the melting point. Several things may occur, among them solution in the solid or liquid form, and compound formation. The solid and liquid equilibrium conditions in the systems, cobalt-tungsten, nickel-tungsten, and iron-tungsten, are similar, and cobalt, nickel, and iron all behave in a similar manner when evaporation from bare tungsten wire is attempted. All these metals evaporate readily at temperatures slightly above their melting points, but if too much evaporating metal is present the filament burns out quickly. In the systems named, there is complete mutual liquid solubility of tungsten and the evaporating metal. A drastic lowering of the liquidus curve from the melting point of tungsten at the pure tungsten

composition to a temperature close to the melting point of the evaporant, at an evaporant composition of about 50 percent by weight, occurs. At 35 percent evaporant composition, however, the liquidus temperature is several hundred degrees above the evaporating temperature, and at the evaporating temperature it might be hoped that the solid tungsten required by the equilibrium diagram might be in the form of undissolved filament. In such a case the heater structure might retain sufficient strength to avoid fracture during the time that fractional distillation of the low melting metal was occurring. Vapor pressure considerations indicate conclusively that the amount of tungsten evaporated from the liquid solution would be entirely negligible. As evaporation proceeded in such a case, solid tungsten would be reformed and if conditions were sufficiently uniform, the filament would be restored to its original shape.

An explanation substantially the same as the above has been advanced by Strong for the case of aluminum evaporated from tungsten. The present experience supports this view as noted below for cobalt, and in the paragraphs on nickel and iron. In these experiments a series of tungsten helical coils was electroplated with various weight percentages of the metal concerned and careful evaporations were carried out. In all cases the maximum evaporant composition resulting in a successful evaporation turned out to be in the neighborhood of 35 percent, filament fracture occurring at higher evaporant composition.

In the case of cobalt the limiting percentage was found to be around 35 percent by weight of metal to tungsten. This was for tungsten helical coils electroplated with cobalt.

Cobalt was plated on tungsten using a solution of 150 g of $CoCl_2$ and 180 g of $CaCl_2$ in enough water to make one liter of solution. Iron anodes were used and the current density was approximately 20 amperes per square foot. Plating at room temperature produced a fairly hard deposit. The tungsten was cleaned with emery cloth before being formed into a coil and the helical coils were immersed in a sodium hydroxide bath and washed with water before being placed in the plating solution. The current was reversed for the first one-half minute, as this aided in the subsequent depositing of the cobalt on the tungsten.

Weighing the coil before and after evaporation showed that practically all of the cobalt could be driven out. Furthermore, several of the coils were replated and used again. Such coils are brittle and care must be exercised not to break them.

If cobalt were available in small diameter wire or sheets so the tungsten coil could be loaded with clips or wound with wire to give a load of twenty-five or thirty percent by weight, there is reason to believe that satisfactory evaporation would occur.

Cobalt was successfully evaporated in larger quanties from alundum and BeO crucibles. The crucibles were charged with pieces cut from cobalt rundels. It was found possible to recharge these crucibles and carry out additional evaporation without breakdown in spite of the high operating temperatures.

### COLUMBIUM

Columbium was secured in the form of one mil sheets. Strips 1 mm wide and several cm long were tightly wound on the turns of tungsten helical coils. At sufficiently high temperatures the columbium melted rather spontaneously, wetting the filament and some evaporated deposit appeared on the test plates. The columbium disappeared practically as soon as melted and undoubtedly some alloying with the tungsten occurred. Because of the high melting point of columbium, no other filaments or crucibles were tried.

### COPPER

Experiments were conducted with helical filaments, close wound baskets, and crucibles. Iron, nickel, and chromel helical coils reacted somewhat with the molten copper which usually pulled up in droplets on the wires. Little evaporation occurred before the droplet moved and the filament burned out at the place where the drop previously was located. In the case of iron some of these drops evaporated. The evaporated material seemed to contain more iron than copper.

A tungsten helical coil was satisfactory for evaporation of very small amounts of copper. A few turns of fine copper wire wound on the bottom of a coil melted and formed a drop which stuck precariously to the bottom of the coil and evaporated. A larger amount of copper formed a bigger drop which fell away from the coil.

The iron, nickel, and chromel close wound baskets behaved poorly. As soon as the copper melted it shorted out the basket, reducing the

temperature. Increased current caused the leads to the basket to burn out.

The tungsten basket also shorted out when melting occurred. In this case increased current caused the copper to evaporate.

Very satisfactory evaporation of copper occurred from the alundum crucible. The molten copper pulled up into a clean ball from which rapid evaporation occurred. This crucible was recharged and its contents evaporated several times without any damage to it.

A crucible is thus the best source for quantity evaporation of copper, while a tungsten basket serves well for a smaller amount.

### GERMANIUM

Small fragments from fused germanium lumps were successfully melted in, and evaporated from, a conical tungsten basket. When the germanium melted, it wetted the tungsten and some turns of the basket shorted out but increased current produced sufficient heat for a fairly rapid rate of evaporation.

Attempts to evaporate this metal from nickel, iron, and chromel baskets were unsuccessful due to reaction between germanium and these metals which occurred as soon as the germanium became molten.

Quantity evaporation of germanium was accomplished with success from an alundum crucible. Upon sufficient heating the charge melted and pulled up into a shiny ball. Increased heating caused rapid evaporation from a white hot crucible. No reaction of germanium with alundum occurred and the crucible was in perfect condition after the experiment was finished.

### INDIUM

Indium in the form of chips evaporated well from tungsten, iron, nickel, and chromel baskets, the first two basket materials being somewhat superior. The molten indium wetted all these materials but did not short them out too much.

Indium wire used as clips would undoubtedly evaporate well from tungsten and iron and probably also from chromel or nickel.

Very satisfactory evaporation of indium occurred from an alundum crucible. The molten indium evaporated rapidly.

### IRON

Techniques previously described for evaporation of cobalt were equally successful with iron. Small iron clips, small diameter iron wire, or plated iron[3] were all evaporated successfully from tungsten helical coils provided the percentage of iron by weight was kept below 35 percent.

Iron was also evaporated in rather large quantities from alundum and BeO crucibles. Multiple evaporations were carried out from both kinds of crucibles without serious effects on them.

### LEAD

Of the four baskets tried, lead evaporated best from iron. When lead melted, it shorted out the basket somewhat but evaporated rapidly. The nickel and chromel baskets were wetted by the lead and all of the lead evaporated, the rate, however, was slower than with iron and greater care had to be taken to keep from burning out these baskets. The lead did not wet tungsten, consequently the molten material tended to run out of the bottom of the basket. For this reason tungsten is not as good as iron.

Lead also evaporated very easily and rapidly from an alundum crucible.

### MAGNESIUM

It was possible to evaporate magnesium by sublimation from baskets of all four materials. In all cases pieces of magnesium ribbon comprised the charge. Some of these pieces hung over and outside the basket. When evaporation began, these pieces usually fell off but several made contact with the outside of the coils of the basket when evaporation began and stayed in this position until sublimation was complete.

Evaporation occurred rapidly from the alundum crucible. As in other cases where sublimation occurred, the vapor pressure tended to blow the charge out of the crucible, making it necessary to raise the crucible to the sublimation temperature slowly.

### MANGANESE

Manganese was successfully evaporated from tungsten baskets. In this case small pieces of electrolytic manganese were used in a close wound conical basket. Evaporation occurred by sublimation. A similar basket of nickel burned out before any melting or evaporation occurred. Iron and chromel were somewhat more satisfactory in that a little evaporation occurred but

[3] Nathaniel Hall and G. B. Hogaboom, Jr., *Plating and Finishing Guidebook* (Metal Industry Publishing Company, New York, N. Y.).

the melting point of maganese is too close to the melting point of these filament materials to give very satisfactory results.

An alundum crucible was very satisfactory as a heater from which to evaporate manganese. At a sufficiently high temperature evaporation began to occur by sublimation and as the temperature was raised further the rate of sublimation increased. No tendency to "jump" out of the crucible was observed with manganese.

### MOLYBDENUM

It was found impossible to melt molybdenum by means of heat supplied by a tungsten coil even though thin, narrow strips of molybdenum cut from sheet was wound closely on the coil. The sublimed material which was eventually driven off probably contained more tungsten than molybdenum.

A small amount of molybdenum was evaporated by slowly raising a molybdenum filament to the melting point.

### NICKEL

Nickel was evaporated with success by methods similar to those used for iron and cobalt. Nickel plated[3] on tungsten coils was evaporated successfully if the percentage of nickel by weight was less than 30 percent. The plated material draws up in droplets when heated to melting so no advantage is gained over using clips or small diameter wire wound on the tungsten coils.

Successive evaporations of nickel from one BeO crucible were conducted with good results. Large amounts were evaporated from the clean molten nickel in the crucible. Alundum crucibles were also found to be very satisfactory for the evaporation of nickel.

### PALLADIUM

Palladium was evaporated from a tungsten helical coil. A piece of thick sheet palladium was rolled out thin and cut into strips 1 mm wide which were then wound tightly on the helical coils. They melted rather easily, wetted the tungsten, and evaporated rapidly.

### PLATINUM

Partial success in evaporating platinum was secured by winding 3-mil platinum wire tightly on a 25-mil helical tungsten filament. The platinum melted and apparently reacted somewhat with the tungsten. A few small droplets formed on the filament which were finally driven off by intense heating. It is possible that the evaporated material may contain some tungsten due to the intense heating.

### SELENIUM

Selenium evaporated rapidly and easily from close wound baskets of all four materials. Some wetting occurred and temporary, partial shorting of the basket turns was also observed. There seems to be little basis for choosing one basket material rather than another.

Evaporation of selenium also occurred rapidly from the alundum crucible, no difficulties being encountered.

### SILICON

Several attempts to evaporate silicon in the form of small chips from close wound conical tungsten baskets gave mediocre results. A little evaporation was secured, but as soon as the silicon became molten, rapid reaction with the tungsten burned out the basket.

Successful evaporation of silicon was secured from a BeO crucible. As the temperature necessary to melt the silicon is quite high, care had to be taken to construct a good crucible without cracks and the crucible had to be heated slowly.

### SILVER

Silver was evaporated with ease from both helical coils and conical baskets of tungsten. While the silver did not wet the tungsten very well, large clips hung on the helical coils would melt and pull up as a spherical drop attached to the tungsten at only a small point. None of these was observed to drop off. In the conical baskets the lack of wetting made it possible to evaporate the molten silver pellet without difficulty.

Iron, nickel, and chromel were also tried in the form of coils and baskets. The baskets were not successful at all and the coils only moderately so. Care had to be taken not to burn out the helical coils before the silver had evaporated.

Silver was evaporated in quantity and without difficulty from an alundum crucible.

### STRONTIUM

Strontium chips were inserted in conical baskets without first removing the protecting kerosene film, but even so the metal was found to be appreciably oxidized. Several evaporations were carried out from baskets of tungsten, iron,

nickel, and chromel. Evaporation always seemed to occur by sublimation. This is contrary to results reported by Caldwell who states melting occurred. The tungsten basket is probably the best evaporation source. Large size tungsten baskets served well for quantity evaporation of strontium.

The evaporated surface had a shiny metallic appearance in vacuum but oxidized to a fine powder immediately when exposed to air.

### TELLURIUM

Tellurium was evaporated by sublimation from all four kinds of conical baskets with ease. Care had to be taken to keep from blowing the charge out of the basket.

Rapid evaporation from an alundum crucible was observed at quite low temperatures. Large quantities were evaporated with ease.

### THORIUM

Thorium powder, briquetted, and placed in tungsten baskets was evaporated after preliminary heating had outgassed the material. Melting occurred at rather high temperatures, the thorium wetting the tungsten and evaporation proceeding quite rapidly.

### TIN

Of the four kinds of baskets used, tungsten was by far the most satisfactory for the evaporation of tin. Some wetting of the tungsten occurred and good surface tension caused the molten tin to remain in a basket which was nearly cylindrical with a fairly large opening in the bottom. Iron, chromel, and nickel baskets burned out before much evaporation occurred.

Satisfactory evaporation of tin proceeded from an alundum crucible. The molten tin first pulled up in a spherical ball and then later wetted the crucible walls somewhat. Evaporation was rapid and not very active.

### URANIUM

Uranium powder was briquetted into small chunks and placed in conical tungsten baskets. When the charge did not jump out of the basket, evaporation proceeded without difficulty.

### VANADIUM

Vanadium chips in a tungsten conical basket were melted and evaporated successfully. A mild reaction of vanadium with tungsten occurred but did not interfere with the evaporation.

### ZINC

Zinc in the form of small pellets was evaporated readily from all four kinds of conical baskets. In all cases evaporation occurred by sublimation. It was necessary to heat the baskets slowly and to evaporate at low temperature or the vapor pressure would drive the charge out of the basket.

Zinc was evaporated readily from an alundum crucible, again by sublimation. Care had to be taken in heating the crucible to keep the vapor pressure from blowing the charge out of the crucible.

Caldwell indicates that zinc reacts readily with such materials as chromel, iron, and nickel, burning out the filament before evaporation occurs. No such reaction was observed in the experiments described above, but in these experiments the temperature was always raised rather cautiously. In an attempt to reproduce Caldwell's results, a trial was made with zinc and an iron basket. The temperature of the basket was slowly raised to a dull red at which point sublimation of zinc occurred. The basket temperature was then raised rapidly, causing the zinc to melt and wet the iron after which solidification of the whole mass took place. No evaporation from the resulting solid was observed, and a further rise in temperature resulted in filament failure.

The above observations may be interpreted in terms of the zinc-iron equilibrium diagram in which appear two rather stable intermetallic compounds of high zinc composition. Zinc melting at 419°C may be pictured as reacting with iron to form one or both of these compounds which do not decompose until approximately 700°C is reached. These compounds may be supposed to be stable enough that little fractional sublimation would occur from them at temperatures below their decomposition temperature, which latter temperature is, however, very near the liquidus temperature at high zinc composition. Hence decomposition of and evaporation from these compounds would be closely followed by melting and failure. The zinc-nickel equilibrium relations are similar to those of zinc-iron. Caldwell's observations as well as the present reproduction of them would then seem to be explained in terms of the above picture.

The successful zinc evaporations from iron and

nickel recorded here would appear to be due to the fact that sublimation was allowed to proceed at relatively low temperatures where the physical contact between the two metals is small (no wetting), and where diffusion and reaction rates are low. It may be suggested that low temperatures and long times are a general cure for many apparently unsuccessful evaporation techniques.

**ZIRCONIUM**

This material was available in the black amorphous form. Initial heating caused considerable outgassing. Further heating caused melting of the zirconium and evaporation proceeded for a short time. Reaction of the zirconium with tungsten destroyed the basket after some evaporation had occurred.

## Recent Applications of Physics

Prepared by CLARK GOODMAN, Associate Editor

Material to be included in this section should be submitted to Dr. Clark Goodman, Massachusetts Institute of Technology, Cambridge 39, Massachusetts.

**Lissajous Figures** A number of techniques have been used in the study of compound harmonic motion. Coupled tuning forks carrying small mirrors were used by Lissajous in his extensive studies. The Harmonograph, Kaleidophone, and, more recently, the cathode-ray oscillograph are standard methods for obtaining patterns of Lissajous figures. W. B. Hales[1] has obtained unusually striking effects using a simple Blackburn pendulum (Y-shaped). The heavy brass bob of this pendulum carries dry cells and a flashlight bulb completely shielded except for a collimating system that gives a very fine pencil of light. This light beam traces the path of the pendulum on photographic paper placed immediately below. The bob is released simultaneously with the turning on of the light and starting of the chronometer. There is sufficient damping to prevent overlapping of the lines even near the end of the exposure. No particular applications of this technique have been found. It would appear that the patterns obtained should be useful in commercial art and textile designing, as the accompanying photograph clearly indicates.

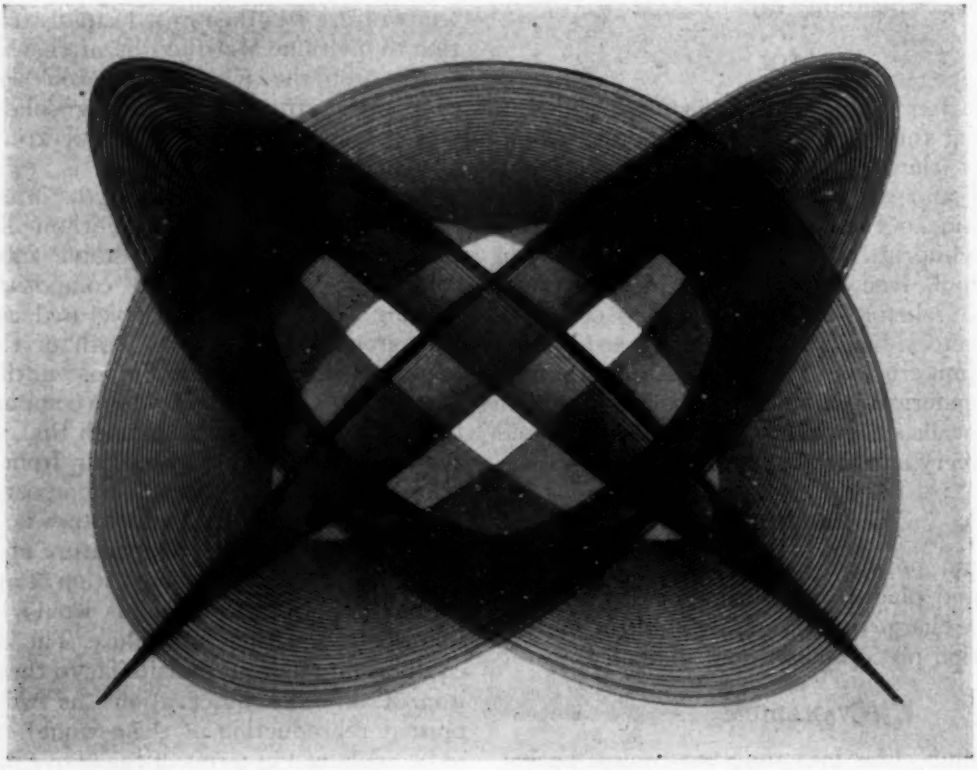

[1] J. Acous. Soc. Am. 16, 137–146 (1945).